MICROINSTABILITIES IN HIGH POWER ELECTRON CYCLOTRON HEATING OF PLASMAS

Andrew Gilbert Miller

A Thesis Submitted for the Degree of PhD
at the
University of St Andrews

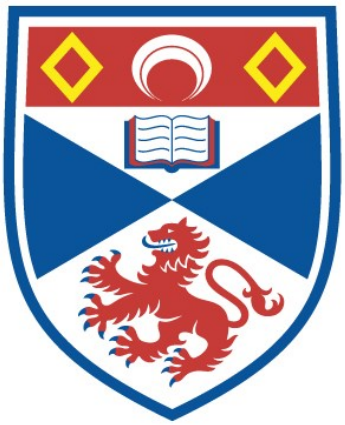

1991

MICROINSTABILITIES IN HIGH POWER ELECTRON CYCLOTRON RESONANCE HEATING OF PLASMAS

ANDREW GILBERT MILLER

THESIS SUBMITTED FOR THE DEGREE OF DOCTOR OF PHILOSOPHY OF THE UNIVERSITY OF ST ANDREWS

ProQuest LLC.
789 East Eisenhower Parkway
P.O. Box 1346
Ann Arbor, MI 48106 – 1346

Certificate

I certify that Andrew G Miller has satisfied the conditions of the Ordinances and Regulations and is thus qualified to submit the accompanying application for the Degree of Doctor of Philosophy.

MICROINSTABILITIES IN HIGH POWER ELECTRON CYCLOTRON RESONANCE HEATING OF PLASMAS

Abstract.

Electron cyclotron resonance heating has been successfully used in a number of experiments, firstly to raise the plasma temperature and secondly to drive currents noninductively. Recently the microwaves in tokamak experiment (MTX) has been proposed at the Lawrence Livermore Laboratory, which will involve pulsed heating at powers much higher than have previously been possible, using a Free Electron Laser (FEL). The physics of such an experiment differs greatly from the physics of experiments using less powerful but continuous operation gyrotron sources.

An analytical model of the interaction between a wave and an electron is presented on the assumption that the wave amplitude experienced along the electron guiding centre changes slowly with time as it passes through the beam. This model is tested numerically by integrating the equations of motion governing the electron's motion as it interacts with the wave.

Finally this model is used to predict the possible growth of instabilities in a plasma heated by a FEL. The growth rates of these waves may be large enough to act on the plasma in time scales much shorter than typical electron collision times.

Acknowledgements.

It is with much reluctance that I leave St Andrews for pastures new having had so many friends and so many pleasant experiences.

Firstly I wish to thank my supervisor Dr Alan Cairns for his patient help and guidance through the last three years. I also wish to thank the other members of the Plasma Physics group past and present for their support and friendship - Professor Jeffrey Sanderson, Alastair McGowan, Ruhul Amin, Ashley Buckner and Helen Holt.

Secondly I wish to thank all my colleagues at Culham who have been so patient in listening to all my computing problems - Dr Chris Lashmore - Davies my supervisor at Culham, Martin Cox, Paul Haynes, Richard Dendy and especially to Martin O'Brien who has spent many long and frustrating hours teaching me to use the computing resources at Culham.

I feel indebted also to all those who have taught me in past years and who have given me the grounding I needed to undertake this work. In particular I would like to thank the Mathematics and Physics departments of Queen Elizabeth School and Community College and Dr John Dougherty of Pembroke College, Cambridge.

Next I would like to thank all those at St Andrews who have been helpful in arranging computing facilities for me especially Dr Hania Allen and Julian Crowe.

My thanks go to the Science and Engineering Research Council and the United Kingdom Atomic Energy Authority for their financial assistance.

I would like to thank all those at Sallies and Stanley Smith for their support and encouragement as well as many friends in the Celtic Society and the Bridge Club.

Finally thanks to Mum and Dad for putting up with a perpetual student for a son.

AGM

Declaration

I declare that the following thesis is a record of research carried out by me, that the thesis is my own composition and that it has not previously submitted in application for a higher degree.

In submitting this thesis to the University of St Andrews I understand that I am giving permission for it to be made available for use in accordance with the regulations of the University Library for the time being in force, subject to any copyright vested in the work not being affected thereby. I also understand that the title and abstract will be published, and that a copy of the work may be made and supplied to any bona fide library or research worker.

Postgraduate Career

I was admitted into the University of St Andrews as a research student under Ordinance General number 12 in October 1987 to work on the theory of electron cyclotron resonance heating under the supervision of Dr R A Cairns. I was admitted under the above resolution as a candidate for the degree of PhD two terms later.

CONTENTS

CHAPTER ONE

INTRODUCTION

CHAPTER ONE

Introduction

1.1 General Introduction

The study of plasma physics is the study of ionised materials and the way electric and magnetic fields behave in them. Plasmas are generally electrically neutral but the separation of electrons and ions gives rise to properties much different from those of gases. They can be studied as a fluid using magnetohydrodynamics (MHD) or using a kinetic model which more accurately describes the detailed physics. For some purposes the effect of collisions between electrons and ions has to be calculated while for other purposes, for phenomena occurring in time scales shorter than typical times between collisions, interactions between single ions or electrons may be neglected. The two cases are referred to as collisional and collisionless plasma physics respectively.

The Debye length.

One of the most important quantities in the theory of plasma physics is the *Debye length.* Suppose a positive charge is placed in a vacuum. The electric field potential will fall off as 1/r, r being the distance from the charge. Now suppose it is placed in a plasma instead. It will attract electrons and repel ions creating a screen of negative charge around it, so that the potential falls off faster than 1/r. The characteristic length in which it falls off is the Debye length.

Formally we have

$$n_e(r) = n_0 e^{\frac{e\phi_p(r)}{T}} \approx n_0\left(1 + \frac{e\phi_p(r)}{T}\right)$$

where the units are such that the Boltzmann constant is unity, T is the temperature, e is the electronic charge of an electron, $\phi_p(r)$ is the electric field potential, n_0 is the average electron density, and $n_e(r)$ is the electron density at distance r from the charge. The expansion of the exponential is clearly only valid when $|e\phi_p/T| \ll 1$.

From Poisson's equation we have

$$\nabla^2\phi_p = \frac{n_0 e^2 \phi_p}{\varepsilon_0 T}$$

ε_0 being the dielectric constant for a vacuum. Now suppose we have spherical symmetry, then Poisson's equation becomes

$$\frac{1}{r^2}\frac{d}{dr}\left(r^2\frac{d\phi_p}{dr}\right) = \frac{\phi_p}{\lambda_D^2}$$

where

$$\lambda_D^2 = \frac{\varepsilon_0 T}{n_0 e^2}$$

so that

$$\phi_p = A\frac{e^{-\frac{r}{\lambda_D}}}{r}$$

A being a constant. The Debye length is therefore λ_D.

The more particles there are within the Debye sphere the more uniformly they will be distributed around our original test particle, and hence the smaller the chance of imbalances producing a net force on the charge. Now the number of particles in the Debye sphere is approximately $4\pi n_0 \lambda_D^3/3$, which will be an extremely large number for the plasma under consideration in this thesis. Therefore on long time scales the effect of individual collisions will be relatively weak. It is for this reason that the study of plasmas differs greatly from the study of gases where the collisions are far more important.

Cold plasma theory.

Despite our earlier assumption that $|e\phi_p/T|<<1$ some phenomena in a plasma may be described by *cold plasma theory*. Essentially cold plasma theory considers the effect of electric and magnetic fields on the plasma by neglecting the temperature of the plasma. Formally cold plasma theory is derived from the equations

$$\underline{J}_{CD} = \sum_s q_s n_s \underline{v}_s$$

(current equation)

$$\frac{d\underline{v}_s}{dt} = \frac{q_s}{m_s}\left(\underline{E} + \underline{v}_s X \underline{B}\right)$$

(Lorentz equation)

$$\frac{dn_s}{dt} = 0$$

(particle conservation equation)

where the subscript s denotes a plasma species, n refers to the density, q to the charge, $\underline{E}$ and $\underline{B}$ to the electric and magnetic fields, $\underline{v}$ to the velocity, $\underline{J}_{CD}$ to the current density, m to the mass and t to time. Frequently we deal with only two plasma species eg electrons and singly charged ions, and sometimes we even neglect the effect of the ion species.

This is not the place for a full review of cold plasma theory although we will use some basic results from the theory in this introduction. In particular we shall remark that for an inhomogeneous plasma the theory enables us to calculate the approximate positions of *cutoffs* and *resonances* . A cutoff is a point at which a wave may travel no further in the direction of travel, generally because the density of the plasma becomes too high, and a resonance is a point at which there may be an exchange of energy between the plasma and the wave allowing the wave to be partly or completely damped.

Although cold plasma theory is in very common use, many of the results in this thesis require the use of hot plasma theory which may be subdivided into

nonrelativistic and relativistic theory. The essential difference between hot theory and cold theory is that in the former we define a distribution function for particle velocities f_s and replace the equations forming the cold plasma theory with

$$\underline{J}_{CD}(\underline{r},t)= \sum_s q_s \int \underline{v} f_s(\underline{r},\underline{v},t) d^3\underline{v}, \qquad \rho_c(\underline{r},t) = \sum_s q_s \int f_s(\underline{r},\underline{v},t) d^3\underline{v}$$

and the Vlasov equation for each species

$$\frac{\partial f_s}{\partial t} + \underline{v}.\frac{\partial f_s}{\partial \underline{r}} + \frac{q_s}{m_s}(\underline{E} + \underline{v}\times\underline{B}).\frac{\partial f_s}{\partial \underline{v}} = 0 \qquad (1.1)$$

where ρ_c is the charge density. These equations are valid for the nonrelativistic case only; for a generalisation to the relativistic case see Clemmow and Dougherty (1969). More about hot plasma theory will be said later.

The electric and magnetic fields in equation (1.1) must be found self-consistently from Maxwell's equations and our expressions for $\underline{J}_{CD}$ and ρ_c. Formally the Vlasov equation is obtained as the lowest order approximation depending on the large parameter $n_o\lambda_D^3$ (roughly the number of electrons in the Debye sphere).

As it stands, in the absence of electric and magnetic fields, the Vlasov equation would be valid for an arbitrary distribution. In this thesis we shall be interested in plasmas with a uniform magnetic field so that the general form becomes $f = f(V_\perp, V_\parallel)$, $V_\perp$ and $V_\parallel$ being the velocities perpendicular and parallel to the magnetic field. However, introducing the effect of two body collisions by adding another term to (1.1), the distribution will relax back to thermal equilibrium (a Maxwellian).

Equation (1.1) is one of the most important equations in the theory of hot plasmas, and much of the work in this depends upon it. It is therefore fitting it should be the first numbered equation in this thesis.

1.2 Nuclear Fusion and Magnetic Confinement.

Although plasmas are relatively rare on earth and abundant in space, much of the study of plasmas to date has been related to nuclear fusion. Fusion is a process that may occur between (usually) light nuclei in which the participating bodies coalesce forming a new element and releasing energy. An example of a reaction which may be feasible is

$$_1D^2 + {}_1T^3 \rightarrow {}_2He^4 + n + 17.56\ MeV.$$

Two other reactions which may occur, but only at higher temperature than the temperature at which this one takes place, are

$$D^2 + D^2 \rightarrow He^3 + n^1 + 3.27\ MeV \text{ and}$$
$$D^2 + D^2 \rightarrow T^3 + H^1 + 4.03\ MeV.$$

Nuclear fusion is in many ways preferable to its fission counterpart and it is the method used by stars to create energy so it is unfortunate that attempts to generate energy on earth through this method have so far proved elusive. Until the 1960's when inertial confinement was first proposed, magnetic confinement of the plasma was the only method considered, and it is still the main focus of attention. Three problems that have prevented the success of the fusion programme are

(1) the presence of macroinstabilities which hinder confinement of the plasma within reactor walls,

(2) the very high temperature required in order to allow fusion, typically 10 keV for magnetic devices and

(3) the relatively poor energy confinement of tokamak plasmas.

A great variety of approaches has been tried, but in this thesis attention is restricted to the tokamak, a toroidal chamber in which currents can be induced by using it as the secondary of a transformer. The external coils on a tokamak provide a strong toroidal field and the plasma current provides a much weaker but nonetheless important poloidal magnetic field. A changing current is driven through coils around an iron core passing through the centre of the torus as in

figure 1.1a, after Taylor (1987), driving the current. As the poloidal magnetic field is essential for containment of the plasma, tokamaks can be used only in pulsed operation without another source of current. Ions and electrons spiral around magnetic field lines and so their guiding centres follow a path almost parallel to the minor axis of the torus. The poloidal field however introduces a second much slower rotation around the minor axis and creates approximately circular surfaces on which electrons travel called flux surfaces, again illustrated in figure 1.1a. The heating effect obtained as the current heats the plasma is known as *ohmic heating* and the electric field producing this current is known as the *ohmic field* . The variation of plasma parameters within the tokamak as a function of distance from the major axis is of great importance to the physics, and the variations of toroidal and poloidal magnetic fields are shown schematically in figure 1.1b also after Taylor. The density and temperature both have a maximum near the minor axis of the torus and fall off towards the edges of the machine whereas the magnetic field strength increases towards the inside wall of the torus. For a fuller review of the operation of tokamaks see Wesson (1987).

Figure 1.1 (after Taylor)

Figure 1.1a Schematic of a Tokamak.

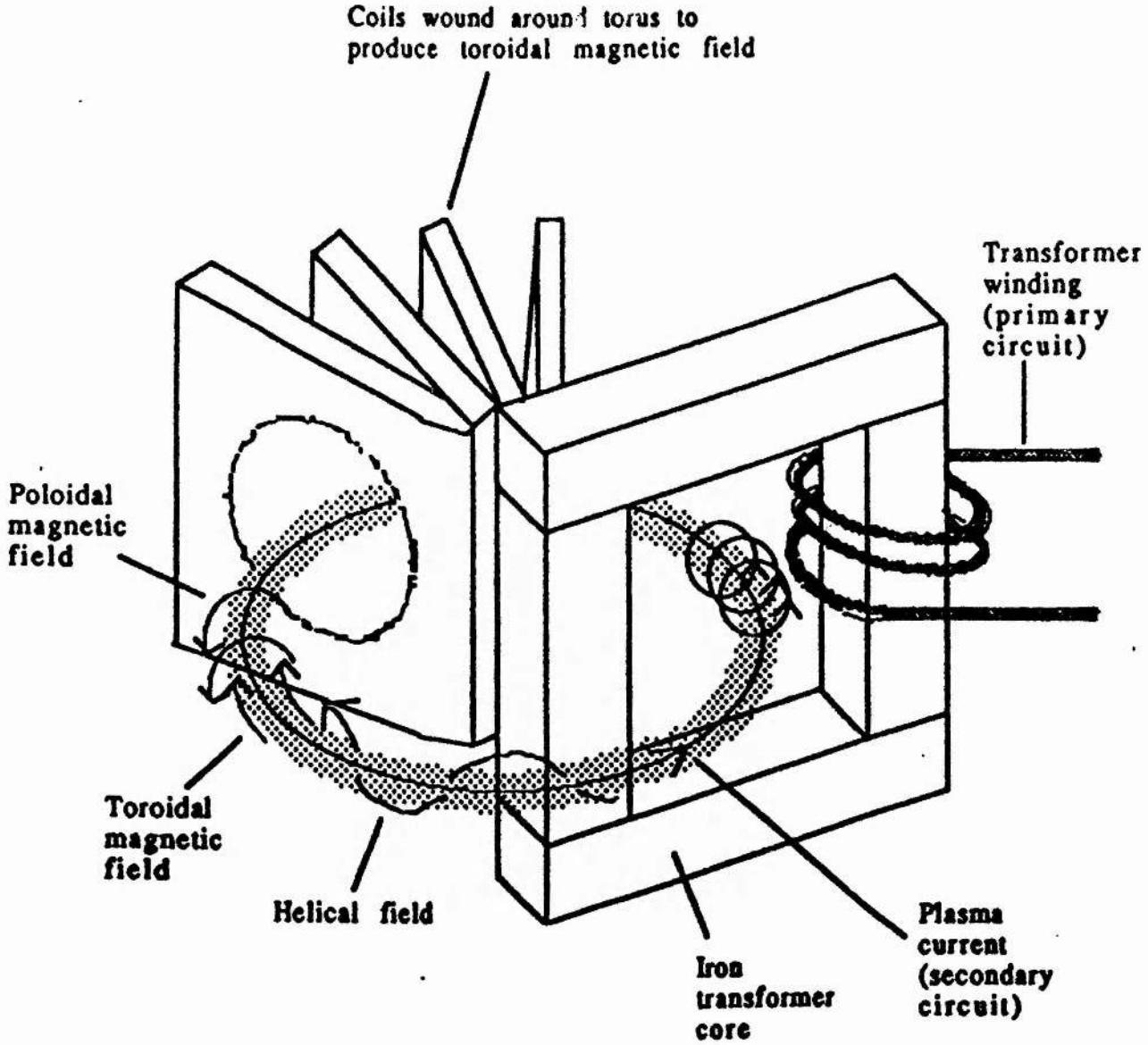

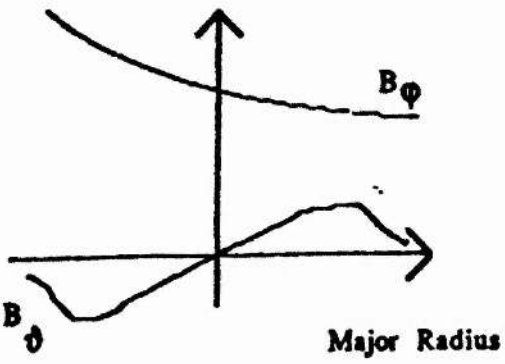

Figure 1.1b Distribution of Toroidal and Poloidal Fields in a Tokamak.

1.3 Additional Heating in Tokamaks.

A plasma may only undergo fusion when the Lawson criterion is met (that $n_d\tau_{con}$ is sufficiently large where n_d is plasma density and τ_{con} is the particle confinement time) and the temperature is high enough. The temperature which can be achieved by ohmic heating is limited because the resistivity is proportional to $T^{-3/2}$, T being the temperature. To satisfy this criterion it is desirable to heat the plasma to temperatures higher than those obtained using ohmic heating and in a tokamak this may be done in a variety of ways, referred to as additional heating. The two main methods are Neutral Beam Injection and Radiofrequency Heating.

Neutral Beam Injection

Charged particles are hindered from penetrating far into the centre of the plasma by the large toroidal magnetic field, but beams of neutral particles, eg deuterium atoms, created by first creating an ion beam and then neutralising it, can penetrate the plasma and heat it. This technique is powerful, but can lead to degradation of energy confinement and to sawtooth oscillations - Bickerton et al (1986) and Gill et al (1986).

Radiofrequency (RF) Heating.

Energy can also be transported to the plasma by high frequency electromagnetic (e/m) waves which can be absorbed locally through resonances in the plasma. The four main RF schemes use Alfven, Ion Cyclotron (ICRH), Lower Hybrid (LH) and Electron Cyclotron (ECRH) waves in ascending order of frequency.

Alfven wave heating relies on exciting localised Alfven waves of frequency 1-10 MHz along magnetic field lines - Behn et al (1984).

ICRH uses fast magnetosonic waves of frequency 25 - 100 MHz which are absorbed by ions at the ion cyclotron frequency or harmonics thereof. The main heating schemes considered are heating at the second harmonic and heating in the presence of a minority ion species. This is a commonly used method of additional heating but suffers from the drawback that the large wavelengths involved require large antennae.

The next highest frequency regime, 1-5 GHz, is lower hybrid heating. The waves' shorter wavelengths allow them to be carried by a waveguide, one of the main advantages of this scheme over ICRH. Heating is achieved by exciting plasma waves near the lower hybrid resonance, at a frequency given by

$$\omega_{LH}^2 = \frac{\omega_{pi}^2}{1+\frac{\omega_{pe}^2}{\Omega_{ce}^2}} \quad .$$

Here $\Omega_{ce}=eB/m_e$ is the electron cyclotron frequency where m_e and B are the rest mass of an electron and the magnetic field strength, ω_{pi} is the ion plasma frequency $\frac{n_i e^2}{m_i \varepsilon_0}$ where m_i is the ion mass and n_i is the ion density, ω_{pe} being similarly defined for the electron. One of the drawbacks of the scheme is that the wave is evanescent at the edge of the plasma and suffers from severe accessibility constraints, particularly in a reactor regime. Nonetheless it is a successful heating scheme - Bernabei et al (1982).

Lastly we consider ECRH, the subject of this thesis.

1.4 Electron Cyclotron Resonance Heating.

Although by no means the most commonly used method of additional heating, in many ways ECRH is the simplest. It is possible to heat electrons without the need for a large antenna, and without the EC wave having to cross an evanescent region, avoiding problems with the plasma edge. When waves are incident perpendicular to the background magnetic field they may travel in two modes viz the ordinary (O) and the extraordinary (X) mode. The O mode is a transverse wave whose electric field oscillates along the direction of the magnetic field while the X mode is a mixed transverse and longitudinal wave which has no electric field component in the direction of the magnetic field. The X mode's field can be composed into two rotating electric field components E_+ and E_-, the latter rotating in the same sense as the electrons (and the former in the same sense as the ions). As $|E_-| \approx |E_+| v_{th}/c$ near the cyclotron frequency (Stix, 1962), v_{th} being the thermal velocity and c the velocity of light, the E_- component vanishes in the cold plasma approximation. Furthermore for electron cyclotron heating the E_+ component is ignored as it rotates in the opposite sense to the electrons. It is therefore clear that the X mode cannot heat electrons at the electron cyclotron frequency in the cold plasma approximation. However in the hot theory E_- does not vanish and heating may take place. Charged particles in uniform magnetic fields move by spiralling around the magnetic field lines at the electron cyclotron frequency. When the cyclotron frequency matches that of electromagnetic waves the particle may interact strongly with the wave, either receiving or giving up energy from or to the wave and enhancing its perpendicular velocity. Resonance is also possible at harmonics of the cyclotron frequency, and, for the X mode, at the upper hybrid frequency $\omega_{UH}^2 = \omega_{pe}^2 + \Omega_{ce}^2$. (This resonance does exist in a cold plasma).

Figure 1.2 after Taylor shows the schematic arrangement of the tokamak and the waveguide carrying the incident ECRH wave for outside launch.

The O mode also has a resonance at the cyclotron frequency in a warm plasma but not at the upper hybrid frequency. It might seem strange at first that a wave

Figure 1.2 (after Taylor) A Schematic Diagram of ECRH.

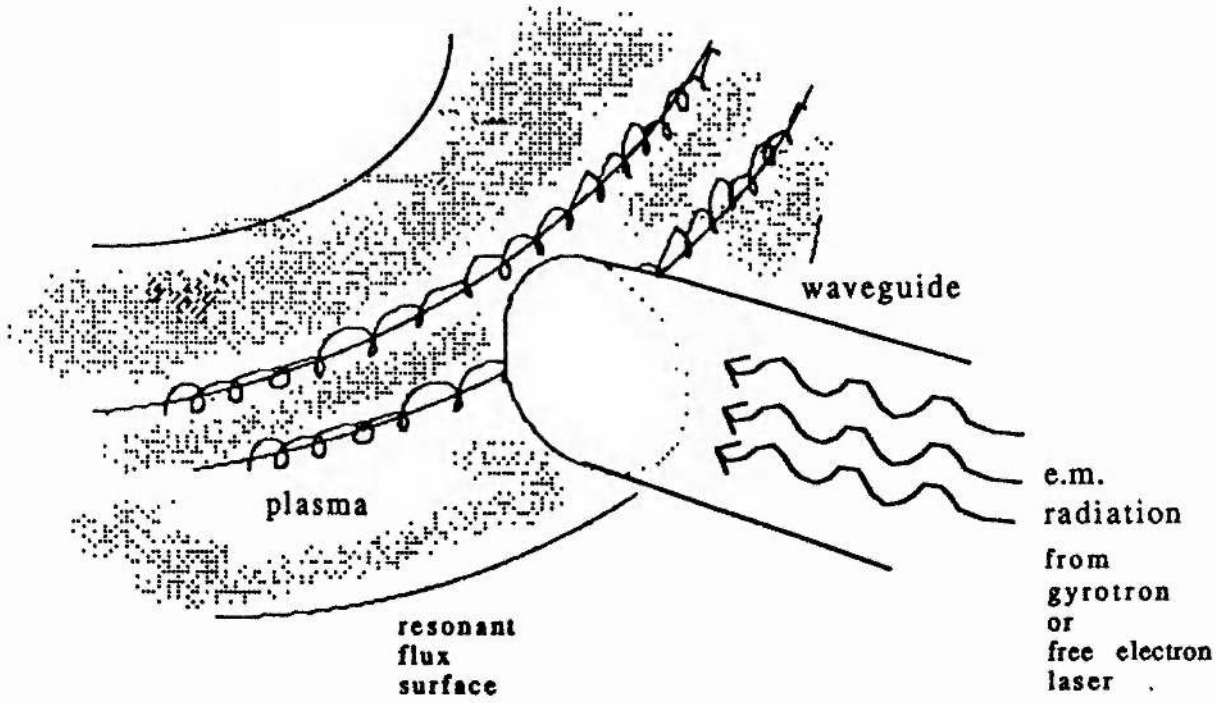

whose electric field is polarised in the direction of the magnetic field may increase the perpendicular velocity of electrons, just like the X mode, and indeed cold plasma theory does not predict a resonance at the cyclotron frequency for the O mode either. A resonance does however exist and the physical basis of the heating is the $\underline{v}X\underline{B}$ force in the Lorentz equation, which explains why heating by the O mode is proportional to the parallel velocity of the electron being heated.

Accessibility

Accessibility conditions for ECRH differ for each mode and are summarised for wave propagation perpendicular to the magnetic field in the Clemmow-Mullaly-Allis (CMA) diagram (figure 1.3 after Wesson, 1987). The cutoffs are determined by zeros of the perpendicular component of the refractive index vector $\underline{n}$ given by the equation

$$\underline{n}X(\underline{n}X\underline{E}) = \underline{\varepsilon}\underline{E} \qquad (1.2)$$

where $\underline{\varepsilon}$ is the dielectric coefficient tensor.

Using cold plasma theory and neglecting the effect of ions we obtain the Appleton-Hartree dispersion relation

$$|\underline{n}^2| = 1 - \frac{2\alpha_{rat}^2\,\omega^2\left(1-\alpha_{rat}^2\right)}{2\omega^2\left(1-\alpha_{rat}^2\right)-\Omega_{ce}^2\sin^2(\theta) \pm \Omega_{ce}\Gamma}$$

where

$$\Gamma = \sqrt{\Omega_{ce}^2\sin^4(\theta)+4\omega^2\left(1-\alpha_{rat}^2\right)^2\cos^2(\theta)} \quad ,$$

$\alpha_{rat} = \omega_{pe}/\Omega_{ce}$ and where θ is the angle the direction of propagation of the wave makes to the magnetic field. What is of significance is whether or not each mode can reach a resonance which depends on the point at which $n_\perp$ becomes zero according to the Appleton-Hartree (A-H) equation. This equation also indicates the position of cold plasma resonances at points where $n_\perp \to \infty$. The O mode can

Figure 1.3

X mode Accessibility (after Wesson)

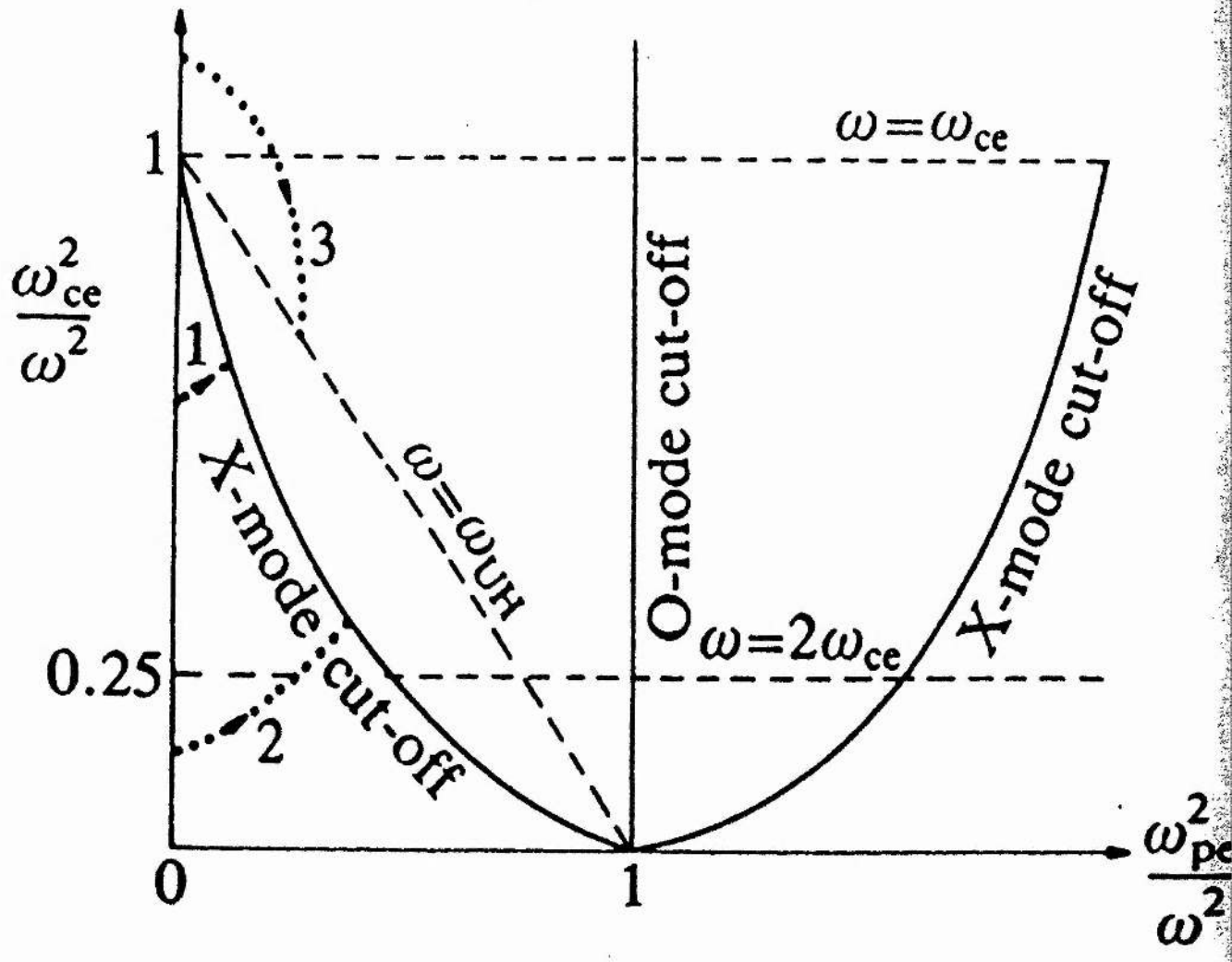

The straight lines___ represent cutoffs, the dashed lines --- represent cold plasma resonances and the dotted lines ..... represent three X mode trajectories.

reach its warm plasma resonance (which the A-H equation does not predict) at the cyclotron frequency provided $\omega > \omega_{pe}$, but the accessibility of the X mode is more complicated and depends on whether it is launched from the low or the high field side of the tokamak. Launched from the low field side with $\Omega_{ce} < \omega$ it cannot reach the cyclotron frequency owing to the X mode cutoff (trajectory 1), but it may reach the second harmonic (trajectory 2). Launched from the high field side with $\Omega_{ce} > \omega$ the X mode can reach the fundamental and the upper hybrid resonance (trajectory 3). It may be absorbed at the cyclotron frequency but does not experience a cutoff there. Any part of the wave that is not absorbed there will continue through the plasma and may be absorbed at the upper hybrid frequency instead. As launch from the high field side is inconvenient technologically, X mode heating is most commonly employed at the second harmonic.

The relativistic resonance condition.

Electrons and perpendicularly propagating waves may exchange energy when $\omega = n_{harm}\Omega_{ce}/\gamma$ where γ is the relativistic factor and n_{harm} is an integer referred to as the harmonic number. Henceforth we drop the ce subscript, Ω referring to the cyclotron frequency in the absence of any subscript. When propagation is oblique the effect of the Doppler shift on the resonance condition must be considered, so the resonance condition becomes $\omega - k_{||}V_{||} = n_{harm}\Omega/\gamma$ where $\underline{k}$ is the wave vector and $_{||}$ denotes the component of a vector parallel to the magnetic field. When $n_{harm}=1$ the resonance is referred to as the *fundamental resonance* . The presence of velocity dependent terms in both conditions allows a broadening of the resonance, so that absorption does not occur at a single wave frequency. As we shall see later for very high fields strong cyclotron interaction exists for electrons for which there is a small frequency mismatch. Relativistic effects also formally appear in the resonance condition for ion cyclotron resonance heating but because the mass of ions is much greater than that of electrons relativistic

effects play a much smaller role.

The dielectric tensor coefficients near resonances.

The dielectric tensor coefficients $\varepsilon_{i,j}$ are very important properties of a wave travelling through a plasma. They depend on properties of the wave and the plasma, and are frequently used in one of a variety of approximations. Exact calculation of the dielectric tensor coefficients is particularly complicated in a plasma where the ion or electron distribution of velocities is non-Maxwellian. Knowledge of the dielectric tensor coefficients enables calculation of the absorption or emission of waves and determines their dispersion. In general the tensor may be complex and may be split into hermitian and antihermitian parts. The latter largely determine the absorption or emission properties of waves and later in this thesis we will consider calculation of some of these elements for particular non-Maxwellian velocity distributions in order to determine the growth rates of unstable waves in the plasma.

ECRH current drive.

Current drive using rf waves was first proposed by Ohkawa (1970), but the first current drive scheme in which no net momentum needed to be injected into the plasma was suggested by Fisch and Boozer (1980) and confirmed by Start et al (1982) who observed ECRH current drive in the Culham Levitron. Using the Doppler shift electrons with parallel velocities in one direction or the other may be heated preferentially enabling them to collide with ions less often than those electrons travelling in the opposite direction. This asymmetric heating transfers net momentum to the ions and there is a consequent net current. The efficiency of the scheme depends on the typical parallel velocity of the heated electrons - the higher the parallel velocity, the greater the efficiency of the method.
Fisch and Boozer write the Fokker-Planck equation in the high velocity limit and distinguish the energy loss rate $\nu_e \propto 1/V^3$ and the parallel momentum loss rate $\nu_m = (2+Z)\nu_e$, Z being the effective charge of the ions in units of e. From these equations they derive the contribution to current drive efficiency from a single

electron. If $V_{||i}$ and V_i are the initial parallel velocity and speed of a heated electron and $V_{||f}$ and V_f are the final quantities the contribution to the current drive is proportional to $V_f^3 V_{||f} - V_i^3 V_{||i}$ while the absorbed power is proportional to $V_f^2 - V_i^2$. The total current drive efficiency is therefore proportional to

$$\frac{\sum\left(V_f^3 V_{||f} - V_i^3 V_{||i}\right)}{\sum\left(V_f^2 - V_i^2\right)}$$

where the summation is over all heated electrons. A comparison of ECRH current drive and other methods is shown in figure 1.4 (after Wesson). Although other methods of additional heating are able to provide noninductive current drive, ECRH has the advantage of easy localisation of current which enables the spatial temperature profile to be controlled.

More recently current drive has been studied by Cairns et al (1983) who presented relativistic calculations, Dendy and O'Brien (1989) who included a loss term, Fidone et al (1984) who considered combining ECRH and LH current drive, Nevins (1987) who showed that pulsed ECRH could give rise to a continuous current and many others, for example the references in the review of current drive by Fisch (1987).

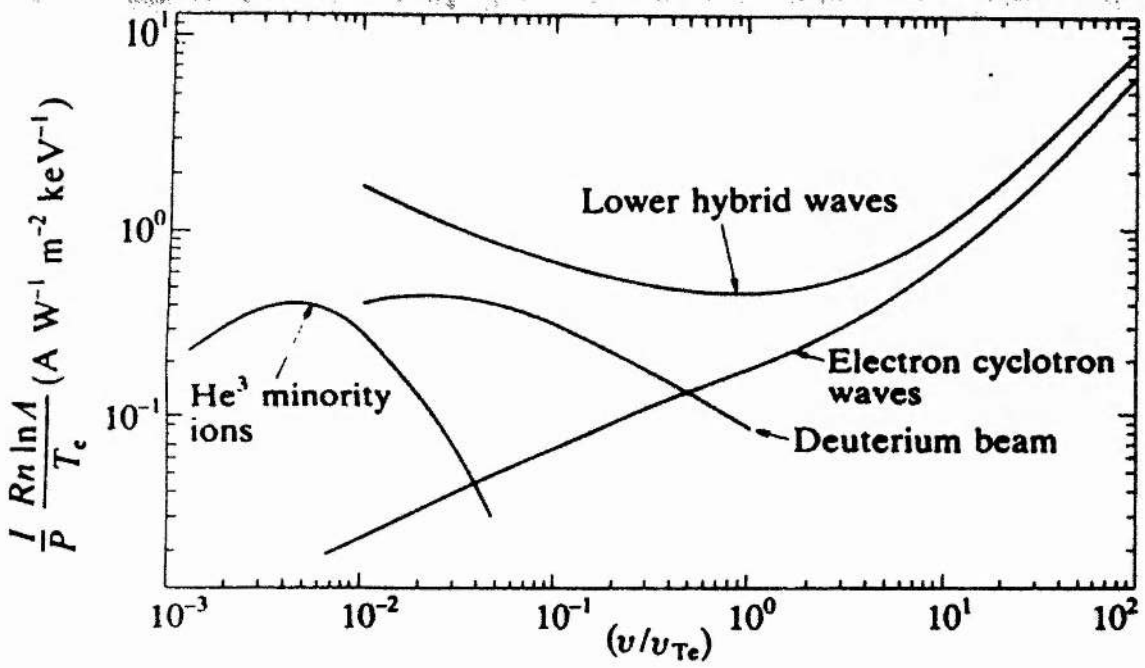

Figure 1.4 (after Wesson)

Comparison of theoretical current drive efficiency for: (i) deuterium beams injected into a D–T plasma; (ii) Landau damping of lower hybrid waves; (iii) electron cyclotron waves; and (iv) He^3 minority ions in a deuterium plasma. The scale gives the ratio of the total current I (A) to the total power injected, P (W), into a tokamak plasma of major radius R (m), density n (10^{20} m^{-3}), and temperature T_e (keV). v is the wave phase velocity, or beam ion velocity, and v_{Te} the electron thermal velocity.

1.5 Sources of Electron Cyclotron Waves.

To date the main source of high power waves capable of attaining the desired frequency to obtain ECRH has been the gyrotron, capable of providing continuous power of about 1 MW at frequencies around 10^{11} -10^{12} Hz. Despite the high power of these devices, a quasilinear theory of the interactions of electrons and the waves has been successful eg O'Brien et al (1986A). We discuss this theory towards the end of Chapter two and confirm that it is applicable to heating using gyrotrons.

Very recently an experiment - the Microwaves in Tokamak eXperiment (MTX), involving a Free Electron Laser (FEL) has been proposed at the Lawrence Livermore Laboratory - Thomassen (1988). A FEL can produce highly tuned, pulsed waves, at the desired frequency and at peak powers of about 1 GW in pulse lengths of 50 ns and repetition rates of 10 kHz. The detailed operation of a FEL is beyond the scope of this thesis, but the underlying idea is that intense waves are produced by a high powered electron beam in a magnetic field. This field, known as a wiggler field, oscillates at the desired pulse repetition rate and forces the electrons to give up energy to the laser beam in very short pulses. The high repetition rate means that a quasi continuous operation can be achieved with reasonably large average power and enormous peak power. We show in Chapter two that the linear theory of O'Brien et al is not applicable to the wave intensities of FELs but that a newer theory, outlined by Nevins et al (1987) and developed in this thesis, may be applicable. We show that whereas gyrotrons heat only resonant electrons, FELs may heat a large number of off-resonant electrons and may substantially distort the original distribution function.

The object of this thesis is to investigate ECRH at powers typical of FELs and to make qualitative predictions about the behaviour we may expect from these experiments. First however we outline linear absorption theory.

1.6 Geometrical Optics and Linear Absorption and Emission Theory.

Provided absorption of the incoming cyclotron wave is weak, and provided the EC wave may be described by geometric optics, one can use Maxwell's equations and the linearised Vlasov equation to derive a spatial absorption coefficient for the heating. The wave is considered to have a complex wave vector $\underline{k} = \underline{k}_r + i\underline{k}_i$, and it is the complex part $\underline{k}_i$ which is responsible for the absorption of the wave. Weak absorption corresponds to $|\underline{k}_i| << |\underline{k}_r|$. We can therefore determine a spatial absorption coefficient defined by (Bornatici et al, 1983A section 2.2.1 and 2.2.2)

$$\frac{d\underline{S}}{d\underline{r}} = -\alpha_{abs}|\underline{S}| \qquad \text{where}$$

$$\underline{S} = \frac{c}{4\pi}\ \underline{E}x\underline{B}^{*} - \frac{\omega}{8\pi}\ \frac{\partial \varepsilon_{h,ij}}{\partial k} E_i^{*} E_j$$

where * is the complex conjugate, $\underline{S}$ being the total power flux density and α_{abs} the absorption coefficient which after a little algebra and use of the WKB approximation (geometrical optics) can be shown to be approximately

$$\alpha_{abs} = \frac{\frac{\omega}{4\pi} E^{*} \varepsilon_a E}{|\underline{S}|} \quad . \qquad (1.3),$$

(equation (16) of Bornatici et al).

Here $\varepsilon_{h,a}$ denote the hermitian and antihermitian parts of the dielectric tensor coefficients respectively. We can find an expression for the dielectric tensor elements using a linearisation of the Vlasov equation.

The details of the calculation of these coefficients are well known - Bornatici et al section 3.1.2.4. Using the expression for these coefficients, also given in Bornatici et al, and using (1.2) and (1.3), we may obtain the absorption coefficient for a given propagation mode. An important assumption here is that perturbations to the distribution function are small, allowing linearisation of the Vlasov equation.

At perpendicular incidence the most strongly absorbed modes are the O mode at the fundamental and the X mode at the second harmonic, for which $\alpha_{abs} \approx \omega_{pe}^2/(c\Omega)$ for low density regimes where the wave frequency is close to the cyclotron frequency or its second harmonic. More exact expressions including relativistic calculations which are particularly important near perpendicular incidence are again given by Bornatici et al. Another important related quantity is the optical depth, which gives a length scale for absorption of the EC wave depending not only on the absorption coefficient but also on the length scale of the gradient in magnetic field.

Linear theory can also be used to determine the emissivity of a plasma, or to determine growth rates of instabilities. In the particular case of thermodynamic equilibrium (the electron velocity distribution is Maxwellian) Kirchoff's law enables the emissivity to be found by first calculating the absorption coefficient. This is important as EC emission (ECE) is a valuable diagnostic tool.

In this thesis we are concerned with modelling nonlinear interactions with EC waves where the assumption that the distribution function suffers small perturbations is invalid, and where the electron distribution is not Maxwellian. This is achieved by examining particle orbits in greater detail and using a Markov approach rather than the linearised Vlasov equation to obtain the new distribution function. However in Chapter five we use linear theory to examine stability to electromagnetic waves other than the incoming ECRH. This is valid because in the initial stages of the growth of an instability the disturbance to the distribution function is small.

1.7 Particle Orbits and Nonlinear Cyclotron Interaction.

The involvement of the relativistic correction factor introduces a far greater degree of nonlinearity into the equations describing interaction of electrons and ECRH than their nonrelativistic counterparts, rendering them insoluble in terms of elementary functions despite their apparent simplicity. This is especially true in the case of high power interactions. Without prohibitively extensive computation progress may be made only by making simplifying assumptions and approximations suitable for specific purposes.

Particle orbits (including nonlinear particle orbits) have been studied for some time - Clemmow and Dougherty (1969), Lieberman and Lichtenberg (1973), Jaeger et al (1972) and Lichtenberg and Lieberman (1983). Suvorov and Tokman (1983), Rognlien (1983) and Taylor et al (1988) have integrated equations of motion averaged on the fast time scale to determine the effect of an rf wave on particles in a background magnetic field.

A scaling law for nonlinear power absorption in MTX was given by Nevins et al (1987) using their theory of nonlinear interaction. In this thesis we will examine this theory critically and use it to estimate growth rates of instabilities in plasmas heated by this means.

1.8 Microinstabilities in Laser Produced ECRH.

A microinstability in a plasma is a state in which the plasma supports a steadily growing wave which does not move the plasma as a whole, and can be contrasted with macroinstabilities which do move the plasma as a whole. There are many different kinds of microinstabilities possible in plasmas generally. Some of the more common varieties found in tokamaks involve interaction between electrons and ions eg the many types of drift instability which give rise to electrostatic or low frequency electromagnetic waves. In this thesis we investigate whether new instabilities may arise as a result of the application of intense ECRH using some approximate models and concluding that ECRH using a FEL may well create instabilities to high frequency electromagnetic waves in MTX, particularly the whistler wave, a wave propagating parallel to the magnetic field with $\omega<\Omega_{ce}$ and with a purely E_- component. We also give numerical examples to show that such instabilities do not occur in distributions typical of those used in experiments with gyrotrons, using numerical distributions produced by the BANDIT code (O'Brien et al, 1986A and 1986B).

1.9 Thesis Outline

In Chapter two we review and extend the work of Taylor on gyroaveraged equations for cyclotron interaction. We discuss the applicability of the **resonant** heating theory of O'Brien et al to gyrotron heating and also to FEL heating. We demonstrate that although it is valid for the former where the heating is dominated by resonant heating, it is not suitable for studying the latter. In Chapter three we review and extend the work of Nevins et al on nonlinear cyclotron interaction, and confirm that it is applicable for FEL heating. We demonstrate that in contrast to gyrotrons, FELs may heat large numbers of **off resonant** particles. In Chapter four we discuss application of the Nevins et al model to the problem of determining the distribution function obtained after a single pulse of FEL ECRH interacts with a given initial distribution, compare the model with purely numerical tests and conclude that although the model has severe limitations it is sufficient for our purposes. In Chapter five we show that gyrotron heating does not give rise to distributions which are likely to be unstable to whistler waves but use the model distribution function obtained in Chapter four to calculate the growth rates of waves which will be unstable in the model distribution. We show that the inverse growth rates are small compared with typical collision times and that the subsequent evolution of the distribution function in time will be dominated by instabilities rather than collisions.

CHAPTER TWO

ELECTRON MOTION IN AN ELECTROMAGNETIC FIELD

A REVIEW OF THE LINEAR THEORY OF ECRH

CHAPTER TWO

Electron Motion in an Electromagnetic Field and the Effect of ECRH on the Electron Distribution Function - A Review of the Linear Theory of O'Brien et al (1986A) and Taylor et al (1988).

2.1 Nonmaxwellian Electron Velocity Distribution Functions

For short time scales the distribution function of a plasma species in equilibrium obeys the Vlasov equation, equation (1.1). In the case of electrons in a strong constant magnetic field the equilibrium distribution function takes the general form $f = f(v_{||},v_{\perp})$ where || and $\perp$ denote components of velocity parallel and perpendicular to the magnetic field, as the distribution is independent of the phase angle $\phi = \tan^{-1}(v_y/v_x)$. Here we denote x and y as representing distances in directions perpendicular to the magnetic field and v_x, v_y as the corresponding velocity components.

Should the distribution function in a collisional plasma be altered instantaneously it will usually relax back to its steady state distribution, through collisions with other particles in the plasma. In a tokamak plasma with an ohmic toroidal electric field and a continuous beam of ECRH we must replace the Vlasov equation with the Fokker-Planck equation

$$\frac{df}{dt} = \left(\frac{\partial f}{\partial t}\right)_E + \left(\frac{\partial f}{\partial t}\right)_C + \left(\frac{\partial f}{\partial t}\right)_W \qquad (2.1)$$

where the subscripts E, C, W refer to the effect on the distribution function of the electric field, the collisions between particles and the wave respectively. It is the presence of the collision operator which tends to bring the distribution back to a Maxwellian.

We shall now consider the situation in which electrons pass through a beam of ECRH and shall ignore for the moment any other contributions to df/dt. If the probability of an electron with velocity $\underline{v}$ receiving a change in velocity $\Delta\underline{v}$ after passing through a beam in time Δt is $P(\underline{v},\Delta\underline{v})$ and the probability that an electron

does pass through the beam is $Q_{pass}(\underline{v},\Delta t)$ $(=Q_{pass}(v_{||},\Delta t))$ the new distribution of electrons is

$$f_{new}(\underline{v},t+\Delta t)= \int Q_{pass}(\underline{v}-\Delta\underline{v},\Delta t)\, P(\underline{v}-\Delta\underline{v},\Delta\underline{v})\, f_{old}(\underline{v}-\Delta\underline{v},t)\, d^3\Delta\underline{v}$$
$$+ \{1-Q_{pass}(\underline{v})\}\, f_{old}(\underline{v},t)$$

where the integration is over all allowable values of $\Delta\underline{v},\Delta t$ being the time during which the change in velocity occurs. NB we use the notation $f=f(\underline{v},t)$ only when the time dependence of the function is of significance and suppress the time dependence otherwise.

The phase angle is related to another important quantity, ψ the phase difference between the electric field and the particle's rotation around its guiding centre, by $\phi=\psi+\omega t$. As the change in $v_{||}$ can always be neglected for ECRH in an inhomogeneous magnetic field, and as f is independent of ϕ, the equation for the new distribution may be simplified to

$$f_{new}(v_{||},v_{\perp},t+\Delta t) = \int Q_{pass}(v_{||},\Delta t)P(v_{||},v_{\perp}-\Delta v_{\perp},\Delta v_{\perp})f_{old}(v_{||},v_{\perp}-\Delta v_{\perp},t)d\Delta v_{\perp}$$
$$+ (1- Q_{pass}(v_{||},\Delta t))f_{old}(v_{||},v_{\perp},t) \qquad (2.2).$$

We can now construct a form for $(\partial f/\partial t)_W$ viz

$$\left(\frac{\partial f}{\partial t}\right)_W = \frac{1}{\Delta t}\left(\int Q_{pass}(\underline{v}-\Delta\underline{v},\Delta t)\, P(\underline{v}-\Delta\underline{v},\Delta\underline{v})\{f(\underline{v}-\Delta\underline{v})-f(\underline{v})\}\, d\Delta\underline{v} \;-\; Q_{pass}(\underline{v},\Delta t)f(\underline{v})\right)$$

which is similar to (3.44) of Taylor.

If the applied ECRH is continuous in operation the latter equation can be balanced against the other terms in (2.1) to obtain a steady state distribution. Alternatively if the ECRH is of finite duration and Δt is short compared to the time scales involved in the other terms of (2.1) we can obtain the distribution immediately after the ECRH stops using (2.2) and then calculate the evolution in time of the distribution afterwards using (2.1) but with $(\partial f/\partial t)_W=0$.

2.2 The Lorentz Equation and Single Particle Motion.

The equations of motion for an electron in a magnetic field and interacting with an electromagnetic wave are

$$\frac{d(mc\underline{p})}{dt} = -e(\underline{E}_1(\underline{x},t) + \underline{v}x\underline{B}_1(\underline{x},t) + \underline{v}x\underline{B}_0) \qquad (2.3a)$$

where $\underline{E}_1(\underline{x},t)$ and $\underline{B}_1(\underline{x},t)$ are the electric and magnetic fields due to the wave, $\underline{B}_0$ is the background magnetic field, $\underline{v}$ is the velocity and $\underline{p}$ is the relativistic momentum normalised to mc. The wave fields vary sinusoidally in space and time but we may regard B_0 as constant at present. Equation (2.3a) has to be combined with the equation for the particle position

$$\frac{dx}{dt} = \underline{v} \qquad (2.3b)$$

giving a set of six ordinary differential equations. In the work of Taylor (1987) and Taylor et al (1988) equations (2.3a) and (2.3b) were simplified for wave frequencies close to the cyclotron frequency using the gyroaveraging approximation and the six equations were reduced to four. Taylor et al used a gyroaveraged Lagrangian, first developed by Littlejohn (1983) to obtain equations of motion first order in the wave amplitude $\underline{E}_1$ in special conditions. They considered cases where the wave propagated perpendicular to the background field with a particular spatial magnetic field variation and where initially $\Omega/\gamma = \omega$. They assumed a top hat profile of form

$$E_1(\underline{x},t) = \hat{\underline{z}}E_{||}(z)\ e^{i(k_\perp x + k_{||} z - \omega t)}$$

$$\text{where } E_{||}(z) = \begin{cases} E_{||peak} \text{ for } -w/2 < z < w/2 \\ 0 \text{ otherwise} \end{cases}$$

$\underline{k}$ is the wave vector, w is the length of the beam and z is the distance along the magnetic field line. In practice wave output from gyrotrons or FELs does not have a tophat profile, but can be quite complicated. More realistically the beam can be assumed to be spatially Gaussian in the two directions perpendicular to the direction of the beam:

$$E_{||}(z) = E_{||peak}\, e^{-\left(\frac{z}{L_z}\right)^2 - \left(\frac{y}{L_y}\right)^2}$$

where we have chosen x as the distance along the direction of the beam. Here L_z and L_y are the Gaussian widths in the horizontal and vertical directions respectively. It is not necessarily the case that $L_y = L_z$ though typically $L_y \approx L_z \approx 5$ cm. Henceforth we drop the -peak part of the suffix and refer only to $E_{||}$ unless the distinction between $E_{||}(z)$ and $E_{||peak}$ is unclear. The form of the spatial profile turns out to be important as we demonstrate later in this chapter and again in Chapter four. In their final equations Taylor et al used the small Larmor radius approximation $k_\perp U_\perp/\Omega << 1$ where $U_\perp = \gamma V_\perp$. Finally they neglected the self consistent effects on the wave amplitude, a common approximation (Nevins et al, 1987) which is retained in this work. The details of the derivation of their approximate equations are straightforward if lengthy. Similar but more general calculations are outlined in Appendix one.

2.3 Relativistic Detuning.

One of the key aspects of the resonant heating of electrons with large fields is that the resonance condition is dependent on the velocity of the electron, possibly through the Doppler shift of the incoming wave if heating is not perpendicular to the background magnetic field, and always through the relativistic factor. As the electron is heated, so the relativistic factor changes. In the laboratory frame the mass of the electron increases which decreases the cyclotron frequency and detunes the electron from resonance. If the detuning effects are particularly strong and the wave intensity is great enough the phase of the electron with respect to the wave, ψ, and the velocity may perform oscillations in phase space as is discussed in greater detail in Chapter three. When the phase of the wave changes in this way approximations such as $\psi=\psi_0$ or $\psi=\psi_0+\text{const}*t$ where ψ_0 is the initial phase are no longer valid and the equations no longer have approximate analytic solutions.

In this chapter we will consider analytic theory which is valid only when ψ changes relatively little, and give examples of cases where the theory is invalid. In contrast in Chapter three we consider the opposite case where ψ changes rapidly and the electron oscillates many times around a fixed point in phase space while traversing the beam.

2.4 The SPEECH Codes of Taylor et al.

The SPEECH (Single Particle Experiments in Electron Cyclotron Heating) codes were written by Dr A W Taylor as a part of his PhD and by kind permission we have been able to use and adapt them. The codes solved the differential equations of motion, either exact or averaged, for particles at an initial position in $(U_\perp, U_\parallel)$ space where $U_\parallel$ is defined by $U_\parallel = \gamma V_\parallel$ but with random initial phases with respect to the wave, the integration proceeding in time until the particle has finished crossing the beam when the final velocities are recorded. Assuming the initial phase of the electron is random there is a probability distribution function for the change in velocity, and the numerical form was compared with theoretical approximations. The integration was performed using the Runga-Kutta technique and the codes used the NAG library routine D02BBF.

The codes assumed that exact resonance occurred somewhere in the beam and assumed a particular form for the magnetic field strength along the guiding centre of the electron's path. Although the codes could solve the equations of motion for either the O or the X mode only perpendicular propagation was considered. The averaged equations solved by Taylor were:

$$\frac{dU_\parallel}{dt} = -\frac{U_\perp^2 \Omega_0 (\dot{\psi}+\omega)}{2\Omega^2 G} + \frac{eE_{eff} U_\perp \Omega_0 \sin(\psi)}{2m\Omega^2 G} \qquad (2.4a)$$

$$\frac{dU_\perp}{dt} = \frac{U_\perp V_\parallel \Omega_0}{2\Omega G} - \frac{eE_{eff}\cos(\psi)}{2m} \qquad (2.4b)$$

$$\frac{d\psi}{dt} = \frac{\Omega}{\gamma} - \omega + \frac{eE_{eff}\sin(\psi)}{2mU_\perp} \qquad (2.4c)$$

$$\frac{dz}{dt} = V_\parallel \qquad (2.4d).$$

We have for convenience introduced

$$E_{eff} = \left| E_{\|} \frac{k_{\perp} V_{\|}}{\omega} + E_{-} \left(1 - \frac{k_{\|} V_{\|}}{\omega} \right) \right|$$

the effective electric field. The angle ψ is a slowly varying quantity if the wave is near the electron cyclotron frequency. For consistency with Taylor we define G, a quantity denoted by R in Taylor et al, by assuming that the magnetic field gradient along the particle's path can be approximated by a linear function, so that the cyclotron frequency is $\Omega = \Omega_0(1+z/G)$, z being the distance along the particle's path. This latter equation for $\Omega(z)$ introduces an extra term in the equations of motion (included in Taylor's work) through the time derivative of Ω as $d\Omega/dt = V_{\|} d\Omega/dz = V_{\|}\Omega/G$. Finally the equations above are valid only if E_{eff} is constant; the equations otherwise involve expressions for the rate of change of the electric field amplitude.

Taylor's form for the magnetic field along the guiding centre of the particle's orbit depends on a number of parameters including the safety factor

$$q = \frac{1}{2\pi R} \oint \frac{B_T}{B_p} ds$$

on the flux surface, where the line integral is over a poloidal circuit following the direction of the magnetic field lines until one complete toroidal rotation has been made, the major radius is R and B_T and B_p are the toroidal and poloidal fields. Physically it represents the number of times an electron following a magnetic field line rotates about the minor axis while it makes one complete orbit of the major axis. Figure (2.1) shows the motion of an electron following a field line. This quantity is important because the curvature and gradient of the magnetic field in a tokamak geometry give rise to drifts which separate the ions and electrons (Cairns, 1985). In particular it must be greater than one everywhere in the tokamak for MHD stability.

Figure 2.1

Cross-section of Tokamak (not to scale)

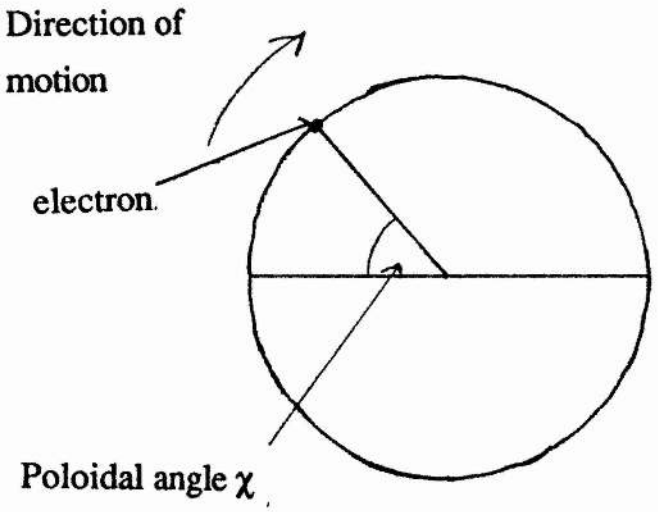

Plan View of Tokamak

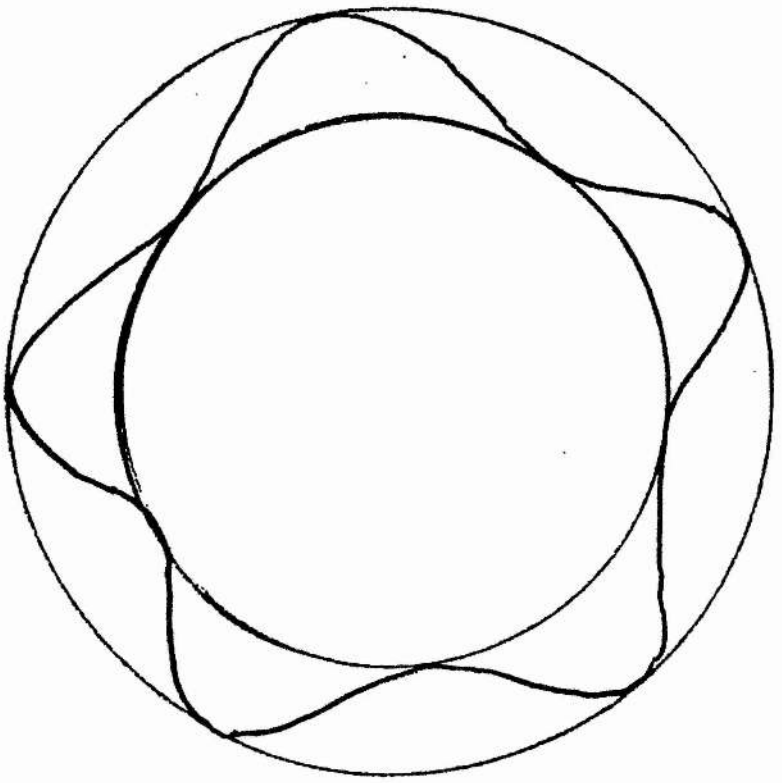

Path of electron
on flux surface
where q ≈ 5

We have $B = B_{axis}(1+x/R)$, $x = \rho\cos(\chi)$ and $z/2\pi R = q(\chi-\chi_0)$, where ρ is the radius of the flux surface, χ is the poloidal angle of the electron as shown in figure (2.1), x is the distance into the tokamak from the minor axis, B(x) is the strength of the magnetic field (mainly in the toroidal direction), B_{axis} is the magnetic field on the minor axis and χ_0 is the poloidal angle at the point z = 0. One can therefore obtain B in terms of z by

$$B = B_{axis}\left\{1 + \frac{\rho}{R}\cos\left(\frac{z}{2\pi Rq} + \chi_0\right)\right\}.$$

For small perturbations about z = 0 we can write

$$\cos\left(\frac{z}{2\pi Rq} + \chi_0\right) = \cos(\chi_0) - \sin(\chi_0)\frac{z}{2\pi Rq} - (1/2)\cos(\chi_0)\left(\frac{z}{2\pi Rq}\right)^2$$

so if

$$\left|\sin(\chi_0)\right| >> \frac{w}{8\pi Rq}\left|\cos(\chi_0)\right|$$

one can write $B \approx B_0(1+z/G)$ for a constant G where

$B_o=B_{axis}(1+\rho\cos(\chi_0)/R)$. When

$$\left|\sin(\chi_0)\right| \leq \frac{w}{8\pi Rq}\left|\cos(\chi_0)\right|$$

this approximation is invalid and it is as well to employ the more accurate expression for B as in O'Brien et al (1986A).

In his thesis Taylor attempted to construct theory to provide an analytic model to account for the change in B through the beam. In this thesis we ignore the change in B with position through the beam for simplicity, noting that the change is minimal if the heating is strongly localised to the median

plane.

We should explain here why ignoring the variation in B throughout the beam makes our work so much easier. Traditionally the magnetic moment μ_{mag} is defined as

$$\mu_{mag} = \frac{V_\perp^2}{2B} \quad \text{or} \quad \mu_{mag} = \frac{U_\perp^2}{2B}$$

depending on whether we are using relativistic or nonrelativistic physics. It can be shown (Cairns, 1985) that this is an adiabatic invariant in the absence of ECRH for an electron which does not suffer collisions. Together with the condition that the energy is constant ie

$$\frac{V_\perp^2 + V_\parallel^2}{2} = \text{constant or } \gamma = \text{constant}$$

we see that $V_\parallel$ may change as B changes. It is this change in $V_\parallel$ which may significantly complicate the physics. It is possible that $V_\parallel$ may become zero and change sign, which leads to the presence of *magnetically trapped* particles. These electrons do not pass around the tokamak completely. Throughout this thesis we shall ignore changes in B along the path of an electron almost completely, and thus the conserved quantity is simply $V_\perp{}^2$; we shall express the equations in terms of

$$\mu = \frac{V_\perp^2}{2c^2} \quad \text{or} \quad \mu = \frac{U_\perp^2}{2c^2}$$

as appropriate. Furthermore references to trapped particles later in this thesis will be to electrons trapped in phase space (about which more will be mentioned in Chapter three) and *not* to magnetically trapped electrons. In the next section we contrast equations (2.4) with more general and accurate averaged equations derived using the same basic method.

2.5 Extensions to the Work of Taylor.

We have very substantially adapted the SPEECH codes used by Taylor. Rederiving the averaged equations and retaining his form for the magnetic field along the guiding centre of an electron's path, but without making any of the other approximations made by Taylor, we arrive at revised equations. Equation (2.4d) naturally remains the same but the remaining equations become (see Appendix one for an outline of the derivation and the meaning of the symbols)

$$\frac{du_\perp}{dt} = \frac{\Omega_0 u_\perp V_\parallel}{2G\Omega} + \frac{e}{m\omega}\dot{E}_- \frac{J_1}{a}\sin\psi + \frac{e}{m\omega}E_- \frac{J_1}{a}\omega' \cos\psi + \frac{e}{2m}E_- \frac{\Omega_0 V_\parallel}{\Omega^2 G}J_0\sin\psi - \frac{e}{2m\omega}\frac{E_\parallel V_\parallel k_\perp J_1}{a}\cos\psi.$$

(2.5a)

$$\frac{du_\parallel}{dt} = -\frac{u_\perp^2(\omega' + \dot{\psi})\Omega_0}{2\Omega^2 G} - \frac{e}{2m\omega}E_\parallel \frac{aV_\parallel}{\Omega}\frac{\Omega_0}{G}J_0\sin\psi + \frac{e}{2m\omega}\frac{\dot{E}_-}{V_\parallel}\frac{d}{dt}\left(\frac{u_\perp}{\Omega}\right)J_0\cos\psi - \frac{e}{m\omega}\frac{\dot{E}_-}{V_\parallel}\frac{(\omega' + \dot{\psi})}{k_\perp}J_1\sin\psi$$

$$-\frac{k_\parallel e}{2m\omega}E_-\frac{d}{dt}\left(\frac{u_\perp}{\Omega}\right)J_0\sin\psi + \frac{e}{2m\omega}E_-\frac{\dot{u}_\perp}{\Omega^2}\frac{\Omega_0}{G}J_0\cos\psi - \frac{e}{m\omega}E_-\frac{d}{dt}\left(\frac{u_\perp}{\Omega}\right)\frac{a}{\Omega}\frac{\Omega_0}{G}J_1\cos\psi - \frac{k_\parallel e}{m\omega}E_-\frac{(\omega' + \dot{\psi})}{k_\perp}J_1\cos\psi$$

$$-\frac{e}{2m\omega}E_-(\omega' + \dot{\psi})\frac{aV_\parallel}{\Omega^2}\frac{\Omega_0}{G}\sin\psi - \frac{k_\parallel e E_\parallel V_\parallel J_1\cos\psi}{m\omega}$$

(2.5b)

$$\frac{d\psi}{dt} = \omega' + \frac{\dfrac{e\Omega E_- J_0 \cos\psi}{2m\omega u_\perp} + \dfrac{eE_-\Omega_0 V_{||} J_0 \cos\psi}{2m\omega\Omega u_\perp G} + \dfrac{eE_-}{2m\omega}\dfrac{d}{dt}\left(\dfrac{u_\perp}{\Omega}\right)\dfrac{k_\perp}{u_\perp} J_1 \cos\psi + \dfrac{eE_{||} V_{||} J_0 k_\perp \sin\psi}{2m\omega u_\perp}}{\left(1 - \dfrac{eE_- J_0 \sin\psi}{2m\omega\ U_\perp}\right)}$$

where $\omega' = \omega - k_{||}V_{||}$ (2.5c).

Equations (2.5a) to (2.5c) reduce to (2.4a) - (2.4c) on making a small Larmor radius expansion, neglecting the rate of change of the magnitude of the electric field along the guiding path of the electron and neglecting second order terms.

One of the most important extensions is the inclusion of terms describing oblique incidence of the beam onto the plasma, ie the inclusion of terms with $k_{||}\neq 0$. Making the small Larmor radius expansion and neglecting terms involving magnetic field gradients, the rate of change of the electric field or second order terms, we have

$$\frac{du_\perp}{dt} = -\frac{e}{2m} E_{eff} \cos\psi \qquad (2.5d)$$

and

$$\frac{du_{||}}{dt} = -\frac{k_{||} e u_\perp E_{eff}}{2m} \cos\psi \qquad (2.5e)$$

$$\frac{d\psi}{dt} = \frac{\Omega}{\gamma} - \omega' + \frac{e E_{eff} \sin\psi}{2mU_\perp} \qquad (2.5f)$$

Inspection of equations (2.5a) to (2.5c) reveals the following generalisations:

(1) Extension to non-perpendicular ECRH.

(2) Inclusion of the Bessel functions J_0 and J_1 so the small argument expansion of those functions is no longer needed. We henceforth refer to the approximation that $J_0 \approx 1$ and $J_1 \approx a/2$ as the small Larmor radius approximation, as it is equivalent to the condition $a_L << \lambda$ where λ is the

wavelength of the e/m wave and $a_L=U_\perp/\Omega$ is the Larmor radius.

(3) Inclusion of second order effects ignored in Taylor's work. These effects arise because the equations of motion for derivatives with respect to time of $(U_\perp, U_{||}, \psi)$ depend on terms of the form

$$\frac{E_{eff}}{B_0 c}\frac{dU_\perp}{dt}.$$

The time derivative $dU_\perp/dt$ is to a first approximation and for small electric fields proportional to the electric field and so the additional terms are approximately second order in the field amplitude. These second order terms are small compared with the first order terms unless the electric field is of order $10^7 Vm^{-1}$.

The following changes have also been made to the code.

(4) The reduction of the order of the equations from four to three by using a theoretically exact value for the relation between $U_\perp$ and $U_{||}$ provided the magnetic inhomogeneity is negligible (see equation (2.8a) later in the chapter) so that we no longer need to solve for $dU_{||}/dt$, greatly enhancing the speed of the code.

(5) Optional inclusion of a Gaussian (or even triangular) profile. In this case new terms may enter into the gyroaveraged equations viz $dE/dt = V_{||}\, dE/dz$, and these are included above.

(6) Allowance for initial frequency mismatches.

(7) Optionally the possibility of comparison of the numerical form of the probability distribution with theoretical approximations other than the ones considered by Taylor.

(8) Optionally the reversal of the equations of motion so that initial velocities may be found in terms of final ones.

(9) Optionally the use of routine D02BGF instead of D02BBF. The former integrates the equations until a specified component of the dependent variable has reached a specified value and is useful in cases where the parallel

velocity changes substantially (see section 2.10).

(10) Optionally the output of solutions to the equations of motion at intermediate points along the electron's path (available only when a single initial phase is chosen). This allows a graph of the trajectory of an electron in $(U_{\perp},\psi)$ space to be plotted.

Relationship of the accuracy to the input tolerance.

The routines D02BBF and D02BGF have as an input parameter TOL which is supposed to be proportional to the output error for all values of TOL in the case of the former and for a restricted range for the latter routine (NAG manual mark 10 1983). The NAG documentation does not guarantee any particular relationship between the two and recommends calling the routine with different values of TOL to establish the accuracy. An alternative approach is to integrate the equations in the forward direction and then to reverse the process. The initial and final answers should be identical. We have done this for test cases in table 2.1. In each case we start with $U_{\perp} = U_{||} = 10^{7}ms^{-1}$, integrate forward to obtain the values in the second and third columns, then integrate in the reverse direction to obtain the values in the last two columns. The extent to which the figures in these last two columns differ from one is a measure of the accuracy of the calculation. Although the accuracy is acceptable using the tolerances 10^{-6} and 10^{-7} the maximum possible relative error can be much larger than the input parameter. For example the fourth particle in table 2.1 has a .2% error in the value of $U_{\perp}$ when integrated forwards and then integrated backwards again to obtain the original $U_{\perp}$ even though the value of TOL is 10^{-6}. It is therefore essential to use small values of TOL to ensure reliability of the final result. This is an important consideration in numerical experiments where the CPU requirements are large as there must inevitably be some compromise in accuracy in return for CPU times of acceptable length. Should the tolerance be too large the results may become unphysical. Throughout the work presented in this thesis TOL has been chosen carefully to be sufficiently small to ensure that the results obtained are meaningful.

Table 2.1

Data:	
Profile	Gaussian
Width	0.025m
Uperp initial	$10^7 ms^{-1}$
Upar initial	$10^7 ms^{-1}$
Psi initial	0, $2\pi/5$, $4\pi/5$, $6\pi/5$ and $8\pi/5$
Mode	O mode
Direction	Perpendicular
Frequency mismatch	0
Wave frequency	$1.75*10^{11}$ Hz
Background field B_0	1T
Electric field	$5*10^5$ Vm^{-1}

The runs represent tolerances of 10^{-6} and 10^{-7} respectively. All velocities in the table are in units of the common initial velocity, $10^7 ms^{-1}$.

Phase	Final $U_\perp$	Final $U_\parallel$	Initial $U_\perp$	Initial $U_\parallel$
I1	I 3.65455	I 1.00021	I 1.00006	I 1.00000 I
I2	I 1.01985	I 1.00000	I 1.00000	I 1.00000 I
I3	I 1.53499	I 1.00050	I 1.00073	I 1.00000 I
I4	I 1.59164	I 1.00064	I 0.998863	I 1.00000 I
I5	I 0.997609	I 1.00000	I 1.00002	I 0.99999 I
Phase	Final $U_\perp$	Final $U_\parallel$	Initial $U_\perp$	Initial $U_\parallel$
I1	I 3.65455	I 1.00021	I 1.00001	I 1.00000 I
I2	I 1.01985	I 1.00000	I 1.00000	I 1.00000 I
I3	I 1.53498	I 1.00050	I 1.00001	I 1.00000 I
I4	I 1.59164	I 1.00064	I 0.999984	I 1.00000 I
I5	I 0.99761	I 1.00000	I 1.00000	I 1.00000 I

2.6 Comparison of the Exact and Gyroaveraged Equations.

In his thesis Taylor gives a comparison of results obtained by integrating the equations of motion for a single particle through the width of the beam in two ways; firstly using the Lorentz equation (2.3a) together with (2.3b) and secondly using his averaged equations (2.4) presenting results for a variety of electric field strengths and the parameter G. According to his table (1) good agreement is obtained for his chosen parameters until the wave amplitude reaches 10^7 Vm^{-1}. This field amplitude is very large indeed and is typical of fields produced by FELs. In table (2.2) we demonstrate that relatively good agreement is possible between the second order averaged equations using Bessel functions (2.5) and the exact equations (2.3) even at this high value of the electric field. Given the enormous saving in CPU time obtained by using the averaged equations rather than the exact ones, we shall assume the former to be accurate enough for our purposes. By also making a comparison with results using equations (2.5), we show that the main source of error in the two approaches lies in the neglect of second order effects and/or the small Larmor radius approximation. In Chapter four we will use the improved equations (2.5) to provide contour plots of possible electron distribution functions that may arise in MTX and so it is essential that the equations used are reliable even in this high power regime. As can be seen agreement is good only when the magnetic field gradient is not too strong. When the magnetic field changes rapidly in space in the plane of the cyclotron motion, the motion is distorted and the frequency of rotation is altered by the gradient, hence the gyroaverage approximation breaks down. The study of the effects of strong magnetic inhomogeneity is gyrokinetic theory and can be quite complicated. In this thesis we largely ignore cases of strong inhomogeneity as it introduces too many extra parameters and complications into a subject area already complicated enough.

Table 2.2 Comparison of Exact and Approximate Equations

Data:

Profile	Tophat
Beam width	0.1m
Uperp initial	$10^7 ms^{-1}$
Upar initial	$10^7 ms^{-1}$
Psi initial	0
Mode	O mode
Direction	Perpendicular
Frequency mismatch	0
Wave frequency	$1.75*10^{11}$ Hz
Background field B_0	1T
Electric field	10^7 Vm^{-1}

G(m)	Uperp final			
	(1)	(2)	(3)	(4)
Infinity	3.55 E7	2.29 E7	3.27 E7	3.44 E7
10^3 m	3.43 E7	2.16 E7	3.34 E7	3.41 E7
10^2 m	2.75 E7	1.37 E7	3.97 E7	3.22 E7

(1) Exact equations of motion (2.3) from table (1) of Taylor.

(2) First order averaged equations of motion (2.4) from table (1) of Taylor.

(3) Second order equations of motion (2.5) with small Larmor radius approximation.

(4) Second order equations of motion (2.5) without small Larmor radius approximation.

2.7 Comparison of Numerical Results and an Analytic Expression for the Change in Velocity after a transit through a beam of ECRH.

In order to determine the new electron distribution function obtained when ECRH is applied to a plasma, one needs to know the change in energy of an electron as it passes through a single beam of ECRH. Without an analytic model we must resort to finding the distribution on a grid and solving the equations of motion at the grid points numerically. This is impractical using the exact equations of motion within the confines of present computing facilities and even use of the averaged equations requires a large amount of computing resources. Calculations along similar lines have been performed by Nevins et al (1987) based on work by Rognlien (1983). The former paper will be discussed in depth later. However in this case the objective was to determine the energy absorption of a beam incident on a Maxwellian plasma, and no numerical plots of the final distributions were produced. However in this thesis, a small number of final distributions are calculated, and displayed in the form of contour plots in Chapter four.

One object of the study of single particle motion in an ECRH beam profile therefore is to try to provide an analytic formula to give the increase in velocity space components after a single pass. O'Brien et al developed a nonrelativistic theory of heating and included the effects of magnetic field inhomogeneity which enabled them to derive a simplified diffusion coefficient for use in a Fokker-Planck equation in the spirit of Fielding (1980) and Cairns and Lashmore-Davies (1986) by finding the change in perpendicular energy

$$\Delta(V_\perp^2) = -V_\perp K \cos(\psi_0) + K^2/4 \qquad (2.6a)$$

and

$$< \Delta(\mu c^2) > = K^2/8 \qquad (2.6b)$$

where

$$K = \frac{e}{m}\left| \int E_{eff}(z) e^{it\left(\omega - k_{\|}V_{\|} - \Omega\right)}\, dt \right|$$

(2.6c)

and where ψ_0 is the initial phase of the particle with respect to the wave, the integral is over the time spent in the beam, and E_{eff} and Ω depend on time through z.

The explicit value of K therefore depends on the profile and the magnetic field profile as seen by the electron, as well as the initial frequency mismatch. For the simplest possible case where there is exact resonance, no magnetic field inhomogeneity and a tophat profile, $K=\frac{eE_{\|}k_{\perp}w}{m\omega}$ for the O mode and $\frac{eE_{-}w\left(1-\frac{k_{\|}V_{\|}}{\omega}\right)}{m\omega V_{\|}}$ for the X mode, where w is the width of the beam, and where we have made the small Larmor radius approximation. More complicated expressions arise in practice and O'Brien et al give an explicit expression for the case where the beam profile is Gaussian and toroidal effects are included.

A relativistic analogue of this analytic form with similar form has been found by Taylor (1987) and Taylor et al (1988):

$$\Delta(U_{\perp}^2) = -U_{\perp}K\cos(\psi_0) + K^2/4$$

(2.7a)

where

$$K = \frac{e}{m}\left| \int E_{eff}(z) e^{it\left(\omega - k_{\|}V_{\|} - \Omega/\gamma\right)}\, dt \right|$$

(2.7b)

but with the condition

$$K^2/4 << U_{\perp}K$$

(2.7c).

In (2.7a) we have included a minus sign not included in the equation in

Taylor et al so that the angle ψ_0 refers to the angle the electric field initially makes with the gyroangle of the electron. The underlying assumption in the derivation of (2.7a) is that the phase remains unchanged throughout heating or changes only linearly according to $\psi=\psi_0+\Delta\omega t$ where $\Delta\omega=\Omega/\gamma$ is the initial frequency mismatch. Neglecting relativistic effects (2.4c) simply reduces to $d\psi/dt = \Delta\omega$ for small electric fields. However with the relativistic effects included, the phase of the particle becomes detuned as the particle is heated or cooled. This reduces the amount of heating and introduces a much greater degree of nonlinearity. The result was originally derived from the Lorentz equation but can be recovered from the averaged equations. For simplicity we consider the X mode at the perpendicular with a tophat profile.

Taking the limit G->∞ (ie ignoring magnetic field gradients) of the equations (2.4) and casting them in a dimensionless form we obtain

$$\frac{dA}{d\tau} = -\varepsilon\cos(\psi) \text{ and}$$

$$\frac{d\psi}{d\tau} = \frac{1}{\gamma} - \frac{1}{\beta} + \frac{\varepsilon\sin(\psi)}{A}$$

where $A=\frac{U_\perp}{U_{\perp 0}}$, $\beta=\frac{n_{harm}\Omega}{\omega}$, n_{harm} being the harmonic number, 1 in this case,

$\varepsilon=\frac{E_-}{B_0 U_{\perp 0}}=\frac{2K}{\tau U_{\perp 0}}$, and $\tau=t\Omega$. We proceed by calculating corrections to the original values of A and ψ iteratively including successive orders of the small parameter $\varepsilon\tau$ each time. Let A_0 and ψ_0 be the values of A and ψ at $\tau = 0$. We denote by ψ_1 the first correction calculated by using the value $A = A_0$ (=1) etc. We obtain

$$A_1 = 1-\varepsilon\tau\cos(\psi_0),$$

$$\psi_1 = \psi_0 + \varepsilon\tau\sin(\psi_0), \qquad \text{and}$$

$$A_2=1-\varepsilon\tau\cos(\psi_0)+\frac{(\varepsilon\tau)^2\sin^2(\psi_0)}{2}$$

where the last equation has been obtained using a Taylor expansion of $\cos(\psi)$. Neglecting terms in $\varepsilon\tau$ higher than $(\varepsilon\tau)^2$ we recover (2.7a). It is clear that the condition $\varepsilon\tau=2K/U_{\perp 0}<<1$ is necessary from examination of next stage of the iteration which involves the term $(1-\varepsilon\tau\cos\psi_0)^{-1}$. Essentially this condition is that the absorbed energy is much less than the thermal energy of the electrons.

To understand why this is important we must understand the work of O'Brien et al, and also earlier work on ECRH by Fielding (1980) and Cairns and Lashmore-Davies (1986). They showed that the heating due to ECRH could be understood as a diffusive process and produced a simplified diffusion coefficient, essentially using equation (2.6b) and the approximation

$$D_o=\frac{\Delta U_\perp^2}{\Delta t},$$

D_o being the diffusion coefficient.

One of the main aspects of Taylor's work was to compare this theory and results of the numerical solution of the gyroaveraged equations. Although he demonstrated that the analytic form certainly did break down when the condition for its applicability was invalid, he failed to provide an alternative better model. In Chapter three we shall discuss another model, proposed by Nevins et al. However the main conclusion of his work was that ECRH is no longer a diffusive process when the intensity of heating becomes sufficiently large, a conclusion we reinforce in this thesis.

2.8 Higher power cyclotron interaction.

Taylor (1987) demonstrated numerically that for perpendicularly propagating waves his theory was invalid for large electric fields. We confirm this with figures (2.2a) and (2.2b) which show examples of the probability density $P(\Delta\mu)$ of the gain in energy of an electron which passes through a beam. In figure (2.2a) we compare the theoretical form (the dotted line) with the numerical form (the solid line), where the electric field is high, demonstrating that the linear theory severely overestimates the heating of electrons. Figure (2.2b) shows an example of an extremely complicated probability density function obtained for a resonant electron at an even higher field. The linear theory overestimates the heating so much that it cannot be compared with the numerical form on the same graph. The function $P(\Delta\mu)$ in figure (2.2b) is such a complicated function of $\Delta\mu$ that even in this thesis no accurate analytic form is found for cases such as this.

For a typical particle with $U_{\perp} \approx 10^7 ms^{-1}$ and $w \approx 0.1m$ (2.7c) is valid in the case of the O mode if

$$E_{||} << 5*10^5 Vm^{-1}$$

and in the case of the X mode for a particle with $V_{||} \approx 10^7 ms^{-1}$,

$$E_- << 1.5*10^3 Vm^{-1}.$$

Both of these conditions are typically satisfied for gyrotrons, but the former is not satisfied for the figures (2.2a) or (2.2b) which explains why the theoretical and numerical forms do not agree.

When the initial frequency mismatch is not nearly zero, ironically, an approximate picture of the heating can be given (see later chapters). Fortunately it is the case that the heating of an individual electron can increase with the frequency mismatch up to a critical value, and that in general the overall heating effect can be dominated by nonresonant rather than resonant electrons.

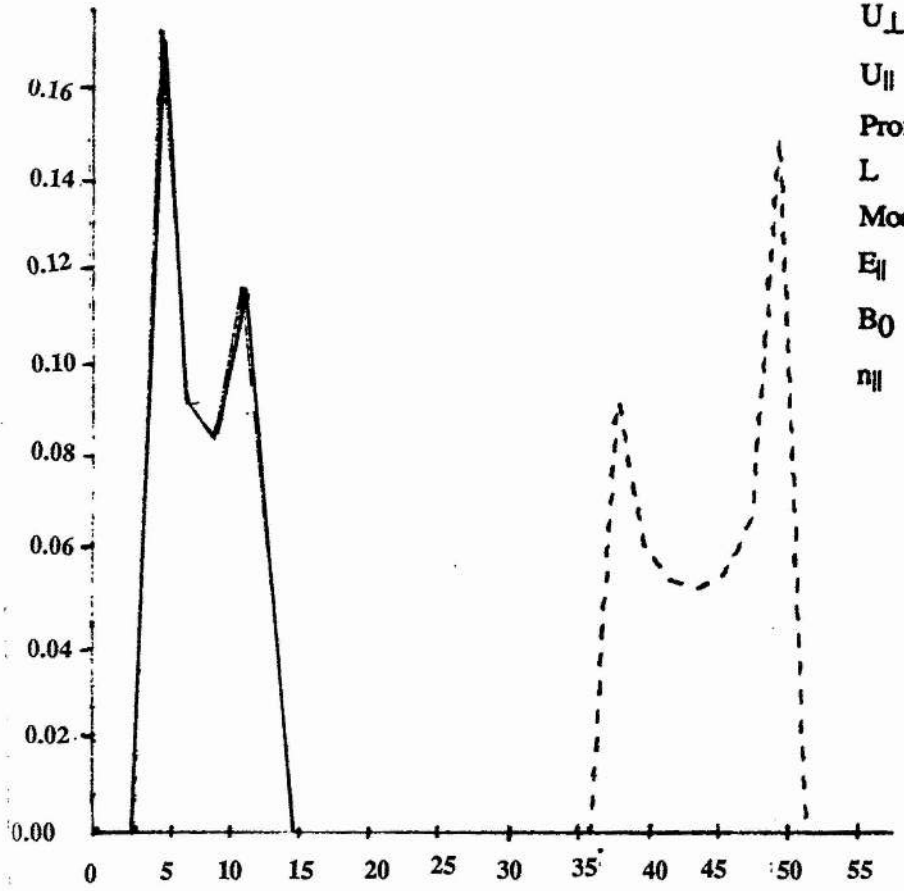

Figure 2.2a

$U_\perp$	$= 10^7$ ms^{-1}	Initial perpendicular velocity
$U_\parallel$	$= 10^7$ ms^{-1}	Initial parallel velocity
Profile		Gaussian
L	= 0.025 m	Gaussian width
Mode		O mode
$E_\parallel$	$= 5*10^6$ Vm^{-1}	Peak electric field
B_0	=1.0 T	Magnetic field.
$n_\parallel$	= 0	Parallel refractive index

Dotted line - theoretical form for the probability

Solid line - numerical form for the probability

Vertical axis probability density P(μ)

Horizontal axis final moment/initial moment

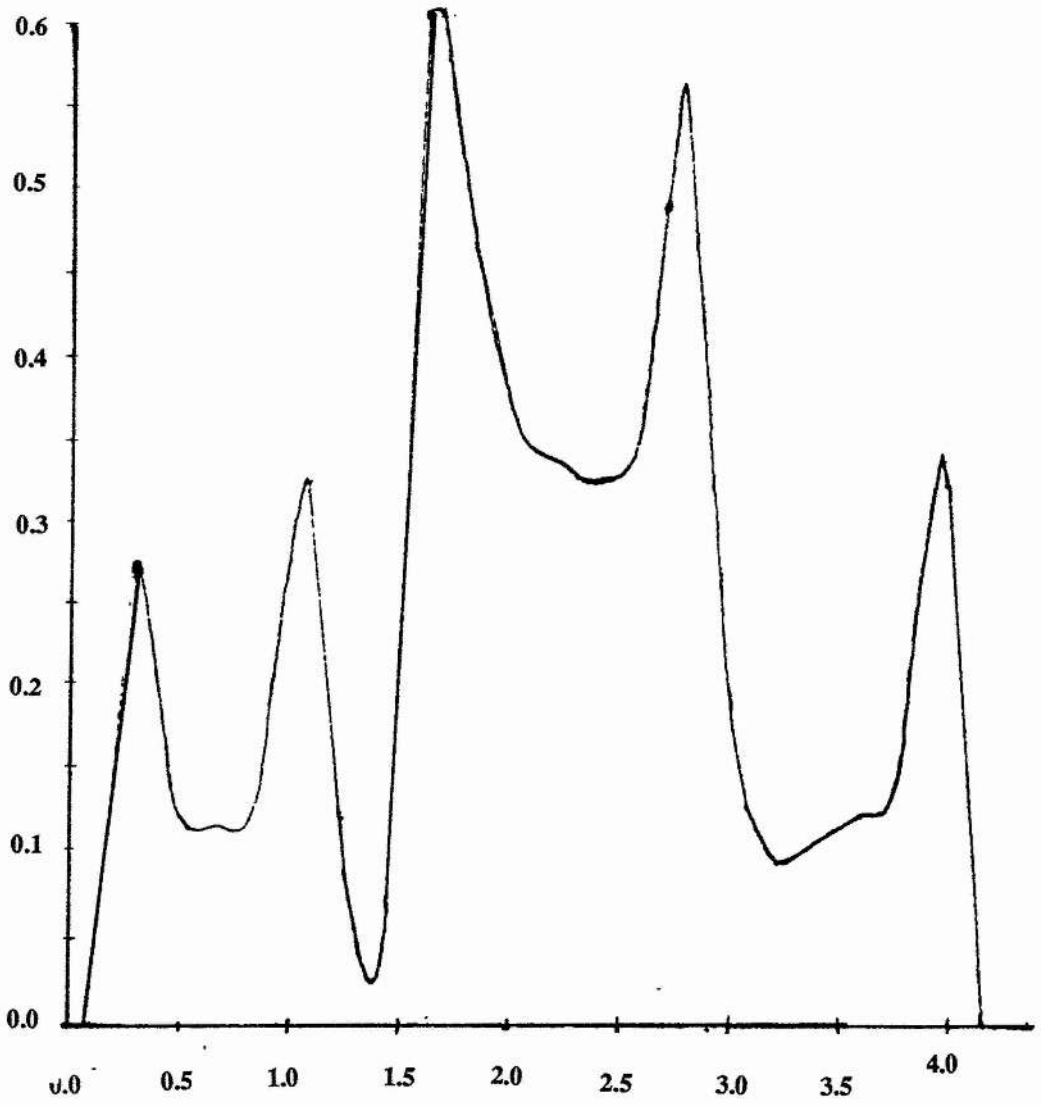

Figure 2.2b

$U_\perp$	$= 10^7$ ms^{-1}	Initial perpendicular velocity
$U_\parallel$	$= 10^7$ ms^{-1}	Initial parallel velocity
Profile		Gaussian
L	= 0.025 m	Gaussian width
Mode		O mode
$E_\parallel$	$= 2*10^7$ Vm^{-1}	Peak electric field
B_0	=1.0 T	Magnetic field.
$n_\parallel$	= 0	Parallel refractive index

Vertical axis probability density P(μ)

Horizontal axis final moment/initial moment

2.9 Oblique Propagation across a Magnetic Field.

When $k_{||} \neq 0$ there is a small change in $U_{||}$ as the particle crosses the beam even if there is no magnetic field inhomogeneity. There are thus now two competing ways which tend to detune the resonance condition - the change in Ω/γ and the change in $k_{||}V_{||}$. A simple relation between $\Delta U_{||}$ and $\Delta\mu$ which is mode-independent (Rognlien, 1983) is

$$\Delta U_{||} = \frac{k_{||}c^2}{\Omega}\Delta\mu \qquad (2.8a)$$

which can be derived from the equations of motion (2.5d) and (2.5e). A more exact expression may be obtained by considering the energy and momentum change in the photons producing the change in energy of the electron:

change in energy of photons $= n\,h\,\omega$

change in parallel momentum $= n\,h\,k_{||}$

Here n is the number of photons required to produce the change in energy of the electron and h is Planck's constant. Using these results we have

$$\frac{\Delta(mU_{||})}{\Delta(\gamma m c^2)} = \frac{k_{||}}{\omega}$$

so that

$$\Delta U_{||} = \frac{k_{||}c^2}{\omega}\Delta\gamma \qquad (2.8b)$$

which reduces to (2.8a) assuming the electron is exactly in resonance and $\Delta\gamma/\gamma \ll 1$. We note (2.8a) and (2.8b) are consistent with Rognlien (1983) equation (26). Defining a resonance quantity $\omega_{FM} = (\Omega - \gamma\omega + k_{||}U_{||})$ (= 0 initially, say) we see the

change in the resonance quantity as a result of the change in energy is

$$\omega_{FM} = \Delta\omega_{FM} = -\omega\Delta\gamma + k_{\|}\Delta U_{\|}$$

$$= \omega\left(\Delta\gamma - \frac{k_{\|}^2\Delta\mu c^2}{\omega\Omega}\right) \text{ from (2.8a)}$$

$$\approx -\omega\Delta\mu\left(1 - \frac{n_{\|}^2}{\beta}\right) \text{ as } \Delta\mu \approx \Delta\gamma.$$

Thus we can see that the Doppler shift is negligible provided

$$\left|\frac{n_{\|}^2}{\beta}\right| << 1.$$

When we have approximate equality instead of the inequality then the two effects may cancel out, and detuning may be prevented or reduced.

2.10 Theoretical implications of heating at $n_{||}^2 \approx ß$.

In this section we digress purely for interest's sake to consider a hypothetical situation in which a wave propagates approximately parallel to the magnetic field in a low density plasma. The purpose is to show that the power absorption may remain linear at high intensities. It is desirable for efficient heating of a tokamak that absorption should be as high as possible, and we have shown in section (2.8) that linear theory generally overestimates the heating of electrons and hence the absorption at high field intensities. We suppose a low density plasma is heated by an e/m wave which couples to the cyclotron motion and propagates parallel to the field. It is the right hand circularly polarised wave (RHCP) which has a rotating component E_- (like the X mode) which couples to the motion. We assume for simplicity that heating occurs near the fundamental, that $n_{||}^2 \approx ß$, that the frequency mismatch is zero and that $G=\infty$. The equations of motion, from (2.5d-f) for the X mode when it is exactly in resonance with the electron are

$$\frac{dU_\perp}{dt} = -\frac{eE_-\left(1-\frac{k_{||}V_{||}}{\omega}\right)\cos(\psi)}{2m} \qquad (2.9a)$$

$$\frac{dU_{||}}{dt} = \frac{ek_{||}E_-\left(1-\frac{k_{||}V_{||}}{\omega}\right)U_\perp\cos(\psi)}{2m\omega} \qquad (2.9b)$$

and

$$\frac{d\psi}{dt} = \frac{eE_-\left(1-\frac{k_{||}V_{||}}{\omega}\right)\sin(\psi)}{2mU_\perp} \qquad (2.9c).$$

The stable solution for ψ is $\psi=\pi$ as $E_->0$, so if the interaction time is

long enough all electrons acquire this phase with respect to the wave and the equations of motion are just (2.9a,b) with cos(ψ) replaced by -1 and (2.9c) is replaced by dψ/dt=0. The maximum heating effect will be for electrons with initial phase ψ=π, so that

$$\Delta\mu_{max}c^2 = \frac{U_\perp K}{2} + \frac{K^2}{8} .$$

We have derived this expression which is similar to (2.7a) without need for the condition (2.7c). When the reverse inequality in (2.7c) applies, we would intuitively expect all electrons to have approximately the same kick in energy ≈ $K^2/8$ and we will have $<\Delta\mu c^2>\approx K^2/8$. This is identical with the expression for $<\Delta\mu>$ which holds for all values of K in the nonrelativistic approximation (2.6b) and for small values of K, ie when (2.7c) is satisfied, in the relativistic case. We see therefore that heating with $n_{||}^2\approx ß$ largely eliminates the nonlinearity caused by relativistic effects, and that wave absorption may remain linear. This does not mean quasilinear theory itself is valid at high intensities however nor that we may follow the procedure of Taylor et al and Cairns and Lashmore-Davies (1986) in attempting to find a simplified quasilinear diffusion coefficient, merely that the expression for $<\Delta\mu>$ remains correct at high intensity if $n_{||}^2$ is close enough to ß. This is because quasilinear theory is valid only when distortions to the distribution function are small and this may not be the case when electrons receive large increases in energy on passing through a beam.

Figure (2.3) shows a comparison between the linear theory (dotted line) and the numerically derived form for the probability of a given increment in energy of an electron passing through a beam of ECRH. The parameters are such that (2.7c) is violated so we would not necessarily expect agreement between the two forms. Nonetheless the theoretical form retains the correct order of magnitude for the heating because the heating is parallel to the magnetic field and (2.6a) appears to be valid. From our previous discussion we would expect the numerical form to have a narrower spread in final velocities than the theoretical form and that the maximum final energies of the two forms should be equal. The

latter expectation is not fulfilled because of the way K is calculated in the theoretical form used in the code, viz

$$K = \frac{eE\_w\left(1 - \frac{k_{\|}V_{\|}}{\omega}\right)}{mV_{\|}}$$

where $V_{\|}$ has its initial value (we note that as $k_{\perp}=0$ for this case we have no need to make the small Larmor radius approximation). Although the change in $V_{\|}$ is virtually never important in ECRH in an homogeneous magnetic field, when the heating is intense and the wave is parallel to the field (2.7) predicts that there *is* a change in $V_{\|}$. The quantity calculated by the code is therefore a slight overestimate of (2.6b). In fact if we consider the change in $U_{\|}$ of an electron whose initial phase is π we see from (2.7), and noting from figure (2.3) that $\Delta\mu \approx 70\mu_i$, that $\Delta U_{\|}/U_{\|} \approx 2$ for figure (2.3). It is interesting to note that the numerical form still has a U shape like the theoretical form (but narrower of course). Qualitatively this behaviour can be understood as follows:

Suppose the heating of an electron can be divided into two stages. In the first stage the electron undergoes heating according to the linear theory. If it is in phase with the wave it is heated and if it is completely out of phase it is cooled. However during this stage the electron is dragged into phase with the wave regardless of its initial state.When it has done so the electron experiences constant heating. The initial stage contributes to the U - shape of the curve, and the second stage simply translates the U curve in $U_{\perp}$ space.

The possibility of sustained interaction of waves and electrons in this manner was first suggested by Davydovskii (1963) in the context of astrophysics. Although it has relevance in that subject, because of the toroidal nature of a tokamak, it is unsuitable as a heating mechanism for ECRH. Furthermore the only wave which interacts strongly with electrons at $n_{\|}^2 \approx ß \approx 1$ is the right hand circularly polarised wave (RHCP) at the fundamental - essentially the X mode.

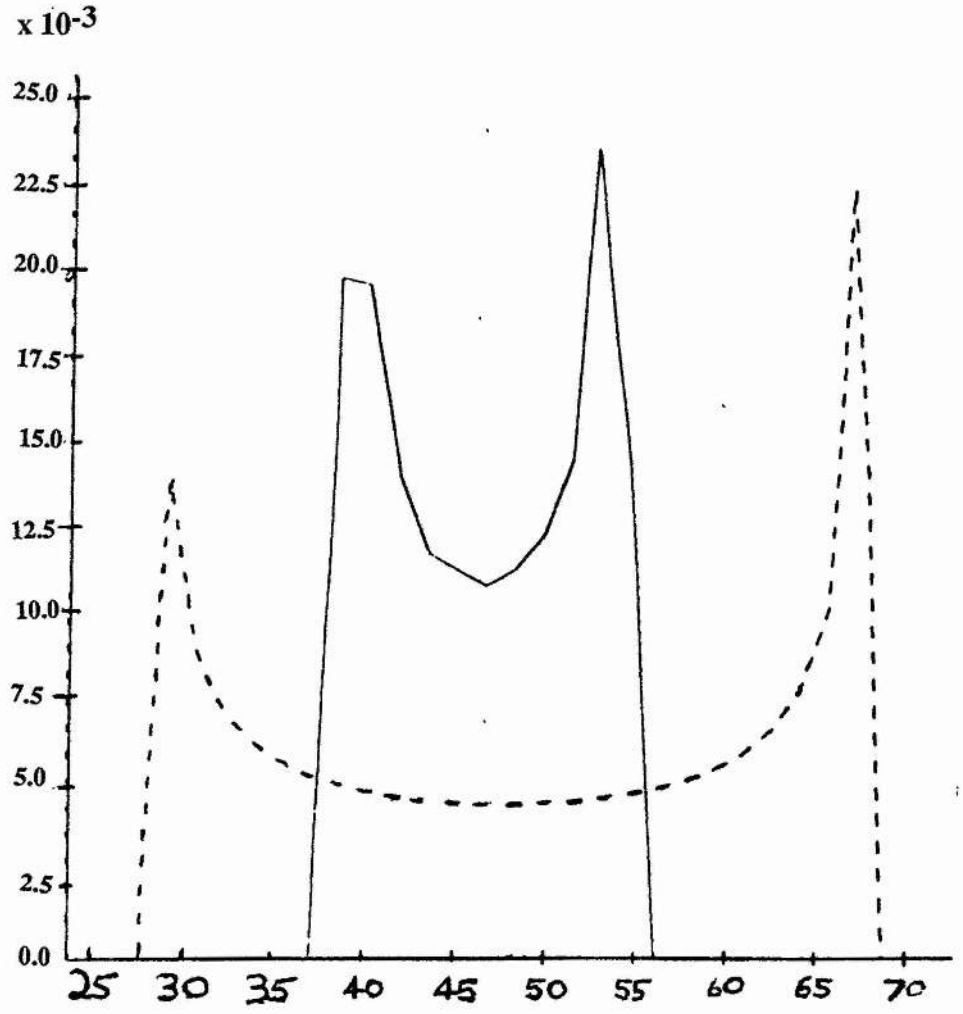

Figure 2.3

$U_\perp$	$= 10^7$ ms^{-1}	Initial perpendicular velocity
$U_\parallel$	$= 10^7$ ms^{-1}	Initial parallel velocity
Profile		Tophat
w	= 0.1 m	Beam width
Mode		X mode
E_-	$= 10^5$ Vm^{-1}	Peak rotating electric field
B_0	=1.0 T	Magnetic field.
$n_\parallel$	= 1	Parallel refractive index

Dotted line - theoretical form for the probability

Solid line - numerical form for the probability

Vertical axis probability density $P(\Delta\mu)$

Horizontal axis final moment/initial moment

All other modes depend on non zero $k_{\perp}$.

We should point out at this stage that two conditions are required if we are to have $n_{||}^2 \approx ß \approx 1$ for a wave propagating just above the electron cyclotron frequency. Not only must the wave propagate nearly parallel to the magnetic field, but the density must be negligible as the total refractive index decreases with increasing density. Thus heating the centre of a dense plasma will certainly be impossible with this scheme. Furthermore the X mode cannot reach the fundamental resonance when launched from the outside of a tokamak, so it is not even possible to obtain a locally near - parallel propagating wave directly (but see Consoli, 1986). If such a wave could be induced in a low density tokamak it might produce sustained heating. The purpose of this section has been to illustrate what would happen in the limiting case when $n_{||}^2 \rightarrow ß$, if that were possible. It should be emphasised that it is **not** being suggested that this can ever be achieved in practical situations.

It is worth mentioning in passing other schemes involving the increase in the energy of charged particles in e/m fields, even though they are *not* based on autoresonance and are not necessarily relevant to tokamaks or even to fusion. Golovanivsky (1985) has considered particle motion in rotating electric fields where there is a background magnetic field whose amplitude changes in time. Menyuk et al (1987) and Menyuk et al (1988) have shown that charged particles can be accelerated to very high energies indeed due to the overlap of resonances (in the context of astrophysics). None of these schemes however seems to have relevance to tokamak heating.

2.11 Conclusion.

In conclusion we have extended the scope of the SPEECH codes considerably and improved substantially on the accuracy while simultaneously making possible a saving in processor time by reduction of the four differential equations to three. We have discussed the theory of resonant cyclotron interaction proposed by O'Brien et al. We have confirmed it is valid for electric field intensities typical of gyrotrons but that for large electric fields - typical of FELs - the theoretical form is invalid and overestimates the gain in energy. We have examined the theoretical implications of heating a plasma with $n_{||}^2 \approx \beta \approx 1$, observing that large accelerations are possible, but have rejected the practicality of this in application to tokamak heating.

CHAPTER THREE

REVIEW OF NONLINEAR CYCLOTRON INTERACTION

CHAPTER THREE

Review of Nonlinear Cyclotron Interaction.

3.1 Review of Nevins, Rognlien and Cohen (1987)

In the last chapter we saw that the linear theory of resonant particle heating failed for large electric fields because of relativistic effects. In this chapter we consider mainly the heating of nonresonant particles in intense fields where condition (2.7c) is not satisfied. In this scenario the parameter $\beta=\Omega/\omega$ does not have to be close to γ for heating to occur. We introduce $p_{\|can}=p_{\|}+e/m\ A_{\|wave}$ the **canonical** momentum of an electron in an e/m wave. Also, remembering that γ can be expressed as $\sqrt{1+p^2}$ we introduce $\gamma_o=\sqrt{1+p_{\|can}^2}$, which in the absence of an e/m wave is simply the relativistic factor for an electron of zero perpendicular energy.

Nevins et al start from an approximate Hamiltonian

$$H=\frac{(\mu-P_r)^2}{2}+\alpha\mu^{¶}\sin(\psi) \qquad (3.1a)$$

whose derivation, which depends on the weakly relativistic approximation, is not given in the paper but is included in Appendix two of this thesis for completeness. Here dimensionless units have been used, p representing momentum normalised to mc, $\mu=\frac{U_\perp^2}{2c^2}$ and $P_r=\frac{1}{\gamma_0}-\frac{1}{\beta}$. For the O mode propagating at the fundamental with perpendicular propagation,

$$\alpha=\frac{E_{\|}}{\sqrt{2}\,cB_0}\,n_\perp\,\frac{V_{\|}}{c} \text{ and } ¶ = 1/2.$$

In this work we are exclusively concerned with fundamental heating, so we

shall take the harmonic number as 1. In quoting (3.1a) from Nevins et al we have made a change of phase so that $\cos(\psi)$ -> $\sin(\psi)$ in order to be consistent with the definition of ψ used by Taylor et al (see Appendix two). It should also be emphasised here that the Hamiltonian and Lagrangian approaches are essentially equivalent and lead to the same gyroaveraged equations we discussed in Chapter two.

In deriving (3.1) Nevins et al have made weakly relativistic approximations and also have assumed $|B_1/B_0|<<1$, where B_1 is the perturbing magnetic field. We retain the latter approximation only. In addition the Hamiltonian is valid only for perpendicular propagation.

In Appendix two we derive a generalisation to oblique propagation without the weakly relativistic approximation, and also demonstrate that using Hamilton's equations the same equations of motion can be derived in an analogous manner to Taylor's Lagrangian approach. Our Hamiltonian is

$$H=\sqrt{1+\left(\underline{p}_{can}+\frac{e}{m}\underline{A}\right)^2}\ -\frac{\mu}{\beta}\left(1-\frac{n_{\|}p_{\|can}}{\gamma}\right) \qquad (3.1b)$$

where $\underline{A}=\underline{A}_o+\underline{A}_{wave}$, $\underline{A}_o$ being the vector potential of the background magnetic field and where the canonical coordinates are μ and $\psi=\phi-\omega' t/\Omega$. We have no need to make further simplifications to this Hamiltonian in the case that propagation is oblique. However when the propagation is perpendicular and the wave propagates in the O mode it is relatively easy to derive the approximate and more useful Hamiltonian, obtained by neglecting $A^2_{\|wave}$ compared with $p^2_{\|can}$:

$$H=\sqrt{1+2\mu+p^2_{\|can}+\frac{e}{m}\underline{p}.\underline{A}_{wave}}\ -\frac{\mu}{\beta} \qquad \text{where}$$

$$\underline{p}.\underline{A}_{wave}=\frac{E_{\|}\ k_{\perp}V_{\|}}{2B_0c\ \omega}\ p_{\perp}\sin(\psi).$$

If we suppose that $E_{\|}$ is constant, ie the beam intensity does not change, then

the Hamiltonian is time-independent and phase space orbits are as shown figuratively in the first frame of figure (3.1a) after Nevins et al. However as the particle moves through the beam the wave intensity changes, and the Hamiltonian is time dependent. If the time dependence is sufficiently slow we can make an adiabatic assumption, that the rates of change of μ and ψ are determined by the local behaviour, with $E_{||}$ regarded as fixed. Figure 3.1b is a plot in time of the perpendicular velocity of an electron against its phase, produced by the SPEECH codes. It demonstrates that as $E_{||}$ changes the orbits are not exactly closed in practice.

Outside the beam the phase space trajectories are just the straight lines μ=constant. As we move into the beam the structure shown in figure (3.1a) develops, with closed orbits around the fixed point at $\psi=\pi/2$ (which are nearly elliptic for small electric fields). Particles with cyclotron frequencies sufficiently close to the resonant frequency are trapped in these closed orbits as the wave grows, then untrapped as the wave leaves the beam again. With the adiabatic assumption particles remain on lines of fixed H, so when the particle is untrapped it gets back to a line μ = constant corresponding to its original value of H. This may be the original value of μ, but there is also a second solution on the other side of the fixed point at which H has an extremum. The second solution fixes the line which coalesces with $\mu = \mu_i$ (the initial value of μ) to form the closed orbit. If the variation is slow enough for the particles to make several rotations about the fixed point while it is trapped in phase space, there will be as many particles on the high μ side as the low μ side after passage through the beam. Assuming that most of the particles start on the low energy side of the fixed point, this leads to the distribution of the general form shown in figure (3.1c). Actual graphical details of distributions for typical parameters are given in Chapter four, but for now we are content with a diagram.

This process can produce effective heating of the plasma, and also give rise to double-peaked distributions which might well be unstable. The remainder of this thesis is devoted to examining in more detail the conditions under which this model gives a good description, refining it in various places, and also to

Figure 3.1a after Nevins, Rognlien and Cohen.

Snapshots of the closed path of an electron as it passes through the beam.

Vertical axis - moment of electron

Horizontal axis - phase of electron with respect to wave

(Nevins et al's definition of phase)

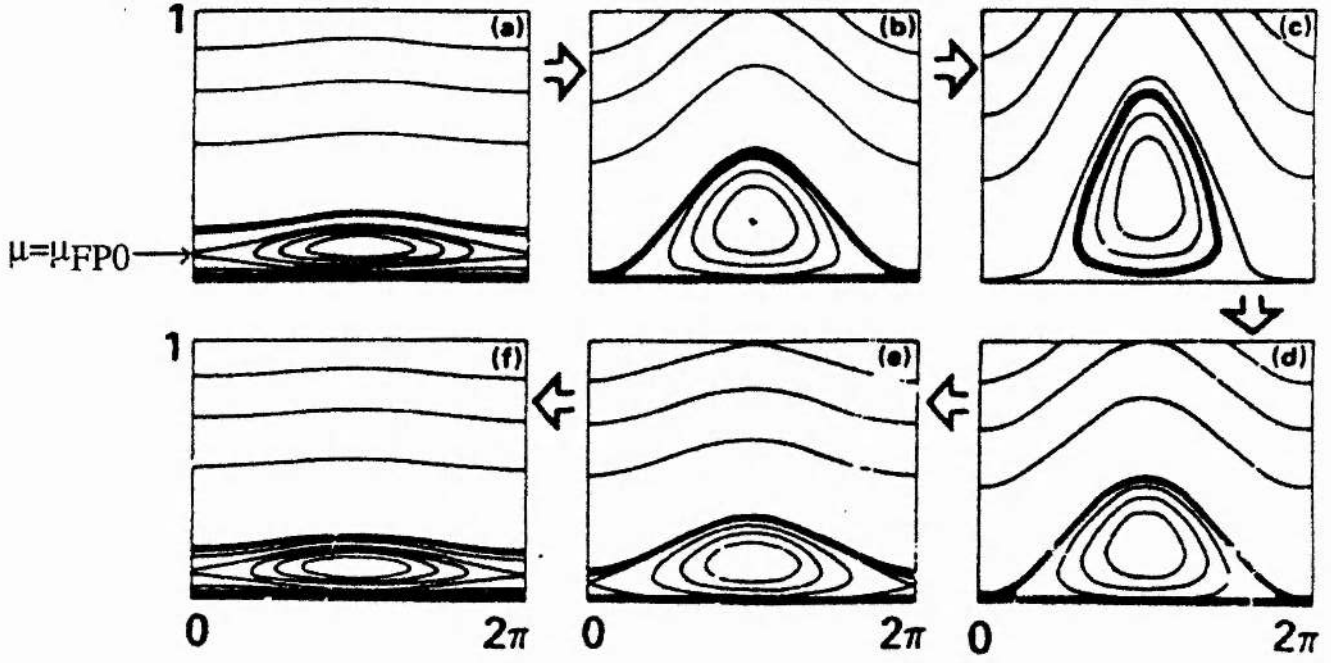

(a)–(f) A sequence of snapshots of phase space moving across the microwave beam illustrating the heating mechanism in the strongly nonlinear regime. The thin lines are surfaces of constant *H*. The particles are indicated by the heavy lines. They are first pulled through the hyperbolic fixed point from below [(a)–(c)]. Half of the particles are expelled above the separatrix [(d)–(f)].

Figure 3.1b

Path of an Electron Through Phase Space

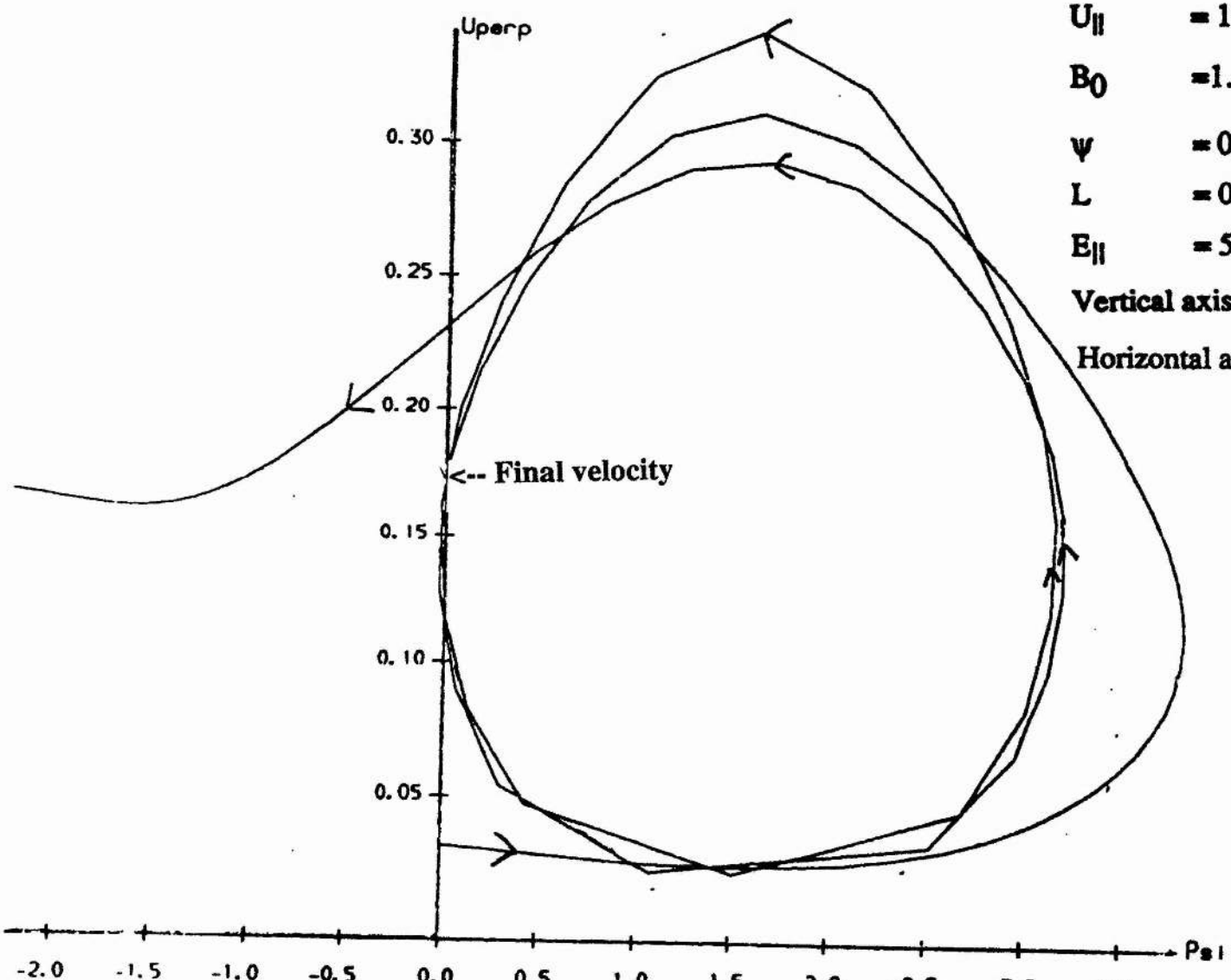

$U_\perp$	$= 10^7$ ms^{-1}	Initial perpendicular velocity
$U_\parallel$	$= 10^7$ ms^{-1}	Initial parallel velocity
B_0	=1.0 T	Magnetic field.
ψ	=0	Initial phase
L	= 0.025 m	Gaussian width
$E_\parallel$	$= 5*10^7$ Vm^{-1}	Peak parallel electric field

Vertical axis - $U_\perp/c$

Horizontal axis - phase of electron with respect to wave

Figure 3.1c

Diagrammatic figure of an electron distribution function before and after a pulse of intense ECRH at a fixed parallel velocity

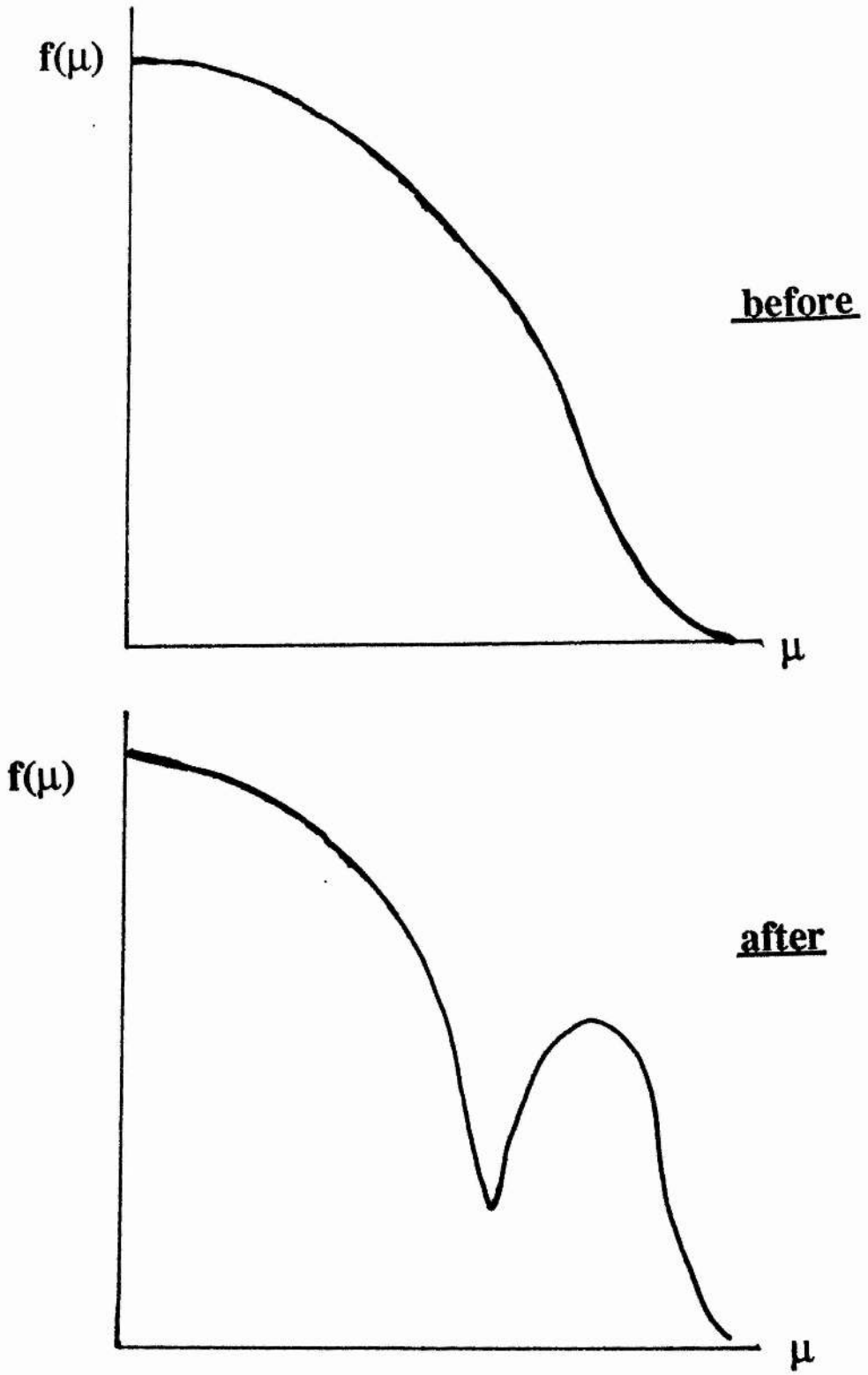

looking at the possibility of instability in the distributions arising from this process.

Restricting attention to the case $n_{||}=0$ and denoting by the subscripts i and f the initial and final states we must have from the equality of Hamiltonians before and after heating, that $H_i=H_f$ ie $\gamma_i - \mu_i/\beta = \gamma_f - \mu_f/\beta$, and as $p_{||}$ is constant

$$\gamma_i - \frac{\gamma_i^2}{2\beta} = \gamma_f - \frac{\gamma_f^2}{2\beta} \qquad (3.2)$$

which leaves two possibilities for γ_f viz

$$\gamma_f = \gamma_i \qquad (3.3a) \text{ or}$$

$$\gamma_f = 2\beta - \gamma_i \qquad (3.3b).$$

This is valid provided $E_{||}$ changes sufficiently slowly, an assumption which will be referred to as the *adiabatic assumption* or *the adiabatic approximation.* We note the solution (3.3b) is possible only if $\gamma_i \leq 2\beta - \gamma_0$. Making the approximation $\gamma_i \approx \gamma_0$ equation (3.3b) reduces to $\Delta\gamma = 2P_r\gamma_i\beta$ where $P_r = 1/\gamma_0 - 1/\beta$ a result which differs from a similar result of Nevins et al viz

$$\Delta\gamma = 2P_r \qquad (3.3c)$$

only by a factor $\gamma_i\beta \approx 1$.

Nevins et al argue firstly that as $|dp_{||}/dt| << |d\mu/dt|$, and the rapid oscillation is approximately in (μ,ψ) plane, and secondly that for a fixed value of the electric field the electrons follow closed orbits around the fixed point at $\psi=\pi/2$ and $\mu=\mu_{FP}(\alpha)$, which are nearly elliptical for small α. A consequence of this is that $p_{||can} \approx p_{||}$. Figure (3.1a) after Nevins et al shows a series of such orbits (we

note again our definition of ψ differs from Nevins et al by $\pi/2$). We suppose that initially most electrons lie below the the line $\mu=\mu_{FP0}$, the fixed point as α->0. As α increases the fixed point moves and a larger number of electrons become trapped by the wave. As α decreases electrons are detrapped, not necessarily with the same energy they started, but on trajectories with the same Hamiltonian. We note that according to figure (3.1a) there may be some electrons with energies too high to become trapped and these correspond to $\gamma_i \geq 2\beta-\gamma_0$.

Using the conservation of phase space for autonomous Hamiltonians they also note that $J_{AC} = \int d\psi \frac{\mu}{2\pi}$, the action in two dimensions (Goldstein, 1950), is also approximately conserved. For untrapped electrons the limits of the integral are $\pm\pi$ and for trapped electrons they are the minimum and maximum ψ that are attained. Again provided that the Hamiltonian changes slowly and that the electrons perform many orbits in phase space during the transit of the beam, J_{AC} is approximately constant through the beam.

If J_{AC} were conserved throughout the beam no heating would be possible at all, as J_{AC}->μ as α ->0 and we must have $\mu_i = \mu_f$ so for a net change in μ the constant J_{AC} must be broken somewhere. This occurs as the electrons pass through the hyperbolic fixed point when the limits of the integral change. A fuller discussion of the change in adiabatic invariants as the nature of motion changes has been given in a different context by Timofeev (1978), but in the present case the approximate equality of the Hamiltonian before and after heating provides the result required.

Particles on open orbits passing sufficiently close to the hyperbolic fixed point are liable to become trapped as the electric field amplitude increases. They rotate about the fixed point in phase space on the same closed orbits until they are untrapped, either above or below the separatrix, again by being expelled close to the hyperbolic fixed point. Each electron has approximately equal chance of being detrapped above or below the line $\mu=\mu_{FP0}$, which we will call the separatrix (we say that the *transition probabilities* are equal). There are thus two possible values of the final value energy as shown above. It should also be noted that it is possible

for an electron to be cooled, a point which Nevins et al do not make as they are interested mainly in the case that the initial perpendicular energy of the electrons can be neglected. Net heating occurs because more particles lie initially on the low energy side of the separatrix.

Much more recently Kotel'nikov and Stupakov (1990) have described the process of breaking the adiabatic invariant in greater detail. They point out that if the electric field is sufficiently small there are exactly three fixed points of the equations of motion (see also Taylor, 1987). Two (those at $\psi=-\pi/2$) coalesce and disappear when the electric field becomes high enough. At such a point the motion of the electron changes producing a change in the adiabatic invariant (but no change in the Hamiltonian). The invariant is permitted to change because on transition between the two trajectories the time scales involved invalidate the assumptions on which the invariant was constructed. As the electric field decreases the reverse change may take place. The approach is essentially the same as that of Nevins et al but is somewhat more lucid in explanation.

In their paper Nevins et al actually refer to two nonlinear regimes. In both $\omega_{rot}T_{transit}>1$ for electrons where ω_{rot} is the frequency of rotation about the fixed point and $T_{transit}$ is the transit time through the beam. Furthermore in both regimes Nevins et al assume that the mean energy gain is proportional to the width of the trapped region. However in the second regime the width of the trapped region in phase space is large compared with the electron temperature so that all of the electrons are trapped, whereas in the first the width of the trapped region is comparable with the temperature. It is for the second regime that the approximate gain in energy is given by the formula (3.3c) - unnumbered in their paper. We are not concerned here with the distinction between the two but rather with the adiabatic assumption. Essentially in the second regime Nevins et al make the cold plasma approximation. This allows approximations which we will not make in this thesis, but which lead to a power absorption scaling law.

Finally we show in figure (3.1b) an example of an electron path in phase space calculated using the SPEECH codes but using data from intermediate points along the electron path (see extension 10 of section 2.5). In this example the

electron makes only three orbits about the fixed point. Note that the largest velocity attained during the orbit is somewhat higher than the final velocity, even though the electron is clearly heated. It is because of the very high velocities involved that it was important to include Bessel functions and second order terms into the equations of motion in the previous chapter. It also helps to explain why the nonlinear theory has no classical limit (ie the limit γ->1) unlike the linear theory.

The work of Davidson et al.

Davidson et al (1989) also consider intense beams, but with a much different profile from a Gaussian. They consider the O mode and a tophat profile (not a physically realistic profile as the infinite derivative $dE_{||}/dz$ at the edge would imply an infinite charge density by Maxwell's equations). Like Taylor et al they derive gyroaveraged equations for the motion, but using the weakly relativistic approximation and not the small Larmor radius approximation. Using the constancy of the Hamiltonian which results from the condition $dE_{||}/dz=0$ everywhere except at the edge, and neglecting any change in parallel velocity, they reduce the equations of motion to a single ODE. From this equation they derive a bound on the minimum and maximum energy allowed during the motion, both for the weakly relativistic and the nonrelativistic cases. They contrast the limit on allowable energy demanded by the relativistic detuning with the limit on allowable energy given by nonrelativistic theory owing to the finite size of the Larmor radius. The two are shown to be vastly different, reinforcing the need for a relativistic approach to the subject. The main point is that relativistic effects **limit** the heating of individual particles, as we have already seen in Chapter two. Davidson et al's paper appears to confirm the scaling law for nonlinear energy absorption derived by Nevins et al (and also Kotel'nikov and Stupakov) though the two papers treat somewhat different spatial profiles.

3.2 Extension to Oblique Incidence.

In moving to oblique incidence we can no longer assume that the rapid motion is completely in the (μ,ψ) plane. However it is approximately confined to a single plane in $(p_{||},\mu,\psi)$ space. Ignoring the terms in the equation for $dU_{||}/dt$ which are second order or depend on $dE_{||}/dt$, the motion is still approximately confined to a 2D manifold defined by equation (2.8b) relating $\Delta(U_{||})$ to changes in $\Delta\gamma$. Although the change in $U_{||}$ is much smaller than $\Delta\mu$, it is still significant as the resonance condition depends on $U_{||}$.

Again using the adiabatic principle that the Hamiltonian has the same value before and after heating, one can obtain a relation between initial and final velocity components (where again we use normalised units):

$$\gamma_i - \mu_i\frac{\left(1-\frac{n_{||}p_{||i}}{\gamma_i}\right)}{\beta} = \gamma_f - \mu_f\frac{\left(1-\frac{n_{||}p_{||f}}{\gamma_f}\right)}{\beta} \qquad (3.4a).$$

Together with (2.8b) (in normalised units, $\Delta p_{||}=n_{||}\Delta\gamma$,) this allows us to determine γ_f and $p_{||f}$ implicitly.

The effect of the heating of a single electron can be seen most clearly if we consider an electron for which $\gamma_i = 1$ and $p_{||i} = \mu_i = 0$. Then we have from (3.4a) that

$$1 = \gamma_f - \frac{\left(\gamma_f^2 - 1 - p_{||f}^2\right)}{2\beta}\left(1-\frac{n_{||}p_{||f}}{\gamma_f}\right)$$

As $\gamma_f = 1 + \Delta\gamma$, $p_{||f} = n_{||}\Delta\gamma$ we have

$$0 = 2\beta\,(1+\Delta\gamma)\Delta\gamma - \left((\Delta\gamma+1)^2 - 1 - n_{||}^2\Delta\gamma^2\right)\left(1+\Delta\gamma-n_{||}^2\Delta\gamma\right)$$

$$\Rightarrow \Delta\gamma = \frac{2(\beta - 1)}{1 - 3n_{||}^2} \qquad (3.4b)$$

provided $\Delta\gamma << 1$.

We see that the maximum possible jump in energy increases as $n_{||}^2$ increases.

In this thesis most attention is devoted to considering the effects of perpendicular propagation. However for completeness we present generalisations to oblique incidence wherever possible and discuss the differences briefly. While the O mode couples best to the plasma at perpendicular incidence (the effective field is proportional to $n_{\perp}$), the X mode at the fundamental (propagating from the high field side) couples better as the angle of incidence increases. Although we have just observed that the maximum possible energy the electron can receive increases with $n_{||}^2$, even for the O mode, the overall heating of the plasma by the O mode will still decrease with $n_{||}^2$ as far fewer electrons will be trapped as E_{eff} decreases (see the next section). Furthermore we will see that when the incidence becomes oblique the position of the heating in the tokamak may change just as in the case of linear heating.

3.3 Three Necessary Conditions for Adiabatic Heating to Occur.

In this section we examine situations in which the adiabatic approximation can be used to describe the heating of a particle. We derive three necessary conditions that a particle must satisfy before it undergoes several phase space rotations such as the ones already described. Only then do we discuss the transition probabilities, ie the probabilities that electrons are finally heated given that they do actually undergo phase space rotations. The first two conditions are essentially conditions that must be satisfied if the electron interacts with the wave at all. The third condition relates to the number of times an electron rotates about the fixed point. In future these conditions will be referred to as the three conditions.

Condition 1 (Maximum parallel velocity)

We first assume that propagation is perpendicular for simplicity.

As $\gamma_i \geq \gamma_0$, $\gamma_f \geq \gamma_0$ and $\gamma_f = 2\beta - \gamma_i$ we have

$$\gamma_f \leq 2\beta - \gamma_0 \qquad (3.5a),$$

and

$$\gamma_i \leq 2\beta - \gamma_0 \qquad (3.5b).$$

Combining the two we have a condition on $p_{||}$ for the maximum parallel velocity an electron can have if it may be heated according to (3.3b):

$$p_{||}^2 \leq \beta^2 - 1 \qquad (3.5c),$$

or simply $\gamma_0 \leq \beta$. The condition is more complicated if propagation is oblique. We will see below that, using the weakly relativistic approximation, the condition

$$\frac{1 + \frac{n_{||} p_{||}}{\beta}}{\gamma_0} - \frac{1}{\beta} > 0 \qquad (3.5d)$$

is required.

Condition 2 (Trapping Condition)

We now consider condition that the particle is trapped assuming condition 1 is satisfied. We follow the approach of Kotel'nikov and Stupakov. We rewrite equation (2.4c) using normalised variables for the O mode, neglecting any contribution E_- might make to E_{eff} should the wave propagate obliquely and suppose that $p_{||}>0$. We have from (2.5f) and (2.5d) that

$$\frac{1}{\Omega}\frac{d\psi}{dt}=\frac{1}{\gamma}\left(1+\frac{n_{||}p_{||}}{\beta}\right)-\frac{1}{\beta}+\frac{E_{||}p_{||}n_{\perp}\sin(\psi)}{B_0c\gamma p_{\perp}} \quad \text{and} \quad \frac{1}{\Omega}\frac{dp_{\perp}}{dt}=-\frac{E_{||}p_{||}n_{\perp}\cos(\psi)}{2B_oc\gamma} \tag{3.6}$$

We now make a number of simplifying approximations. Firstly we assume that the γ in the denominator of the last term may be replaced by 1. Secondly we make a weakly relativistic approximation by assuming $p_{\perp}^2<<1$ and making the following Taylor expansion in the first term on the RHS:

$$\frac{1}{\gamma} \approx \frac{\left(1-\frac{p_{\perp}^2}{2\gamma_0^2}\right)}{\gamma_0}$$

Thirdly we assume $p_{||}$ is constant. Further we consider only the O mode. The particle may become trapped when the two fixed points at $\psi=-\pi/2$ coalesce and disappear, so we consider the equation $d\psi/dt=0$ when $\psi=-\pi/2$. With the help of equation (3.6) this equation may be cast in the form

$$h(p_{\perp}) \equiv a\,p_{\perp}^3-b\,p_{\perp}+c=0.$$

where $a=\dfrac{\left(1+\frac{n_{||}p_{||}}{\beta}\right)}{2\gamma_0^3}$

$$b = \frac{1 + \frac{n_{||}p_{||}}{\beta}}{\gamma_0} - \frac{1}{\beta}$$

and $c = \frac{E_{||}p_{||}n_{\perp}}{B_0 c}$.

We note that a and c>0, and b>0 by condition 1 (inequality (3.5c) or (3.5d)).

For any cubic of this form we must have one negative root. This corresponds to negative $p_{\perp}$ which is unphysical so we ignore this root. The remaining roots disappear when $h(p_{\perp 0})=0$ where $h'(p_{\perp 0})=0$ ie where h has a double root. We note that the condition b>0 is needed as otherwise there are no real solutions of $h'(p_{\perp 0})=0$, no stationary points on the curve $h(p_{\perp})$, no physical solutions to the equation $h(p_{\perp})=0$, and hence no hyperbolic fixed points. This justifies our condition (3.5d) for the obliquely propagating wave . Taking the positive root of $h'(p_{\perp 0})=0$ we see the required condition for electron heating is

$$2\left(\frac{b}{3a}\right)^{\frac{3}{2}} + \frac{c}{a} < 0$$

which becomes

$$\frac{\beta E_{||}p_{||}n_{\perp}}{2B_0 c} > \left(\frac{2}{3}\right)^{\frac{3}{2}}\left(1 + \frac{n_{||}p_{||}}{\beta}\right)\left(\frac{1+\frac{n_{||}p_{||}}{\beta} - \frac{\gamma_0}{\beta}}{1+\frac{n_{||}p_{||}}{\beta}}\right)^{\frac{3}{2}} \qquad (3.7a)$$

from which it is obvious that the position of the heating in the plasma still depends on $n_{||}$, just as in the linear case.

For perpendicular propagation (3.7a) reduces to the simpler

$$\beta-\gamma_0 < \frac{3\beta\gamma_0}{2}\left(\frac{eE_{\|}p_{\|}n_{\perp}}{2m}\right)^{\frac{2}{3}} \qquad (3.7b)$$

which agrees with Kotel'nikov and Stupakov.

It is worth noting that these conditions are independent of the initial perpendicular energy. In particular electrons above the separatrix may be trapped but because there are far fewer electrons above the separatrix for typical electron distributions, adiabatic cooling is a relatively insignificant effect.

Condition 3 (Rotation period).

We now examine the motion about the elliptic fixed point at $\psi=\pi/2$. The quantity $p_{\perp FP}$ is the solution for $p_{\perp}$ of the equation

$$\frac{1}{\gamma}\left(1+\frac{n_{\|}p_{\|}}{\beta}\right)-\frac{1}{\beta} - \frac{E_{\|}p_{\|}n_{\perp}}{B_0 c\gamma p_{\perp}} = 0$$

subject to

$$p_{\|} = p_{\|i} + n_{\|}(\gamma-\gamma_i).$$

The particle will only undergo phase mixing if the rotation period about the elliptic fixed point is less than the transit period:

$$T_{rot} < T_{transit} \qquad (3.8a)$$

where $T_{transit}$ is the total time to cross the beam.

To find the rotation period we linearise about the fixed point. Letting $\tau=\Omega t$, $x=\Delta p_{\perp}$ and $y=\Delta\psi$, then from (3.6) we obtain the following two equations of motion about the fixed point $\psi=\pi/2$,

$$\frac{dx}{d\tau} = Ay \text{ and } \frac{dy}{d\tau} = -Bx$$

where

$$A = \alpha/\sqrt{2} \text{ and}$$

$$B = \frac{p_{\perp FP}}{\gamma_{FP}^2}\alpha_2 + \frac{\alpha}{\sqrt{2}p_{\perp FP}^2}$$

where $\alpha_2 = 1-n_{||}^2/ß$.

Noting $\Omega T_{rot} = \frac{4\pi}{\sqrt{AB}}$ we have

$$T_{rot} = \frac{4\pi}{\Omega\sqrt{\frac{\alpha}{\sqrt{2}}\left(\frac{p_{\perp FP}\alpha_2}{\gamma_{FP}^2} + \frac{\alpha}{\sqrt{2}\,p_{\perp FP}^2}\right)}} \qquad (3.8b).$$

Together with $T_{transit}=2L/V_{||}$ this provides the quantities defined in (3.8a). Intuitively the adiabatic approximation will work very well only if there are several rotations about the fixed point as otherwise the electric field changes substantially during an orbit ie only if

$$T_{rot} << T_{transit} \qquad (3.8c).$$

Typically we might have say $\alpha=1/500$, $p_{\perp FP}=1/20$, $V_{||}=10^7 ms^{-1}$ and L=0.05m so that $T_{rot}/T_{transit} \approx 1/100$. In practice for larger orbits T_{rot} may be larger than the time given in (3.8) and consequently (3.7b) may not always be satisfied. This is because the electron spends increasingly long times near the X points, especially when the electron is very close to the separatrix. A large increase in T_{rot} would only be expected for particles which are so close to the separatrix as to be only marginally trapped.

As we would expect, the linear theory is valid when the electric field is small, while the adiabatic heating theory is valid only when the electric field is large. Now suppose that conditions 1 and 2 are satisfied, but that condition 3 is not and that $T_{rot}>>T_{transit}$. The particle will interact with the wave, but it will not perform an orbit around the fixed point. In fact the heating will be described more accurately by linear theory than by nonlinear theory. When $T_{rot} \approx T_{transit}$, neither theory describes the heating very well at all.

We note here that all of our conditions are substantially simpler when propagation is perpendicular. Further in this case none of the conditions depend on μ_i.

Transition probabilities

Although this section is primarily about the conditions under which equation (3.3b) may be a solution of (3.2), we have not proved or even suggested that all particles which satisfy these conditions, and which consequently orbit about the fixed point, will be heated according to (3.3b), and indeed this is far from the case. Suppose a particle is trapped and does perform many oscillations about the fixed point. It may suffer a change in energy or it may return to its original energy.

An implication of the adiabatic approximation is that there are only two final states available to the electron, with a discrete probability distribution. In contrast the linear theory discussed earlier provided for a continuous set of final states and a continuous probability density function $P(\underline{v},\Delta\underline{v})$. The adiabatic theory provides no clue to the probabilities that should be attached to either final state, but both Nevins et al and Kotel'nikov and Stupakov assume

that for untrapped electrons the probability of an energy gain is zero and for trapped electrons the probability is on average 1/2. However for any given set of parameters (electric field, magnetic field, initial velocity coordinates etc) it is not necessarily the case that the transition probability will be 1/2. More realistically there will be a spread in energy around the two final states, and the total number of electrons emerging close to each of the final states need not be approximately equal, especially if (3.8a) is only marginally satisfied. However it is intuitively obvious that trapped electrons are far more likely to be heated than untrapped ones, and that the transition probability, given random phase and a Gaussian profile, depends mainly and sensitively on $T_{transit}$-$n_{rot}T_{rot}$, n_{rot} being the number of rotations. Formal justification of this is however beyond the scope of this thesis and so in Chapter four we solve the ODEs for a Maxwellian distribution of electrons and compare the final distribution with the adiabatic model. Figures (3.2) show transition probabilities for two sample sets of parameters plotted against the Gaussian width, a quantity which is directly proportional to the transit time. Despite the assertion of Nevins et al and Kotel'nikov and Stupakov it is certainly not the case that the transition probabilities are nearly equal for both possible final states for any given set of parameters pertaining to individual electrons. Nonetheless this does not mean that the overall effect on the plasma cannot be accurately described using this assumption provided the transition probabilities are equal on average for heated electrons. The only conclusion that can be drawn from these figures is that a more accurate analytic evaluation of the transition probabilities must be somewhat difficult.

In this section we have considered the circumstances under which heating may occur if the adiabatic assumption is made. In the next section we consider how good this assumption is and where the approximation breaks down by using the SPEECH code to examine individual points in phase space. In Chapter four we will continue to examine the validity of the approach, but by examining the distribution functions which we would expect after a pulse of FEL ECRH hits a plasma.

Figure 3.2a

Transition probabilities as a function of Gaussian width.

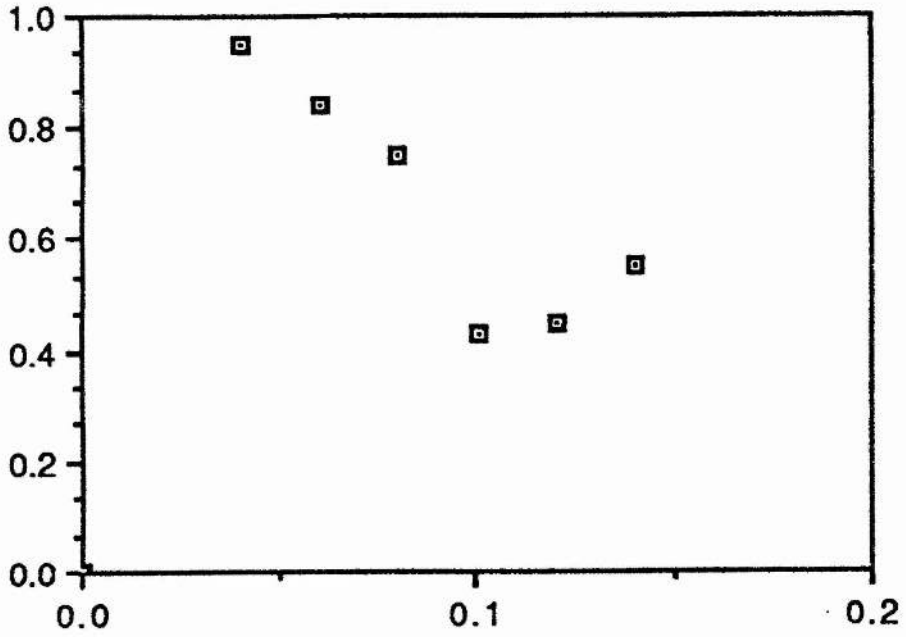

$U_\perp$	$= 10^7$ ms^{-1}	Initial perpendicular velocity
$U_\parallel$	$= 10^7$ ms^{-1}	Initial parallel velocity
B_0	=1.0 T	Magnetic field.
$E_\parallel$	$= 10^7$ Vm^{-1}	Peak parallel electric field
$1/\gamma - 1/\beta$	= 0.001	Frequency mismatch

Horizontal axis - Gaussian width

Vertical axis - transition probability

Figure 3.2b

Transition probabilities as a function of Gaussian width.

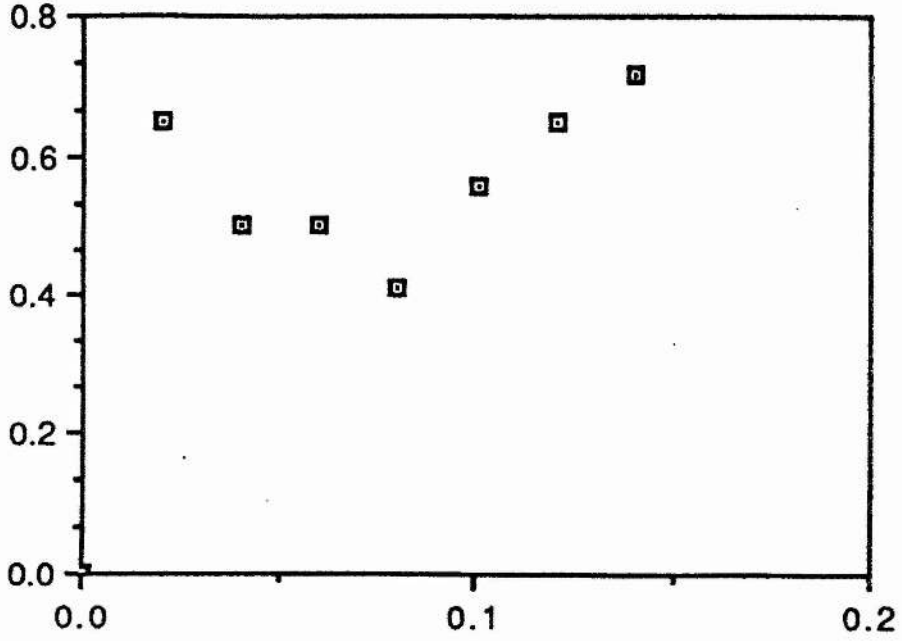

$U_\perp$	$= 10^7$ ms^{-1}	Initial perpendicular velocity
$U_\parallel$	$= 10^7$ ms^{-1}	Initial parallel velocity
B_0	=1.0 T	Magnetic field.
$E_\parallel$	$= 5*10^7$ Vm^{-1}	Peak parallel electric field
$1/\gamma - 1/\beta$	= 0.005	Frequency mismatch

Horizontal axis - Gaussian width

Vertical axis - transition probability

3.4 Comparison of Numerical Results with the Theory of Nevins, Rognlien and Cohen.

In this section we present results of numerical solution of the equations of motion (2.5) and compare the probability distribution $P(\Delta\underline{v},\underline{v})$ (see Chapter two) obtained numerically with the theoretical two valued model obtained using adiabatic theory. In practice the orbits are not exactly ellipses and of course the orbits change with the distance of the electron through the beam. Furthermore there may be nonadiabatic effects due to the change in the electric field as seen by the electron. In figures (3.3a-c) we show an orbit in phase space for an electron with a given initial phase, for three different sets of parameters. These contrast sharply with (3.1b), which follows the Nevins et al idealisation relatively closely. The underlying reason for the discrepancy is that the equations of motion are not given exactly by a time independent Hamiltonian. The Hamiltonian depends on $E_{||}$ which changes as

$$\frac{dE_{||}}{dt} = -2zV_{||}E_{||}$$

along the guiding centre of the electron.

In figures (3.4a-c) we use electrons with many different initial phases, but with the same parameters as (3.3a-c) respectively, to show the probability distribution $P(\Delta\mu)$ as a function of μ_f/μ_i to illustrate some of the ways in which the heating may differ from the adiabatic model. In the first example the model fits very well indeed, in the second case there is a small spread of velocities around the theoretical maximum velocity, while in the third case all the electrons appear to be heated and they have a considerable spread around the theoretical maximum velocity. We certainly do not have unambiguous numerical support for the model. Again however what is important is the overall effect on the distribution function rather than individual heating patterns. the numerical forms differ with the idealised forms as the electron orbits in phase space are not ideal.

Figure 3.3a

Electron Phase Space Paths through the Beam.

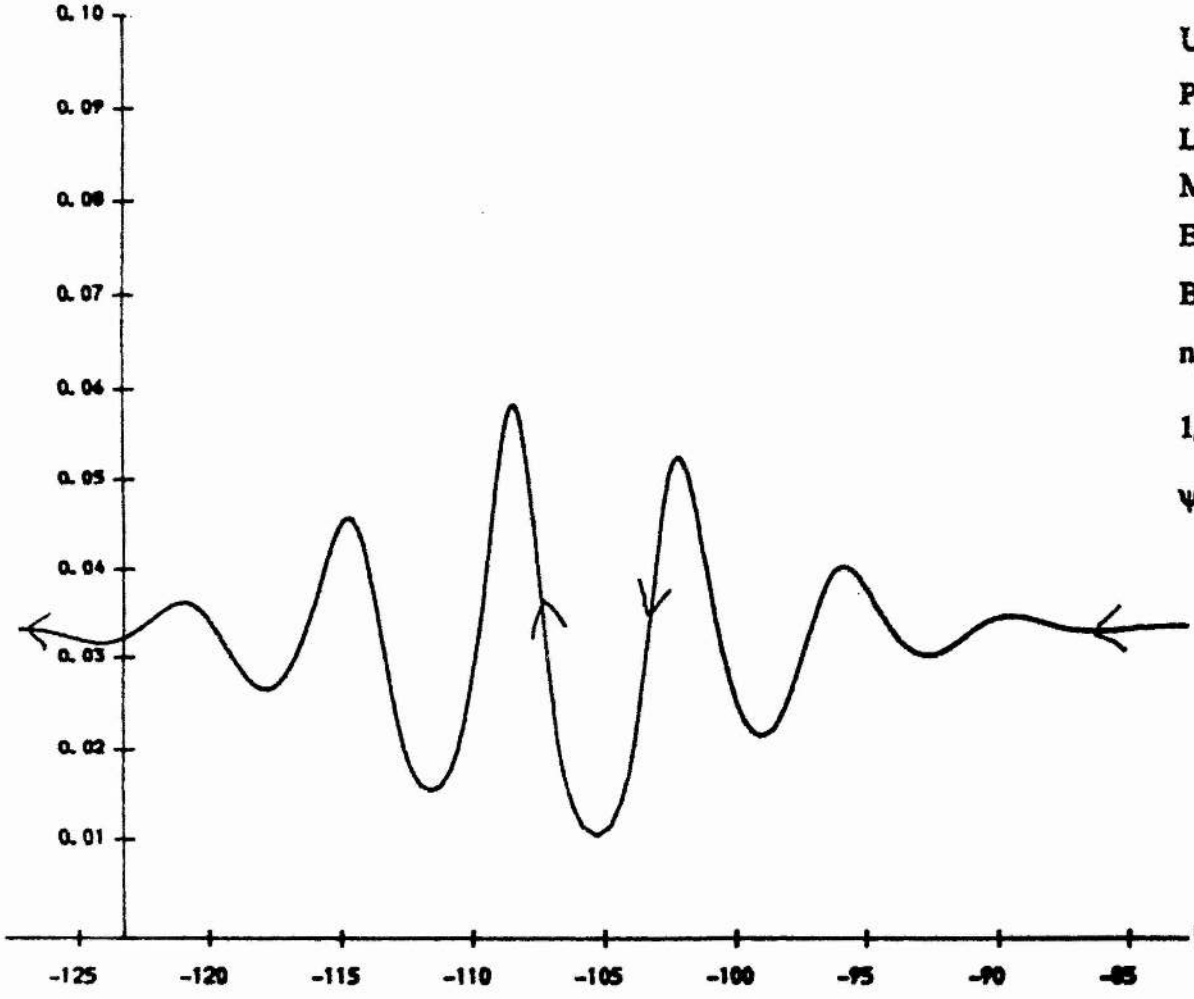

$U_\perp$	$= 10^7$ ms^{-1}	Initial perpendicular vel
$U_\parallel$	$= 10^7$ ms^{-1}	Initial parallel velocity
Profile		Gaussian
L	= 0.025 m	Beam width
Mode		O mode
$E_\parallel$	$= 5*10^7$ Vm^{-1}	Peak parallel electric fie
B_0	=1.0 T	Magnetic field.
$n_\parallel$	= 0	Parallel refractive index
$1/\gamma - 1/\beta$	= 0.005	Frequency mismatch
ψ	= 0	Initial phase

Vertical axis - $U_\perp/c$

Horizontal axis - phase of electron with respect to

Figure 3.3b

Electron Phase Space Paths through the Beam.

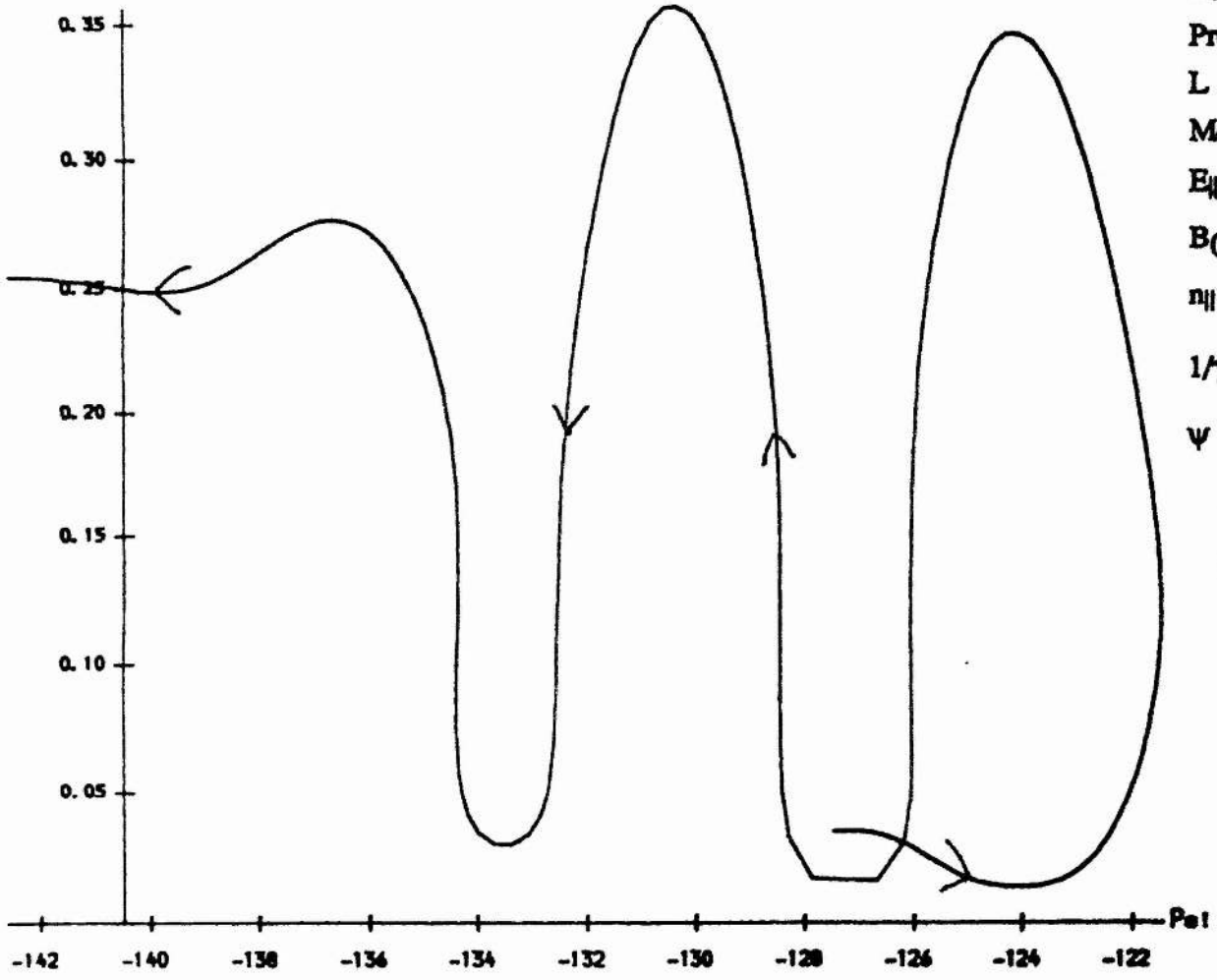

$U_\perp$	$= 10^7$ ms^{-1}	Initial perpendicular ve
$U_\parallel$	$= 10^7$ ms^{-1}	Initial parallel velocity
Profile		Gaussian
L	= 0.025 m	Beam width
Mode		O mode
$E_\parallel$	$= 10^8$vm^{-1}	Peak parallel electric fi
B_0	=1.0 T	Magnetic field.
$n_\parallel$	= 0	Parallel refractive inde
$1/\gamma - 1/\beta$	= 0.005	Frequency mismatch
ψ	= 0	Initial phase

Vertical axis - $U_\perp/c$

Horizontal axis - phase of electron with respect to

Figure 3.3c

Electron Phase Space Paths through the Beam.

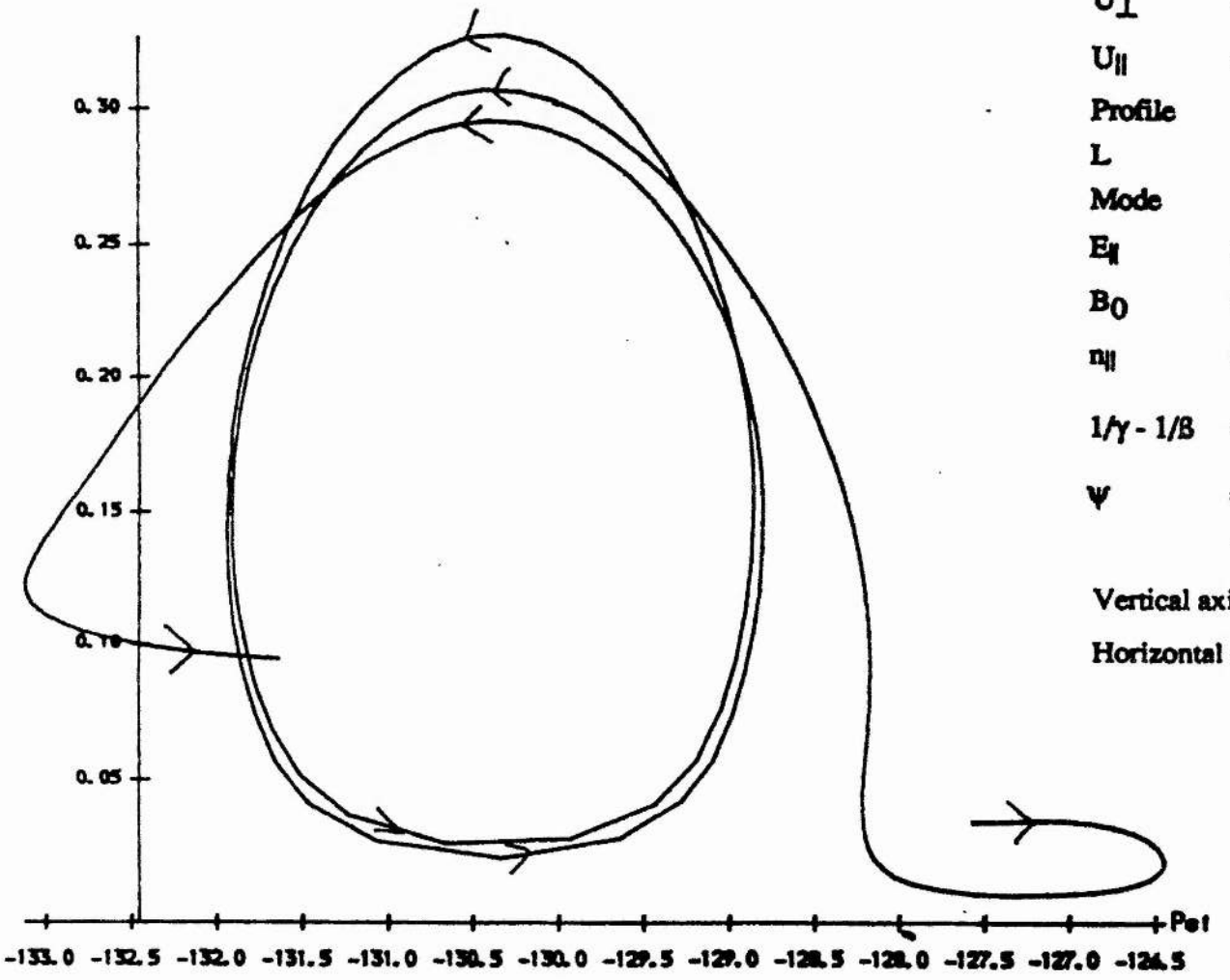

$U_\perp$	$= 10^7$ ms^{-1}	Initial perpendicular velocity
$U_\parallel$	$= 10^7$ ms^{-1}	Initial parallel velocity
Profile		Gaussian
L	= 0.025 m	Beam width
Mode		O mode
$E_\parallel$	$= 2x10^8$vm^{-1}	Peak parallel electric field
B_0	=1.0 T	Magnetic field.
$n_\parallel$	= 0	Parallel refractive index
$1/\gamma - 1/\beta$	= 0.005	Frequency mismatch
ψ	= 0	Initial phase

Vertical axis - $U_\perp/c$

Horizontal axis - phase of electron with respect to wave

Figure 3.4a

Probability distribution functions of final electron perpendicular energy.

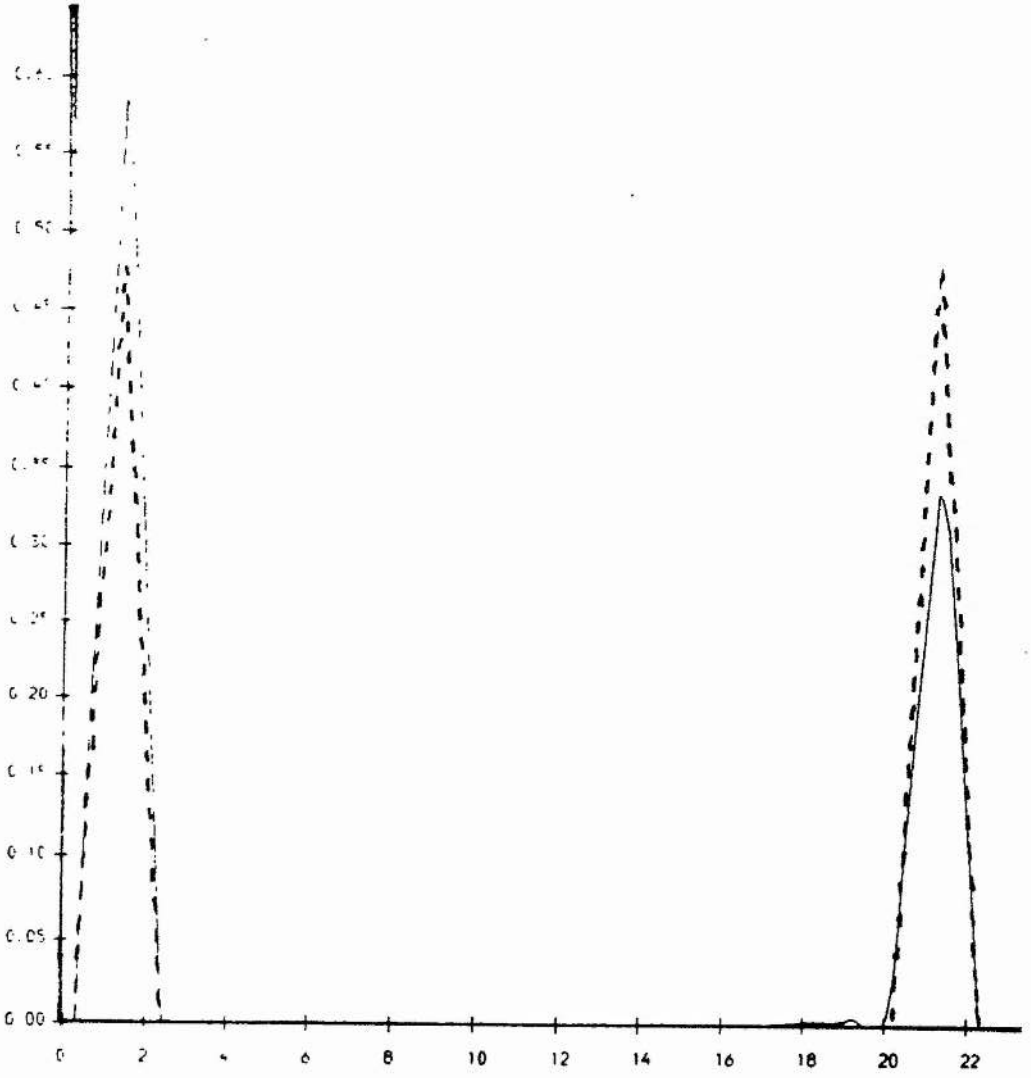

$U_\perp$	$= 10^7$ ms^{-1}	Initial perpendicular velocity
$U_\parallel$	$= 10^7$ ms^{-1}	Initial parallel velocity
Profile		Gaussian
L	= 0.025 m	Beam width
Mode		O mode
$E_\parallel$	$= 5*10^7$ Vm^{-1}	Peak parallel electric field
B_0	=1.0 T	Magnetic field.
$n_\parallel$	= 0	Parallel refractive index
$1/\gamma - 1/\beta$	= 0.005	Frequency mismatch

Dotted line - theoretical form for the probability

Solid line - numerical form for the probability

Vertical axis probability density P(μ)

Horizontal axis final moment/initial moment

Figure 3.4b

Probability distribution functions of final electron perpendicular energy.

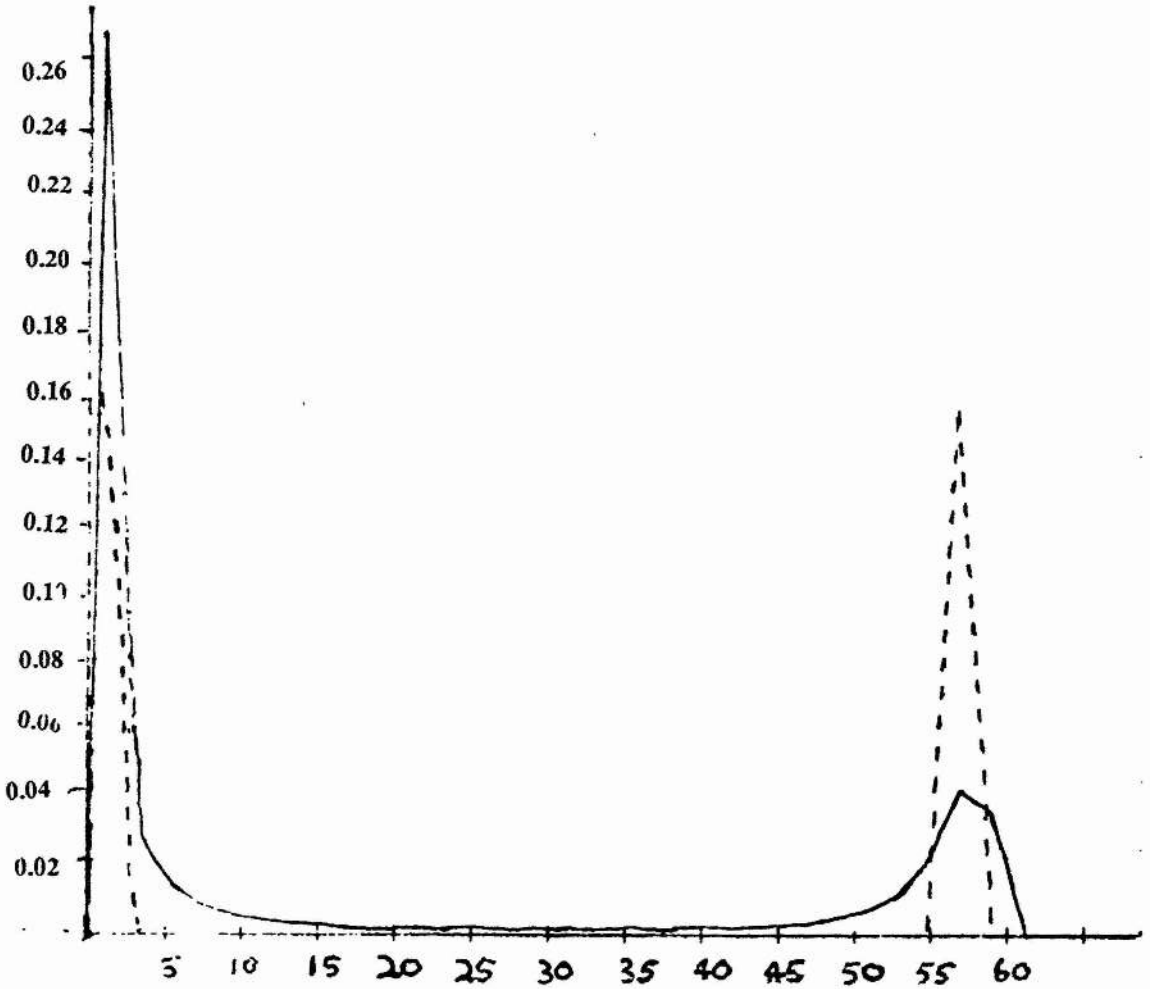

$U_\perp$	$= 10^7$ ms^{-1}	Initial perpendicular velocity
$U_\parallel$	$= 10^7$ ms^{-1}	Initial parallel velocity
Profile		Gaussian
L	= 0.025 m	Beam width
Mode		O mode
$E_\parallel$	$= 10^8$vm^{-1}	Peak parallel electric field
B_0	=1.0 T	Magnetic field.
$n_\parallel$	= 0	Parallel refractive index
$1/\gamma - 1/\beta$	= 0.005	Frequency mismatch

Dotted line - theoretical form for the probability

Solid line - numerical form for the probability

Vertical axis probability density P(μ)

Horizontal axis final moment/initial moment

Figure 3.4c

Probability distribution functions of final electron perpendicular energy.

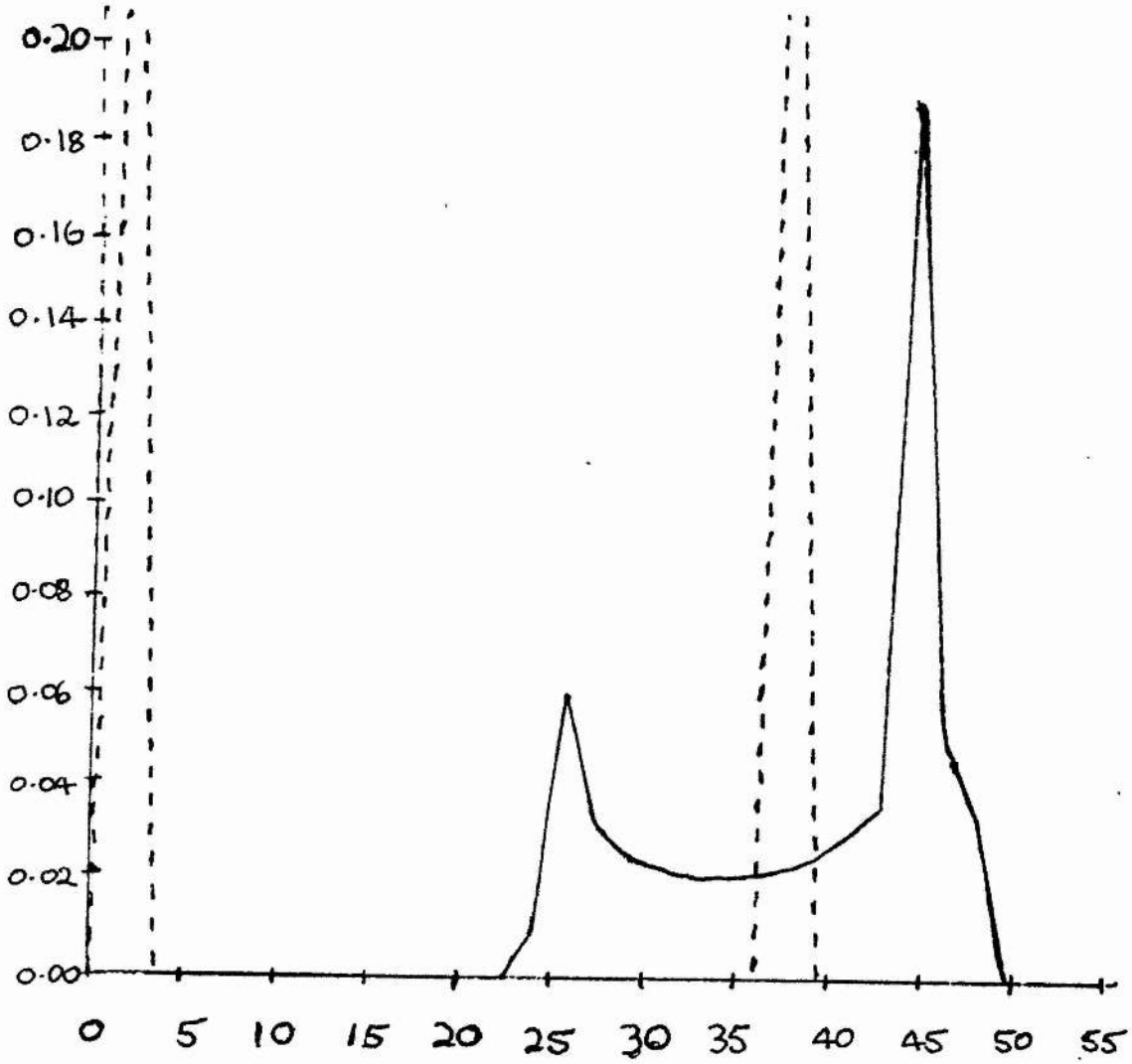

$U_\perp$	$= 10^7$ ms^{-1}	Initial perpendicular veloci
$U_\parallel$	$= 10^7$ ms^{-1}	Initial parallel velocity
Profile		Gaussian
L	= 0.025 m	Beam width
Mode		O mode
$E_\parallel$	$= 2x10^8$vm^{-1}	Peak parallel electric field
B_0	=1.0 T	Magnetic field.
$n_\parallel$	= 0	Parallel refractive index
$1/\gamma - 1/\beta$	= 0.005	Frequency mismatch

Dotted line - theoretical form for the probabili

Solid line - numerical form for the probabili

Vertical axis probability density P(μ)

Horizontal axis final moment/initial moment

In Chapter four we return to the problem of assessing the condition under which the theory is valid, noting here that it appears to work only for particles which are heated but which are not exactly in resonance. More particularly however we note that in figures (3.3a) and (3.3b) the electrons do not actually appear to be trapped, yet in figure (3.3b) the final energy is much higher than the initial energy. We conclude that trapping is not after all a strictly necessary condition that nonlinear heating should take place. (The electrons do however make a number of large oscillations in phase space and are clearly close to being trapped. We will therefore for later work still require that condition 2 be fulfilled, if (3.4b) is to be a possible solution of (3.2).)

It is ironical that figure (3.3c) shows an electron which is trapped, making a small number of rotations, before being detrapped, even though figure (3.4c) shows the least agreement between numerical and analytic form. The reason for the discrepancy is however immediately apparent: the value of the electric field clearly changes considerably during the final orbit so the electron does not travel on an orbit given by an autonomous Hamiltonian. The final velocity depends on how far around the fixed point the electron has travelled, which will in turn depend on the initial phase of the electron.

It is not easy to see how these nonadiabatic influences should be incorporated into a more sophisticated theory of heating and we do not attempt to do this in the thesis. Nonetheless it would clearly be an interesting theoretical challenge. Finally we note figure (3.3c) contains one more interesting feature viz the part rotation about the hyperbolic fixed point at $\psi \approx -127.25 = -\pi/2 \mod 2\pi$ at the start of the electron path in phase space.

Discussion of the beam profile.

In this section we investigate to what extent the exact shape of the profile matters to the heating effect by comparing a Gaussian beam with a triangular and a tophat profile. The form of the triangular beam is

$$E = E_{peak} (T_b - |z|) \text{ for } |z| \leq T_b$$

where T_b is a length scale proportional to the width of the Gaussian chosen to make the power of the two beams equal. One might be forgiven for imagining that the first two profiles might produce identical effects as both go to zero at the ends of the beam and change relatively slowly. The figures (3.5a), (3.5b) and (3.5c) show the probability density for the change in moment of an electron interacting with a Gaussian, a triangular and a tophat beam respectively. Although the first two probability densities are broadly similar there are small differences in shape and maximum moment possible using the two profiles, in particular the spread of velocities around the two theoretical spikes is larger for the triangular beam. The reason for these small differences is that nonadiabatic effects occur at different spatial points for the two beams. (We should point out here that a triangular distribution is not intended to be an approximation to any particular output from a gyrotron or laser, but is used here simply for comparison with a Gaussian. In practice the profile of the output from a gyrotron or FEL will not even be exactly Gaussian, and may be quite complicated especially at the edges.)

In stark contrast figure (3.5c) shows the equivalent picture when a tophat profile is used. The beam width has been chosen to make the total power of the wave equal to that of the triangular and Gaussian beams, while keeping the peak electric fields the same. The theoretical form bears little resemblance to the numerical form as the adiabaticity requirement is not satisfied. The heating of many particles is substantially above the theoretical form, because the fixed point does not alter through the beam. Particles rotate in orbits in the way they would only at the point z=0 in a Gaussian beam, with a fixed point μ_{FP} independent z. The final velocity will depend on how far around the fixed point the electron has

Figure (3.5a)
Gaussian Profile

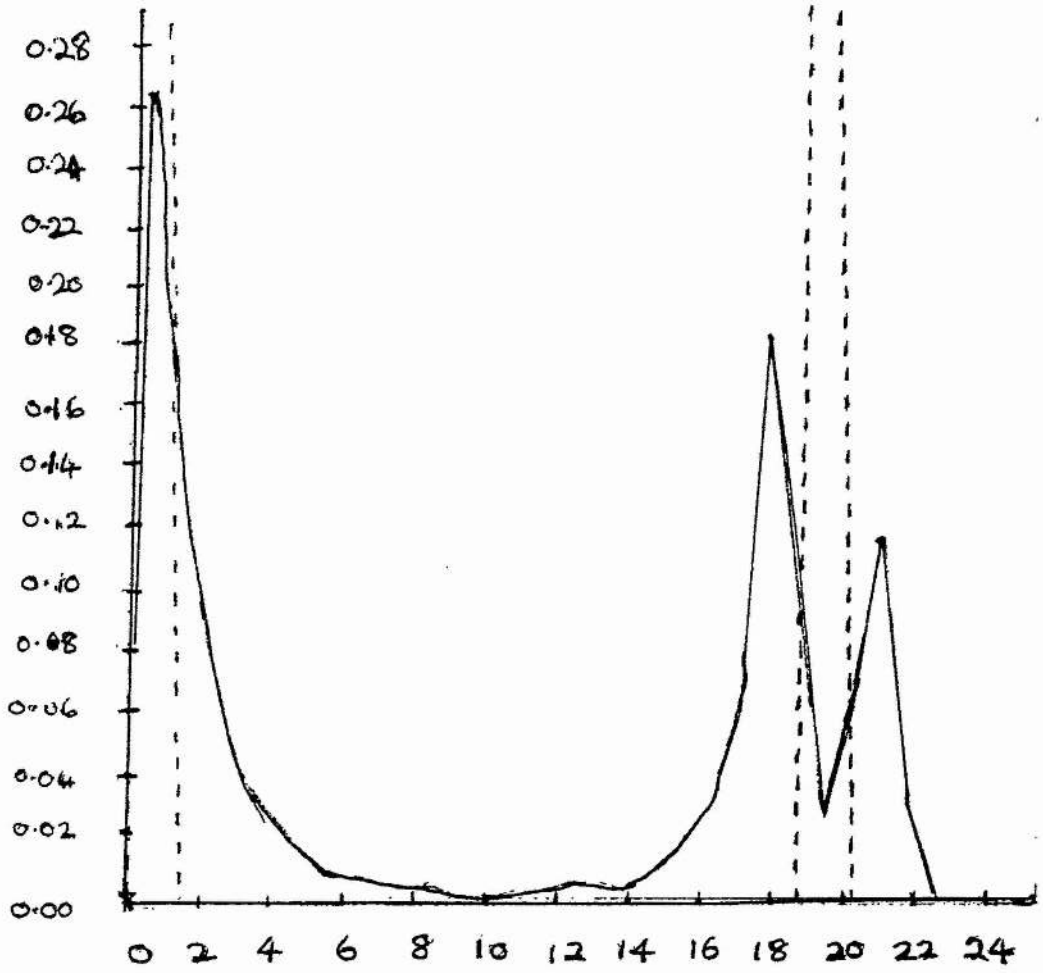

$U_\perp$	$= 10^7$ ms^{-1}	Initial perpendicular velocity
$U_\parallel$	$= 10^7$ ms^{-1}	Initial parallel velocity
L	= 0.025 m	Beam width
Mode		O mode
$E_\parallel$	$= 5*10^7$ Vm^{-1}	Peak parallel electric field
B_0	=5.0 T	Magnetic field.
$n_\parallel$	= 0	Parallel refractive index
$1/\gamma - 1/\beta$	= 0.005	Frequency mismatch

Dotted line - theoretical form for the probability
Solid line - numerical form for the probability
Vertical axis probability density P(μ)
Horizontal axis final moment/initial moment

Figure (3.5b)
Triangular Profile

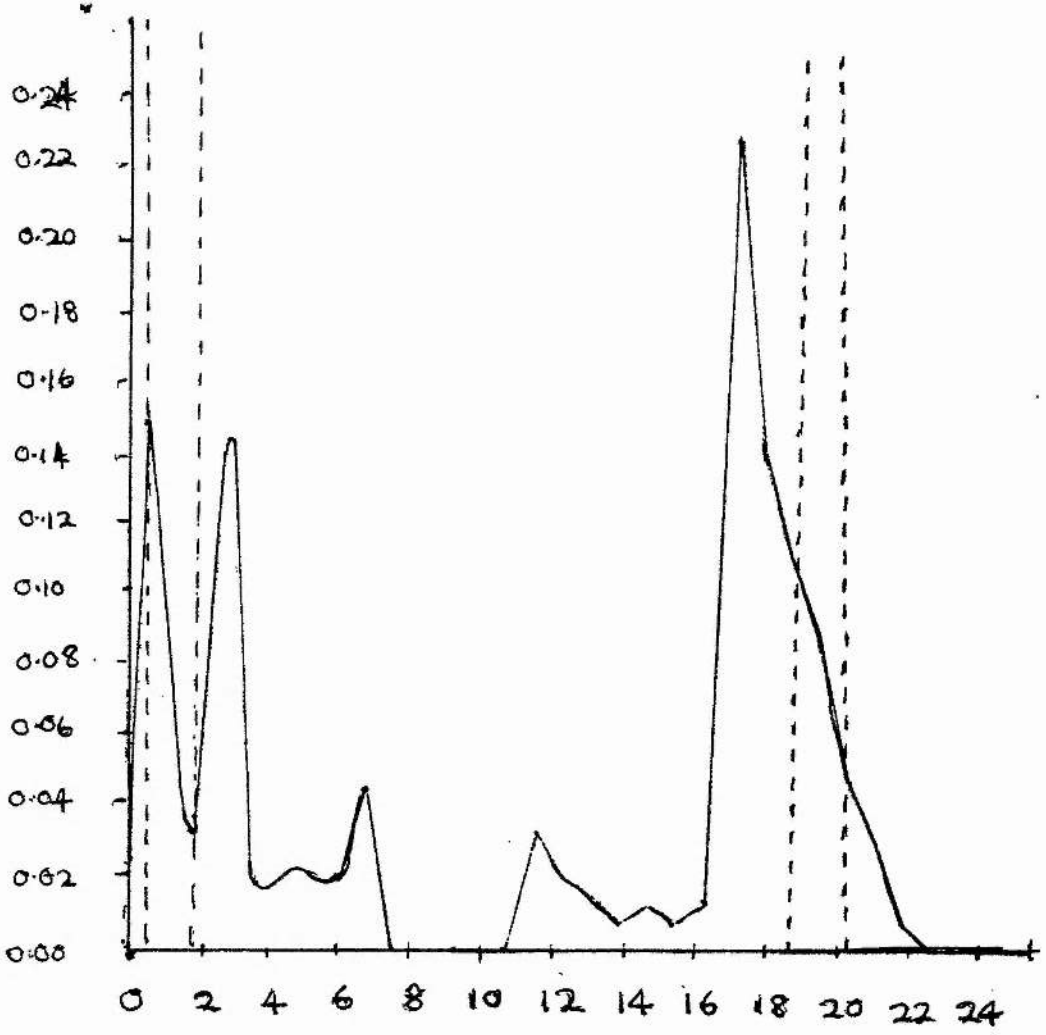

$U_\perp$	$= 10^7$ ms^{-1}	Initial perpendicular velocity
$U_\parallel$	$= 10^7$ ms^{-1}	Initial parallel velocity
T_b	= 0.00392 m	Half beam width
Mode		O mode
$E_\parallel$	$= 5*10^7$ Vm^{-1}	Peak parallel electric field
B_0	=5.0 T	Magnetic field.
$n_\parallel$	= 0	Parallel refractive index
$1/\gamma - 1/\beta$	= 0.005	Frequency mismatch

Dotted line - theoretical form for the probability
Solid line - numerical form for the probability
Vertical axis probability density $P(\mu)$
Horizontal axis final moment/initial moment

Figure (3.5c)
Tophat Profile

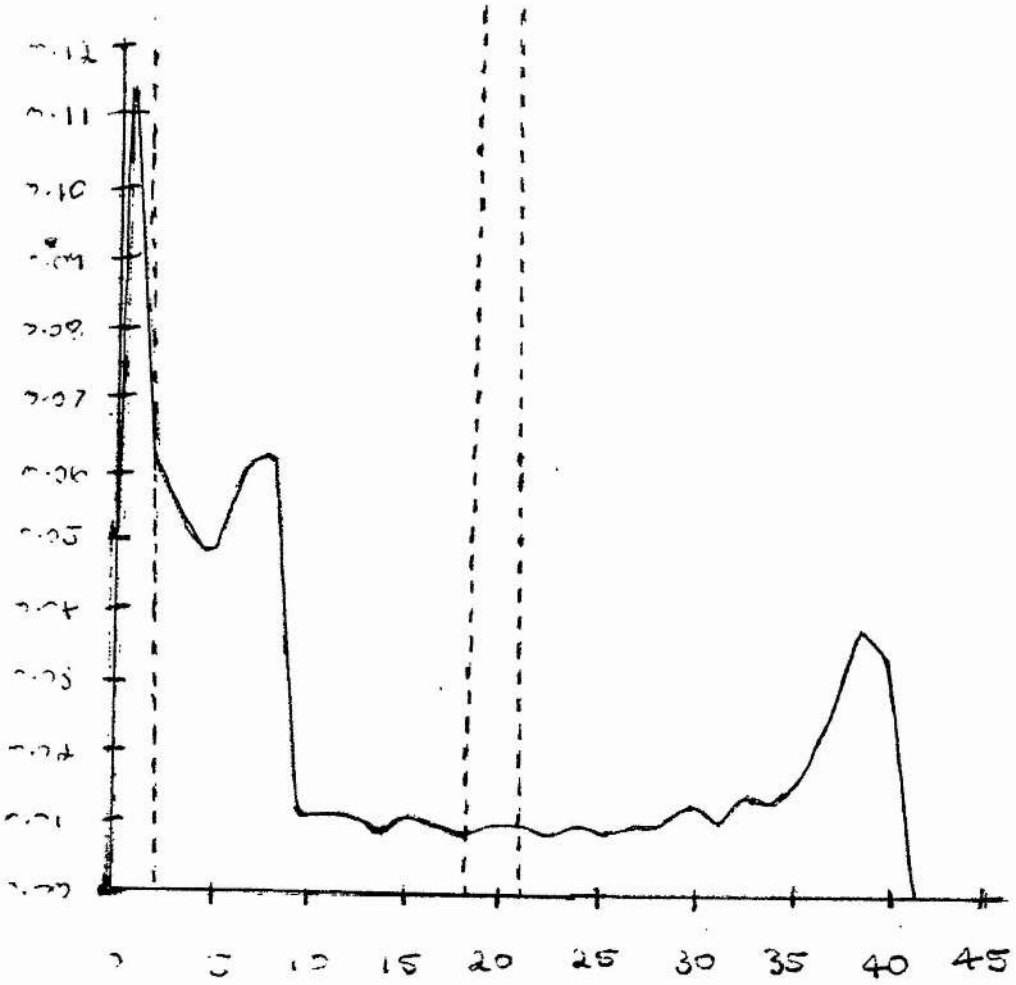

$U_\perp$	$= 10^7$ ms^{-1}	Initial perpendicular velocity
$U_\parallel$	$= 10^7$ ms^{-1}	Initial parallel velocity
T_b	= 0.03133 m	Beam width
Mode		O mode
$E_\parallel$	$= 5*10^7$ Vm^{-1}	Peak parallel electric field
B_0	=5.0 T	Magnetic field.
$n_\parallel$	= 0	Parallel refractive index
$1/\gamma - 1/\beta$	= 0.005	Frequency mismatch

Dotted line - theoretical form for the probability
Solid line - numerical form for the probability
Vertical axis probability density $P(\mu)$
Horizontal axis final moment/initial moment

Figure 3.6

Maximum velocities attained by electrons during heating against beta

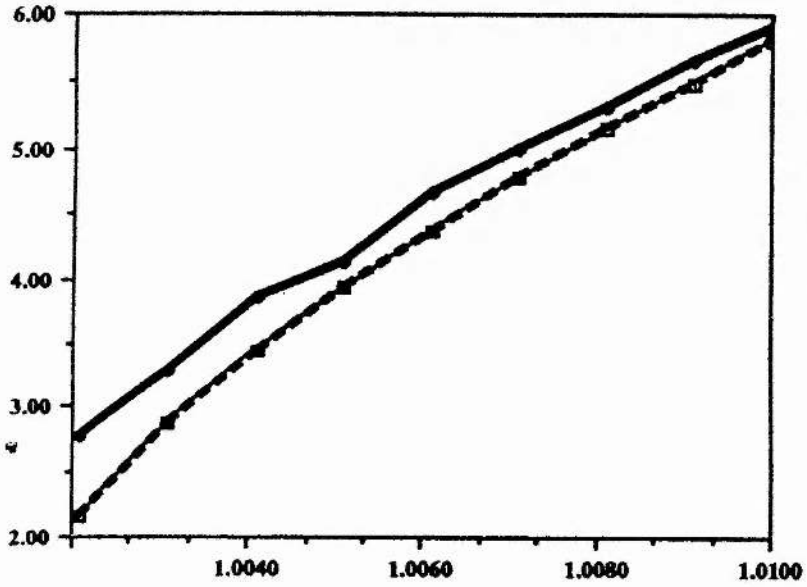

$U_\perp$	$= 10^7$ ms^{-1}	Initial perpendicular velocity
$U_\parallel$	$= 10^7$ ms^{-1}	Initial parallel velocity
Profile		Gaussian
L	= 0.025 m	Beam width
Mode		O mode
$E_\parallel$	$= 5*10^7$ Vm^{-1}	Peak parallel electric field
B_0	=5.0 T	Magnetic field.
$n_\parallel$	= 0	Parallel refractive index

Horizontal axis - ß

Vertical axis - $U_{\perp max}/U_{\perp initial}$

Solid line - numerical result using 25 particles

Dotted line - theoretical result using equation (3.3b)

travelled when it leaves the beam.

Figure (3.5c) raises the interesting question: how can we optimise the profile to maximise heating? It would appear that a profile which is not smooth may be more efficient than one which is. However as mentioned earlier the tophat profile is actually unphysical, and a detailed discussion of exact profiles which experimental apparatus produce is well beyond the scope of this thesis.

Dependency of the accuracy of the nonlinear model on the frequency mismatch.

Finally we demonstrate numerically that the accuracy of the approximation can depend on the frequency mismatch between the wave and the electron. In figure (3.6) we plot $U_{\perp max}/U_{\perp i}$, the maximum perpendicular velocity divided by the original velocity, on the vertical axis and ß on the horizontal axis. The solid line corresponds to the maximum perpendicular velocity found when 25 particles are integrated along the beam profile, while the dotted line represents the maximum velocity according to equation (3.3b). Not surprisingly the numerical maximum is slightly higher than the theoretical maximum, because there is a small spread of velocities either side of the theoretical maximum energy. Secondly and perhaps more surprising at first is that the accuracy of the result improves as the frequency mismatch and hence the maximum velocity increase. This is a critical result which enables us to use the model with confidence in circumstances in which ß is not at all close to 1.

Numerical verification given by Nevins et al of their theory.

We should for completeness briefly mention the numerical support Nevins et al give for their theory. In their paper Nevins et al quote two codes which they use to support their model referring to Rognlien (1983) and Langdon and Lasinski (1976). In each case they have compared the numerical and theoretical absorption by solving the equations of motion for an entire distribution of electrons. In this chapter we have tested the theory for a single point in velocity space only, to illustrate circumstances under which their theory holds well, and under which it is **not** a good approximation. Like Rognlien we

have used averaged equations; however his equations do not include the second order effects mentioned as extensions to Taylor's work in Chapter two. The second code referred to, the ZOHAR code, does not use averaged equations but instead uses the Lorentz equation directly. However the quoted paper deals only with application of this code to laser-plasma interaction and it is not clear exactly how the authors implemented the code to verify their results. In Chapter four we test the applicability of the theory to the problem of determining the distribution functions likely to arise as a result of using FEL ECRH. We plot contours of distribution functions given both by the theoretical model, and also by the integration of the equations of motion through the beam for an entire distribution of electrons. We will also comment on the energy absorption law found by Nevins et al as it is the principle source of numerical verification they give for their theory.

3.5 Discussion

In Chapter two we outlined a theory of heating in which the phase of the electron changed little during the heating, while in this chapter we have considered the opposite limit in which the phase oscillates about a fixed point many times during transit of the beam. The physics of the two scenarios are completely different. In the former case only resonant particles receive substantial amounts of energy from the wave while in the latter case wave absorption is dominated by interaction with nonresonant electrons. In between these two extremes will be cases where $T_{rot} \approx T_{transit}$ and we have no theory to explain this situation. For Maxwellian plasmas of temperature ≈1keV we saw in Chapter two that the theory of O'Brien et al was sufficient to explain heating due to gyrotrons, but not that due to FELs. In this chapter we have shown numerically that the adiabatic theory is applicable to field intensities typical of FELs. In Chapter five we will exploit this fact to consider the linear stability of the distributions to e/m waves both when a plasma is heated by gyrotrons and by FELs.

Conclusion.

We have considered the model of Nevins et al of adiabatic heating of electrons in a spatially Gaussian beam of ECRH. We have derived the change in energy of electrons in a more rigorous manner without weakly relativistic approximations and have extended the theory to oblique incidence. We have given a clearer description of conditions under which the particle is trapped and found an expression for the rotation period of particles which perform small elliptical orbits about a fixed point in phase space. We have shown that the form of the beam profile is important and that a tophat profile may lead to higher heating. Finally we have tested the theory numerically at single points in velocity space and demonstrated that the increment in velocity after a single pulse of ECRH using this model may not always be accurate, especially for nearly resonant particles.

CHAPTER FOUR

ELECTRON DISTRIBUTION FUNCTIONS OCCURRING DURING NONLINEAR ECRH

CHAPTER FOUR

Electron Distribution Functions Occurring During Nonlinear Heating and the Validity of the Adiabatic Approximation

In this chapter we consider distributions which are likely to arise due to nonlinear heating. We use the model of Chapter three to predict a distribution function and examine the circumstances under which it may be valid. First however we review the assumptions made in Chapter three. Our purpose in doing so is to analyse the distribution for linear instabilities, and so we will be particularly interested in the gradient of the distribution with respect to its velocity.

4.1 Review of the Assumptions made in the Nonlinear Model and the Differences between the theory of Nevins et al and the Refined theory presented in Chapter three

Over the course of this thesis a number of approximations have been made in order to obtain the change in velocity of an electron which has passed through a beam of intense pulsed ECRH. Some of the main assumptions are as follows:

(1) that the equations of motion and the Hamiltonian of interaction between an electron and an e/m beam can be averaged over the fast time variations near a resonance, and consequently that only contributions from a single harmonic (the first) need be considered;

(2) that the motion in a Gaussian beam can be considered to be adiabatic;

(3) that some electrons may be trapped in phase space by a beam and that only those which are trapped will be heated;

(4) that the transition probability for the final energy state (3.3b) given

that the conditions (1) to (3) of Chapter three are satisfied is 1/2, and that if these conditions are not satisfied the probability is zero.

Assumption (1) was made by Taylor et al (1988) and was tested numerically in Taylor (1987) and Chapter two of this thesis. Assumptions (2) to (4) can be tested by integrating the equations of motion using the gyroaveraged equations and comparing the final distribution with that obtained adiabatically. As the assumption of greatest interest is the adiabatic assumption we examine it in greater detail in section 4.4.

In the paper of Nevins et al the expression (3.3c) was derived for the energy change of individual electrons and an energy scaling law was derived, for the case that the energy absorption is much higher than the thermal energy of the electrons. They made the following approximations not included above:

(5) the weakly relativistic approximation in obtaining (3.3c), and

(6) the approximation that μ_i could be neglected compared with $\Delta\mu$ for most heated electrons.

Here we emphasise that we have made no weakly relativistic approximation in obtaining our alternative formula (3.3b), but that we do use the weakly relativistic approximation in obtaining condition (2), the trapping condition.

It is worthwhile investigating the difference these extra approximations make for parameters typical of MTX. In figure (4.1) we plot energy absorption against the electric field for a Maxwellian distribution at a single flux surface. The average slope of the curve in figure (4.1)is 5/3. However it would be incorrect to claim that we had discovered a $E_{||}^{5/3}$ scaling law. In fact at higher electric fields the gradient does decline to approximately 4/3, while it is far closer to 2 near the origin. Although these results confirm the 4/3 power law of Nevins et al, Davidson et al and Kotel'nikov and Stupakov for exceptionally high electric fields, there is a significant discrepancy at lower fields. The reason

Figure 4.1

Power Absorption

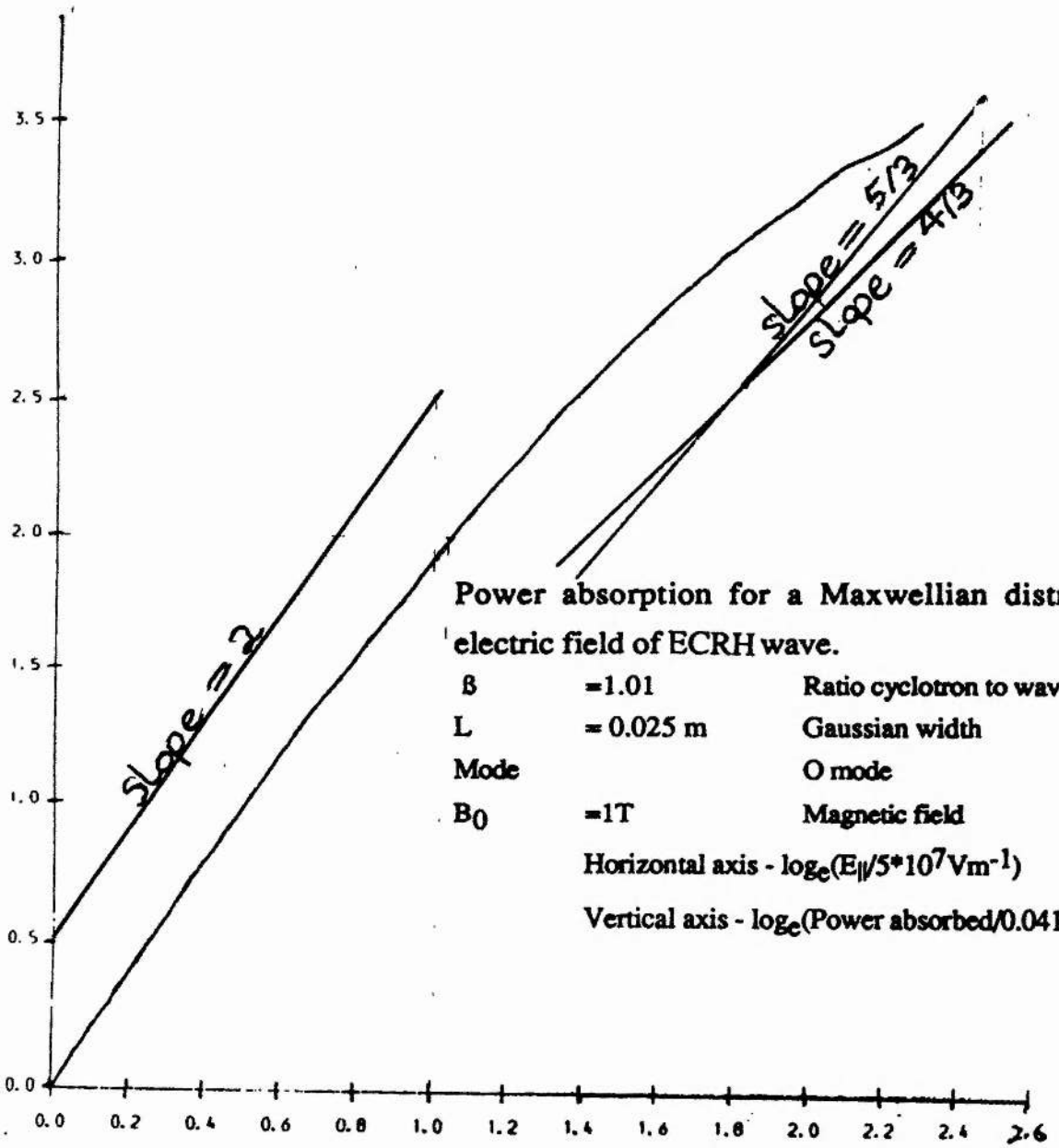

Power absorption for a Maxwellian distribution temperature 1keV against electric field of ECRH wave.

ß	=1.01	Ratio cyclotron to wave frequency
L	= 0.025 m	Gaussian width
Mode		O mode
B_0	=1T	Magnetic field

Horizontal axis - $\log_e(E_{\parallel}/5*10^7 Vm^{-1})$

Vertical axis - $\log_e$(Power absorbed/0.0412*thermal energy)

for this lies in the use of the cold plasma approximation - ie the assumption that the typical gain in energy of electrons is much larger than their thermal energy. Employment of the weakly relativistic approximation instead of the full relativistic expression is relatively unimportant. We shall however see that use of the fully relativistic expression leads to a surprisingly simple analytic formula for the distribution function obtained, given that a single pulse of FEL ECRH interacts with a plasma which has a Maxwellian distribution of electron velocities. In fact in later work it leads to expressions of simpler form than that obtained if we were to use formula (3.3c) instead.

An accurate theoretical model for energy absorption depends ultimately on the distribution function of electrons prior to heating. It is not the purpose of this thesis to consider scaling laws for current drive and energy absorption etc on the basis of this heating model as one of the conclusions we make is that the distribution functions created in the process may be unstable.

4.2 Distributions Given by Nonlinear Heating.

In this section we attempt to explain how we use the adiabatic heating theory to find a model for the distribution of electron velocities immediately after a single pulse of ECRH without considering the effect of collisions. Throughout the section we refer to coordinates in velocity space of an electron after it has passed through the beam with subscript f and we denote a velocity coordinate by a subscript i if it represents the initial velocity of an electron that has been heated according to the nonlinear model presented in Chapter three ($\gamma_f = 2ß - \gamma_i$).

Firstly we recall that electrons in tokamaks are generally confined to flux surfaces, so that our aim will be to find the distribution on a given flux surface. Secondly we recall that our work to date has been in a slab geometry and that toroidal effects, such as the change in magnetic field as the electron travels through the beam, have been ignored. Consistent with this approach we identify each flux surface with the parameter ß, ie $\Omega(x)/\omega$, *at the point where the flux surface interacts with the beam of ECRH* . Of course Ω changes around the flux surface, but if the beam is sufficiently small compared with the major radius of the tokamak and the distance of the flux surface from the minor axis each flux surface will correspond to a single value of ß at the location of the heating.

Next we note from Chapter three that the conditions (1) to (3) hold for a particular position in velocity space if and only if the mirror image position given by (3.3b) or (3.4a) in the perpendicular and oblique cases respectively satisfy these conditions. This is easy to see in the case of perpendicular propagation as $p_{||}$ is constant throughout the heating and the conditions are independent of initial moment. In the case of oblique propagation our statement can be supported by noting that the underlying equations of motion are reversible in time. This will be of help in defining the final distribution function after a FEL ECRH pulse.

Suppose the distribution before application of ECRH is a Maxwellian or Bimaxwellian which we shall denote by f_{max}, and that we assume that exactly half of the particles becoming trapped from below the separatrix are heated. It

is also possible that particles may be trapped from above and be cooled, though the contribution to the overall shape of the distribution function is not much altered due to cooling as there are many fewer particles in the regime in which particles are liable to be cooled. The distribution is now given by

$$f_{ECRH}(p_f) = f_{max}(p_f)/2 + f_{max}(p_i)/2 \qquad (4.1a).$$

The final result is an inversion in the electron population about the resonance position as is clearly seen from the relation $\gamma_f = 2\beta - \gamma_i$ and from the sets of figures (4.2) - (4.4). To see this more clearly, note that for a Maxwellian

$$f_{max} = Ne^{-\lambda_T \gamma} \qquad (4.1a),$$

where

$$N = \frac{\lambda_T}{4\pi K_2(\lambda_T)} \qquad (4.1b),$$

K_2 is the modified Bessel function of the second kind order 2 and λ_T is essentially the inverse temperature.

The inverted distribution takes the form

$$f_{ECRH} = \frac{N}{2}\left(e^{-\lambda_T\left(2\beta-\gamma\right)} + e^{-\lambda_T \gamma}\right) \qquad (4.1c)$$

in the region of phase space in which the three conditions are satisfied. (Note that this distribution cannot possibly be valid for all γ - as $f_{ECRH} \to \infty$ as $\gamma \to \infty$! The first of our three conditions alone however ensures that the integral of f_{ECRH} over permitted velocity space is finite.) Now

$$\frac{d\, f_{ECRH}}{d\gamma} = -\frac{N}{2}\lambda_T\left(1 - e^{-2\lambda_T(\beta-\gamma)}\right)$$

$= 0$ when $\gamma=\beta$.

For $\gamma>\beta$ $df_{ECRH}/d\gamma > 0$, proving an inversion **may** occur. However, it is not the existence of a positive gradient in $df_{ECRH}/d\gamma$ which is a necessary and sufficient condition for an inversion, but the existence of a positive gradient in the overall distribution on a flux surface, f_{flux}. We shall soon examine the relation between f_{ECRH} and f_{flux}. However we shall see that inversions do occur and that they are the cause of instabilities which we shall examine in the next section.

So far we have only discussed the situation in which nonlinear interaction occurs. It may be that an electron at point $\underline{p}_f$ is not trapped by the wave in which case the distribution there is unaltered and we simply have

$$f_{ECRH}(\underline{p}_f) = f_{max}(\underline{p}_f) \qquad (4.2a).$$

As $\underline{p}_f$ satisfies the conditions if and only if $\underline{p}_i$ does, we have completely defined the final distribution function. Furthermore we have considered only the distribution of electrons given that they pass through the beam. In a single pulse typical for example of MTX, most electrons on a given flux surface will not pass through the beam so

$$f_{flux} = Q_{pass} f_{ECRH} + (1-Q_{pass}) f_{max}, \qquad (4.2b)$$

where Q_{pass} represents the probability that an electron will pass through the beam, assumed proportional to $p_{||}$. More specifically we shall define the *mixing parameter* $V_{||c}$ (which has the same dimensions as velocity) such that $Q_{pass}=cp_{||}/V_{||c}$. The magnitude of this quantity will depend on the dimensions

of the tokamak and the beam , the length of the pulse and the distance of the flux surface from the minor radius. It will generally be sufficiently large that no electron will pass through the beam more than once. Suppose the circumference of the tokamak is 10m, the length of the pulse is 50ns and that approximately 1/10 of the flux surface is heated by the beam. Then the appropriate value of $V_{||c}$ will be $2*10^9$ ms^{-1}. A number of complications will arise in practice. Firstly we are neglecting any consideration of **magnetically** trapped particles (see Chapter two) for which the relationship $Q_{pass} \alpha p_{||}$ will not hold. Secondly we have neglected the special case that the heating may occur on a *rational flux surface* eg at q=2, when electrons are effectively confined to a subspace of the flux surface. Both of these considerations are well beyond the scope of this thesis.

Throughout this thesis we shall mainly consider pre-pulse distributions of a Maxwellian form, but we shall also refer to Bimaxwellian distributions of the form

$$f = N_{BM} e^{\frac{-(\lambda_\perp p_\perp^2 + \lambda_{||} p_{||}^2)}{1+\gamma}} \qquad \text{where } \frac{1}{N_{BM}} = \int d^3\underline{p}\, e^{\frac{-(\lambda_\perp p_\perp^2 + \lambda_{||} p_{||}^2)}{1+\gamma}} .$$

We choose this form of the relativistic Bimaxwellian because it reduces to the nonrelativistic Bimaxwellian at low temperature and because the parameters $\lambda_\perp$ and $\lambda_{||}$ are effectively the inverse of the perpendicular and parallel temperature. Finally for $\lambda_\perp=\lambda_{||}$ the distribution reduces to a relativistic Maxwellian. For sufficiently high ratio $T_\perp/T_{||}$ the distribution is unstable to electromagnetic waves (see the next chapter), $T_\perp$ and $T_{||}$ being the temperatures perpendicular and parallel to the magnetic field. Consideration of a Bimaxwellian enables us to estimate the effect of an intense pulse on a distribution whose parallel and perpendicular electron temperatures are unequal.

It is not necessarily the case that the equilibrium distributions existing prior to the application of an ECRH pulse will be Bimaxwellian, but this distribution function is relatively simple and allows for temperature anisotropy.

In order to completely define the distribution function we must determine when adiabatic heating may occur ie when (4.1a) is applicable as opposed to (4.1b). The condition for this is simply that conditions (1), (2), and (3) of Chapter three are fulfilled.

4.3 Integration of the Equations of Motion.

We have integrated the equations of motion for an electron in a beam of ECRH for an entire distribution of electrons in order to determine the shape of the distribution function and compared it with that obtained using the adiabatic model. The numerical tests performed have been done only for the case of no magnetic field inhomogeneity because this allows simplification of the 4 ODEs down to 3 ODEs as demonstrated in Chapter two, and represents a substantial saving in processor time.

Our code chooses a grid in $(p_\perp, p_\parallel, \psi)$ space and simply integrates the electrons through a Gaussian beam using routines from the SPEECH code. At the end the final velocities are put into the same grid at a new location and the new distribution function is determined. Typically a grid size might be 100 by 50 by 50, so there may be 250,000 equations to integrate, which requires extensive computing time. Unfortunately the maximum number of grid points it is possible to take is so small the resultant functions are not smooth (see the figures at the end of the chapter). As it is difficult to numerically differentiate the distribution with respect to its velocity components, and to present straight forward comparisons with the analytic growth rates, we merely give contour plots and cross-sections with respect to $p_\perp$. Due to the prohibitive time required even for relatively modest runs we present results only for three different sets of parameters. The results show increasing validity of the adiabatic model with ß, the ratio of cyclotron to wave frequency.

Our results are shown in the sets of figures (4.2) to (4.4). Each set corresponds to a particular set of parameters. The significant parameter change between the three sets is ß which has the value 1.05, 1.03 and 1.01 in the three sets (4.2) to (4.4) respectively. The first figure in each set is a contour plot of the model distribution function calculated using equations (4.1c) and (4.2). The second is a contour plot of the numerical distribution function calculated using a routine from the SPEECH code which integrates equations (2.5) through a Gaussian beam. This routine is used as part of a code which determines the numerical distribution function, given that the initial distribution has a certain form (Maxwellian in each of these examples). The third figure shows a cross-section of $\log_e(1000f/N)$ against $p_\perp$ for the model distribution at a fixed value of $p_{||}(=0.09)$, and the fourth figure likewise for the numerically calculated distribution. The cross-sections show only points where 1000f/N>1 simply for clarity. A number of features of the model and numerical distributions agree. Firstly they both approximate Maxwellians near $p_{||}=0$ because there $Q_{pass}=0$, cf equation (4.1c). Physically this represents the fact that electrons with no parallel velocity never get to pass through the beam during a pulse in the first place. Secondly away from $p_{||}=0$ the distribution has an inversion in $p_\perp$ (ie $df/dp_\perp>0$ at some points). This is an extremely important feature as we will see in Chapter five that this inversion gives rise to instabilities in the plasma. Henceforth we will refer to the places where $df/dp_\perp=0$ as *critical points* . In addition to these specific points we can see that apart from the jagged nature of the numerical distribution caused partly be the coarseness of the grid used to produce it, the distributions all have qualitatively similar features.

Next we need to look at the differences between the distributions as the parameter ß changes ie as the distance from the centre of the tokamak changes. As ß increases the position of the critical point moves to higher velocities. This is because some particles which satisfy the conditions of Chapter three, and for which $\gamma>ß$, may be cooled, while some of those for which $\gamma<ß$ may be heated. At $\gamma=ß$ a critical point occurs.

Next we need to examine the differences between the numerical and model

distributions. We note that the positions of the critical points differ between the two for each set of parameters. Although in each case the model distribution and the numerical distribution appear to resemble each other closely, the resemblance is qualitative and not quantitative, **as they are plotted on different scales.** In fact the critical point occurs at higher velocities for the numerical distribution than for the model one. This may be seen most easily by examining the cross-sections showing $\log_e(f)$ against $p_\perp$. The reason lies in the presence of nonadiabatic heating discussed at length in Chapter three which is particularly important for nearly resonant particles. It is not surprising that the positions of the critical points differ. We also note that the model and numerical distributions show a little less agreement in figures 4.4 where ß=1.01. The reason is simply that for this parameter and with the 1keV Maxwellian distribution the critical point occurs at $V/V_{th} \approx 2.5$, so a considerable number of electrons experience nearly resonant interaction, so that non-adiabatic effects become very important. Again this finding is in agreement with our findings in Chapter three where we looked at single particle motion in some detail.

It must be stressed that these plots are only approximations to the actual contour plots and cross-sections. Even for the model distribution, the contour details are sufficiently complicated for the exact location of critical points to be hard to determine exactly. The situation is far worse for the numerically produced distribution, hence a large number of small contour rings appear around local maxima of the distribution which appear seemingly randomly. Furthermore the edges of the contours are extremely jagged. The contour plots were produced using a GHOST contour plotting routine, and required relatively large amounts of interactive CPU time simply to plot. Similarly the cross-sections would have appeared extremely hard to interpret had we not employed an artificial smoothing technique to enable the overall shape of the curve to be obtained (for example, we have not plotted $\log_e(1000f/N)$ where it is negative). At the expense of a small loss of numerical accuracy, the overall shape of the cross-section has been plotted. This is justified since our objective is to establish qualitative agreement rather than quantitative agreement, and because the untidy

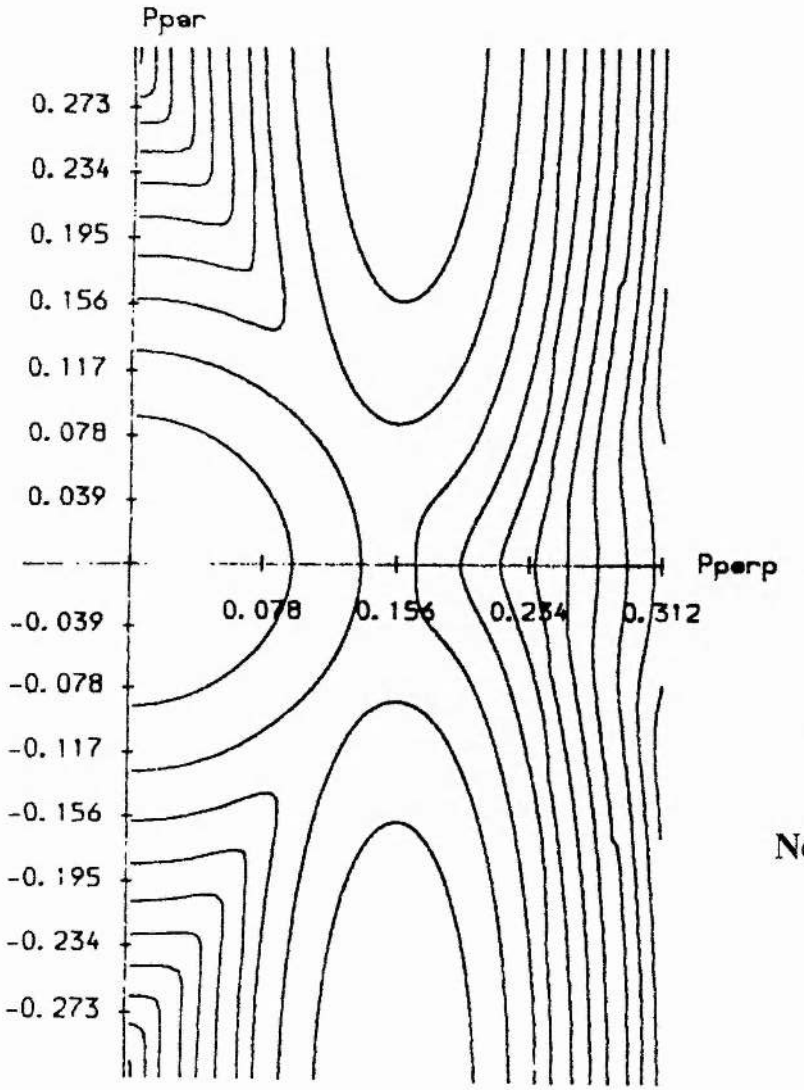

Figure 4.2a - Model Distribution Function.

Contour Plot

ω_{pe}/Ω	Ratio of plasma to cyclotron frequency	= 1/2
$T_\perp$	Perpendicular temperature	= 1 keV
$T_\parallel$	Parallel temperature	= 1 keV
B	Background field	= 2.5T
$n_{\parallel ec}$	Parallel refractive index	= 0
$ß_{EC}$	Ratio of cyclotron to EC wave frequency	= 1.05
$E_\parallel$	Parallel electric field	= 10^8 Vm-1
L	Gaussian beam width	= 0.05m
$V_{\parallel c}$	Mixing parameter	=10^8ms^{-1}

Horizontal axis $p_\perp$

Vertical axis $p_\parallel$

Note: the scale on this plot is not the same as that for Figure 4.2b

Figure 4.2b - Numerical Distribution Function.

Contour Plot

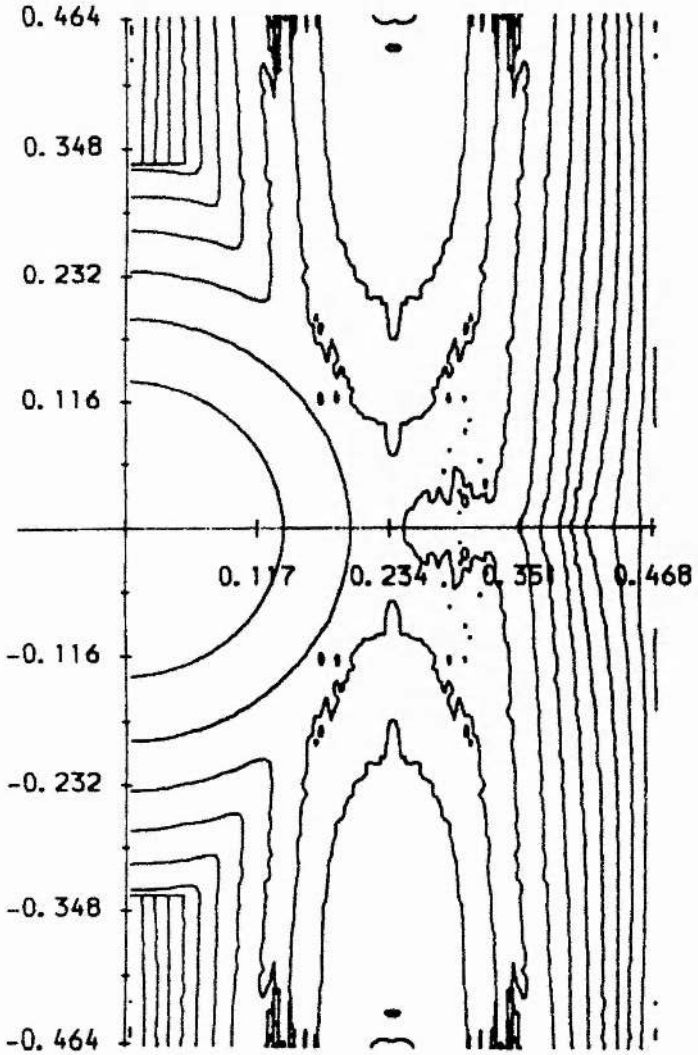

ω_{pe}/Ω	Ratio of plasma to cyclotron frequency	= 1/2
$T_\perp$	Perpendicular temperature	= 1 keV
$T_\parallel$	Parallel temperature	= 1 keV
B	Background field	= 2.5T
$n_{\parallel ec}$	Parallel refractive index	= 0
β_{EC}	Ratio of cyclotron to EC wave frequency	= 1.05
$E_\parallel$	Parallel electric field	= 10^8 Vm-1
L	Gaussian beam width	= 0.05m
$V_{\parallel c}$	Mixing parameter	=10^8ms^{-1}

Horizontal axis $p_\perp$

Vertical axis $p_\parallel$

Note: the scale on this plot is not the same as that for Figure 4.2a

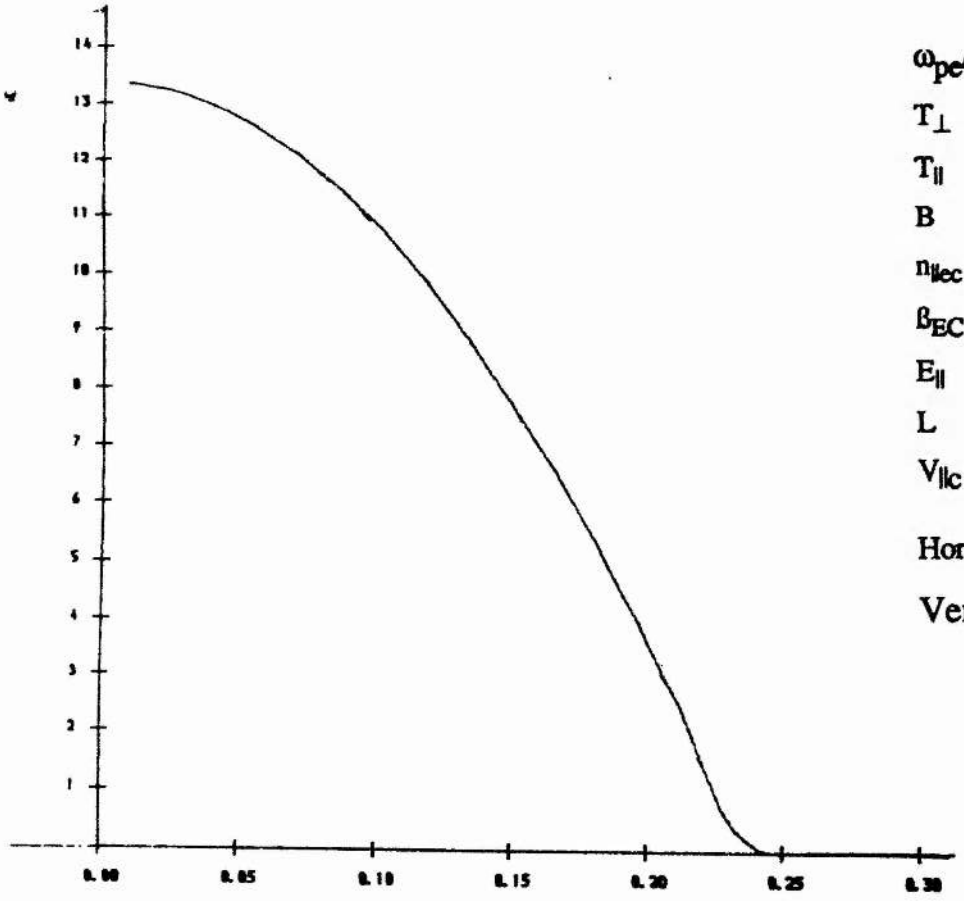

Figure 4.2c - Model Distribution Function.

Log(f) Against $p_\perp$

ω_{pe}/Ω	Ratio of plasma to cyclotron frequency	= 1/2
$T_\perp$	Perpendicular temperature	= 1 keV
$T_\parallel$	Parallel temperature	= 1 keV
B	Background field	= 2.5T
$n_{\parallel ec}$	Parallel refractive index	= 0
β_{EC}	Ratio of cyclotron to EC wave frequency	= 1.0
$E_\parallel$	Parallel electric field	= 10^8 Vm-1
L	Gaussian beam width	= 0.05m
$V_{\parallel c}$	Mixing parameter	=10^8ms^{-1}

Horizontal axis $p_\perp$

Vertical axis $\log_e(1000f/N)$

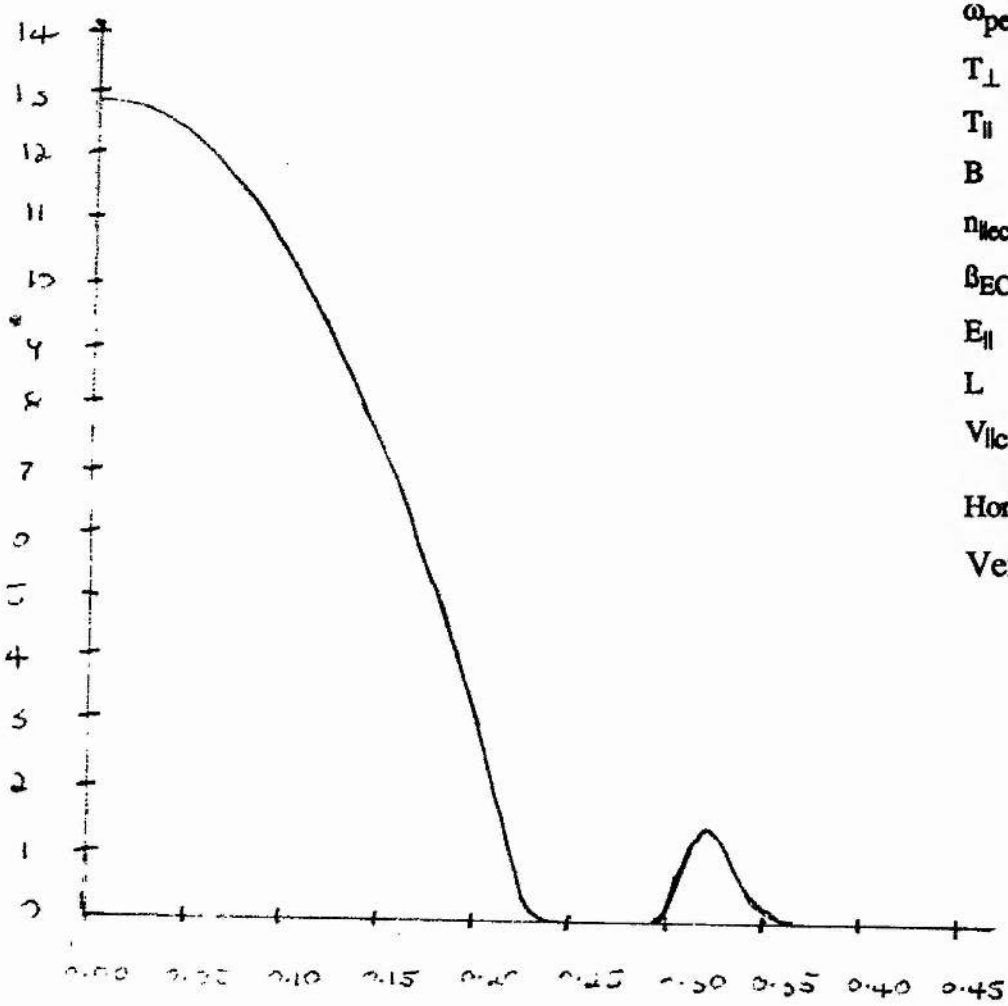

Figure 4.2d - Numerical Distribution Functior

Log(f) Against $p_\perp$

ω_{pe}/Ω	Ratio of plasma to cyclotron frequency	= 1/2
$T_\perp$	Perpendicular temperature	= 1 keV
$T_\parallel$	Parallel temperature	= 1 keV
B	Background field	= 2.5T
$n_{\parallel cc}$	Parallel refractive index	= 0
β_{EC}	Ratio of cyclotron to EC wave frequency	= 1.05
$E_\parallel$	Parallel electric field	= 10^8 Vm-1
L	Gaussian beam width	= 0.05m
$V_{\parallel c}$	Mixing parameter	=10^8ms^{-1}

Horizontal axis $p_\perp$

Vertical axis $\log_e(1000f/N)$

Figure 4.3a - Model Distribution Function.

Contour Plot

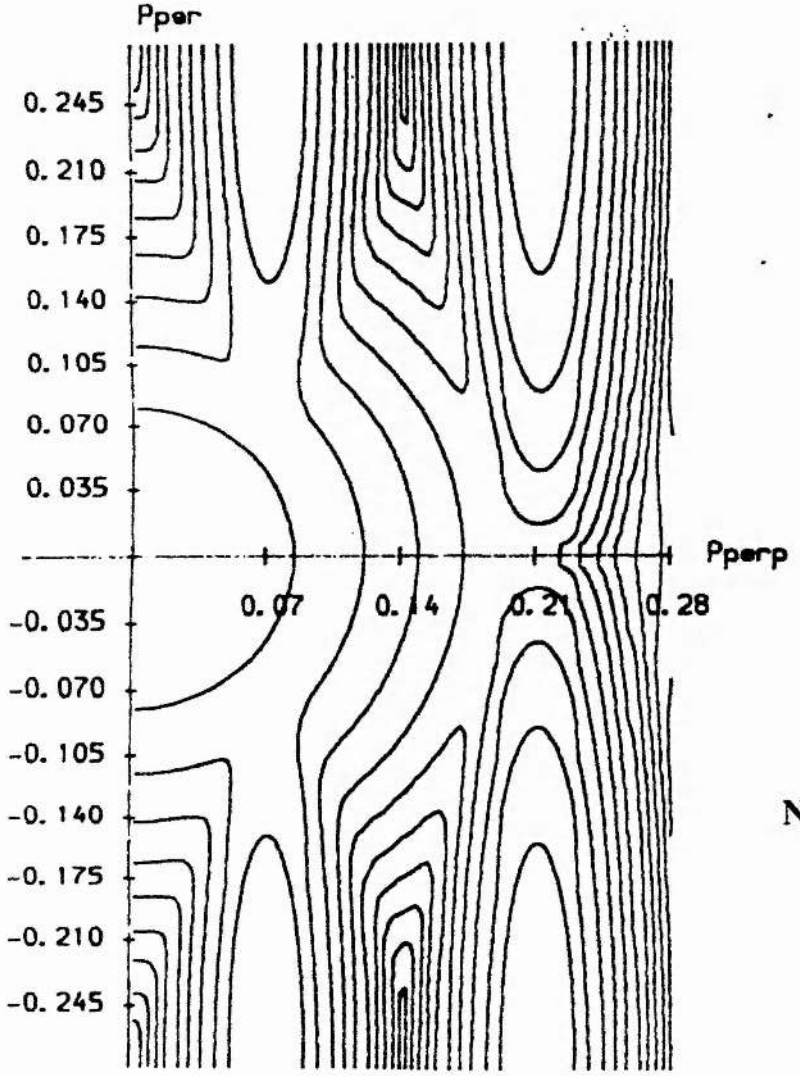

ω_{pe}/Ω	Ratio of plasma to cyclotron frequency	= 1/2
$T_\perp$	Perpendicular temperature	= 1 keV
$T_\parallel$	Parallel temperature	= 1 keV
B	Background field	= 2.5T
$n_{\parallel ec}$	Parallel refractive index	= 0
β_{EC}	Ratio of cyclotron to EC wave frequency	= 1.03
$E_\parallel$	Parallel electric field	= $5*10^7$ Vm-1
L	Gaussian beam width	= 0.05m
$V_{\parallel c}$	Mixing parameter	= 10^8ms^{-1}

Horizontal axis $p_\perp$

Vertical axis $p_\parallel$

Note: the scale on this plot is not the same as that for Figure 4.3b

Figure 4.3b - Numerical Distribution Function.

Contour Plot

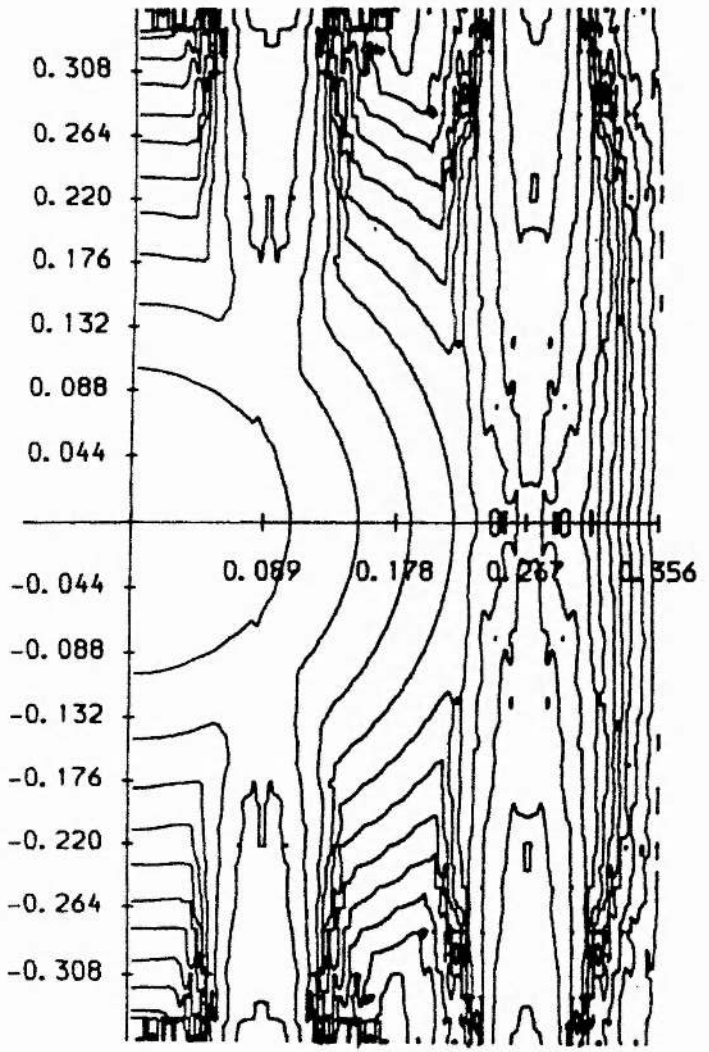

ω_{pe}/Ω	Ratio of plasma to cyclotron frequency	= 1/2
$T_\perp$	Perpendicular temperature	= 1 keV
$T_\parallel$	Parallel temperature	= 1 keV
B	Background field	= 2.5T
$n_{\parallel ec}$	Parallel refractive index	= 0
β_{EC}	Ratio of cyclotron to EC wave frequency	= 1.03
$E_\parallel$	Parallel electric field	= $5*10^7$ Vm-1
L	Gaussian beam width	= 0.05m
$V_{\parallel c}$	Mixing parameter	= $10^8 ms^{-1}$

Horizontal axis $p_\perp$

Vertical axis $p_\parallel$

Note: the scale on this plot is not the same as that for Figure 4.3a

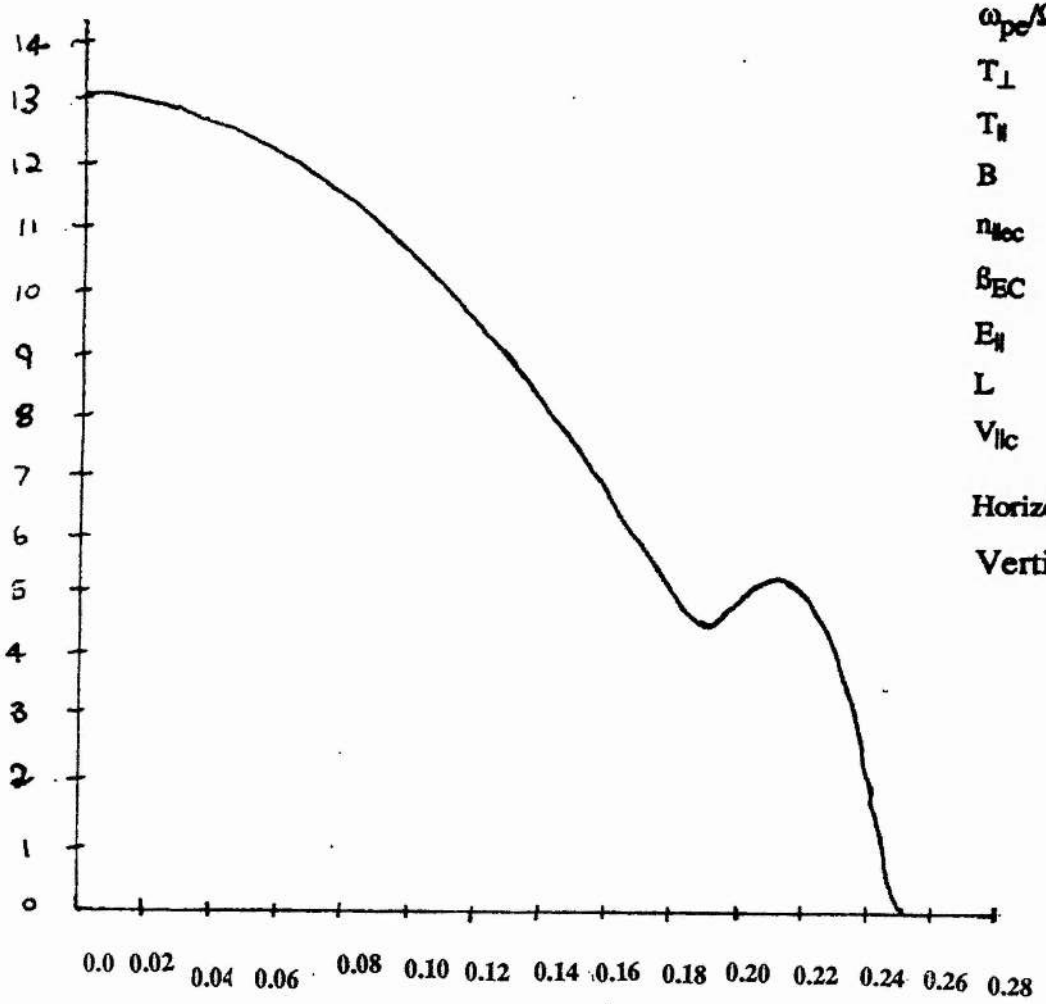

Figure 4.3c - Model Distribution Function.

Log(f) Against $p_\perp$

ω_{pe}/Ω	Ratio of plasma to cyclotron frequency	= 1/2
$T_\perp$	Perpendicular temperature	= 1 keV
$T_\parallel$	Parallel temperature	= 1 keV
B	Background field	= 2.5T
$n_{\parallel ec}$	Parallel refractive index	= 0
β_{EC}	Ratio of cyclotron to EC wave frequency	= 1.03
$E_\parallel$	Parallel electric field	= $5*10^7$ Vm-1
L	Gaussian beam width	= 0.05m
$V_{\parallel c}$	Mixing parameter	= $10^8 ms^{-1}$

Horizontal axis $p_\perp$

Vertical axis $\log_e(1000f/N)$

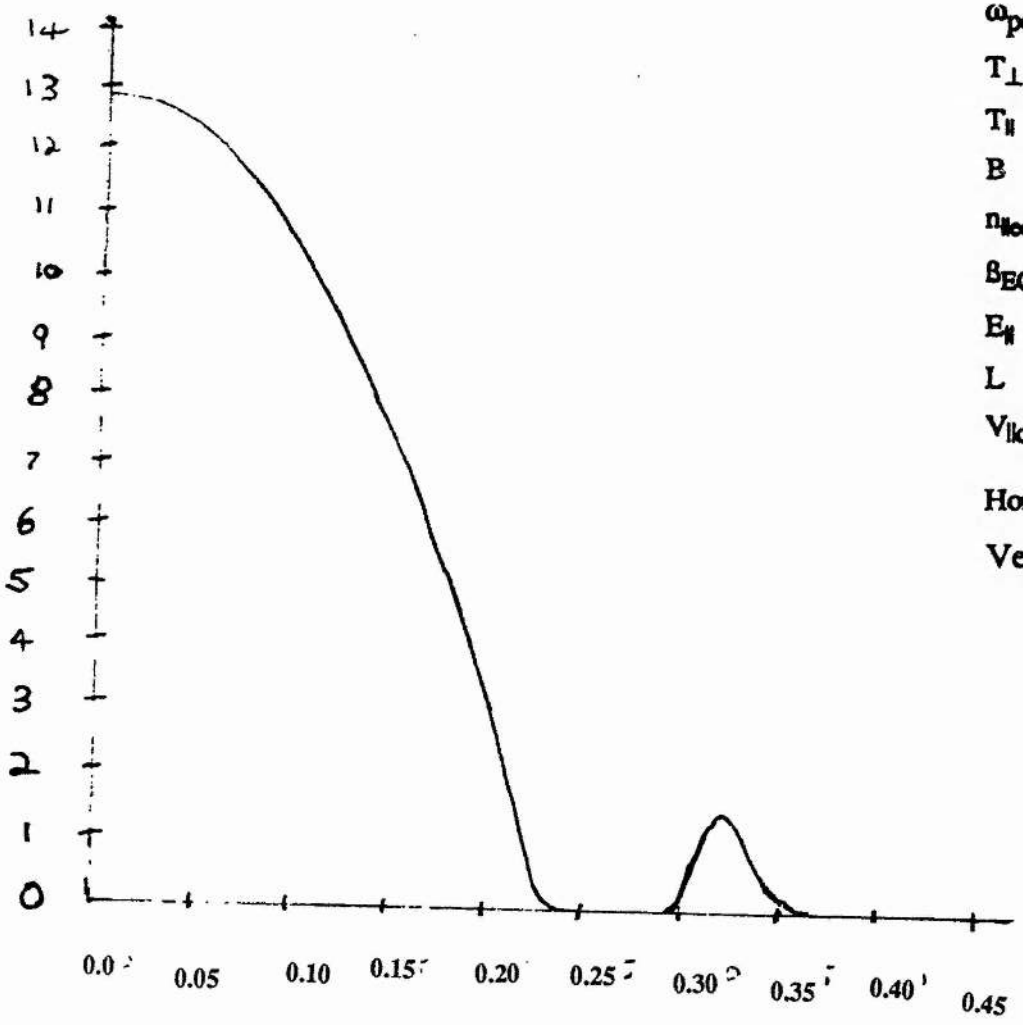

Figure 4.2d - Numerical Distribution Functi

Log(f) Against $p_\perp$

ω_{pe}/Ω	Ratio of plasma to cyclotron frequency	= 1/2
$T_\perp$	Perpendicular temperature	= 1 keV
$T_\parallel$	Parallel temperature	= 1 keV
B	Background field	= 2.5T
$n_{\parallel ec}$	Parallel refractive index	= 0
β_{EC}	Ratio of cyclotron to EC wave frequency	= 1.05
$E_\parallel$	Parallel electric field	= 10^8 Vm-1
L	Gaussian beam width	= 0.05m
$V_{\parallel c}$	Mixing parameter	=10^8ms^{-1}

Horizontal axis $p_\perp$

Vertical axis $\log_e(1000f/N)$

Figure 4.4a - Model Distribution Function.

Contour Plot

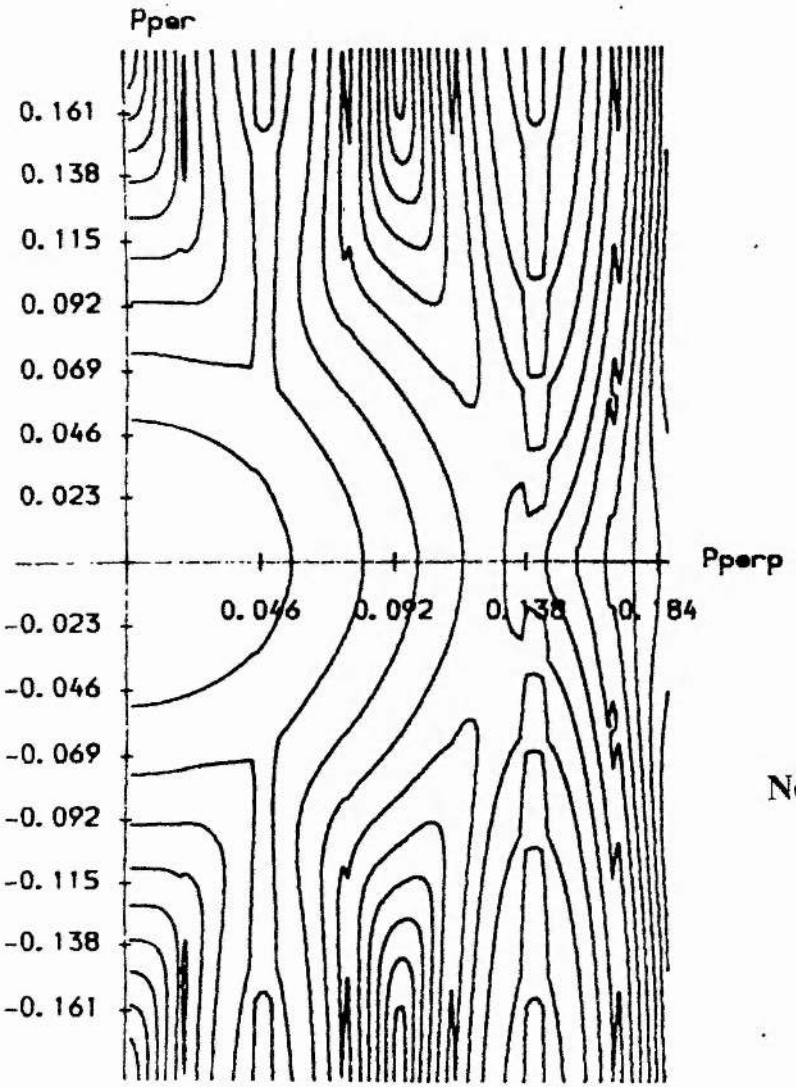

ω_{pe}/Ω	Ratio of plasma to cyclotron frequency	= 1/2
$T_\perp$	Perpendicular temperature	= 1 keV
$T_\parallel$	Parallel temperature	= 1 keV
B	Background field	= 2.5T
$n_{\parallel ec}$	Parallel refractive index	= 0
β_{EC}	Ratio of cyclotron to EC wave frequency	= 1.01
$E_\parallel$	Parallel electric field	= $2.5*10^7$Vm-1
L	Gaussian beam width	= 0.05m
$V_{\parallel c}$	Mixing parameter	= 10^8ms^{-1}

Horizontal axis $p_\perp$

Vertical axis $p_\parallel$

Note: the scale on this plot is not the same as that for Figure 4.4b

Figure 4.4b - Numerical Distribution Function.

Contour Plot

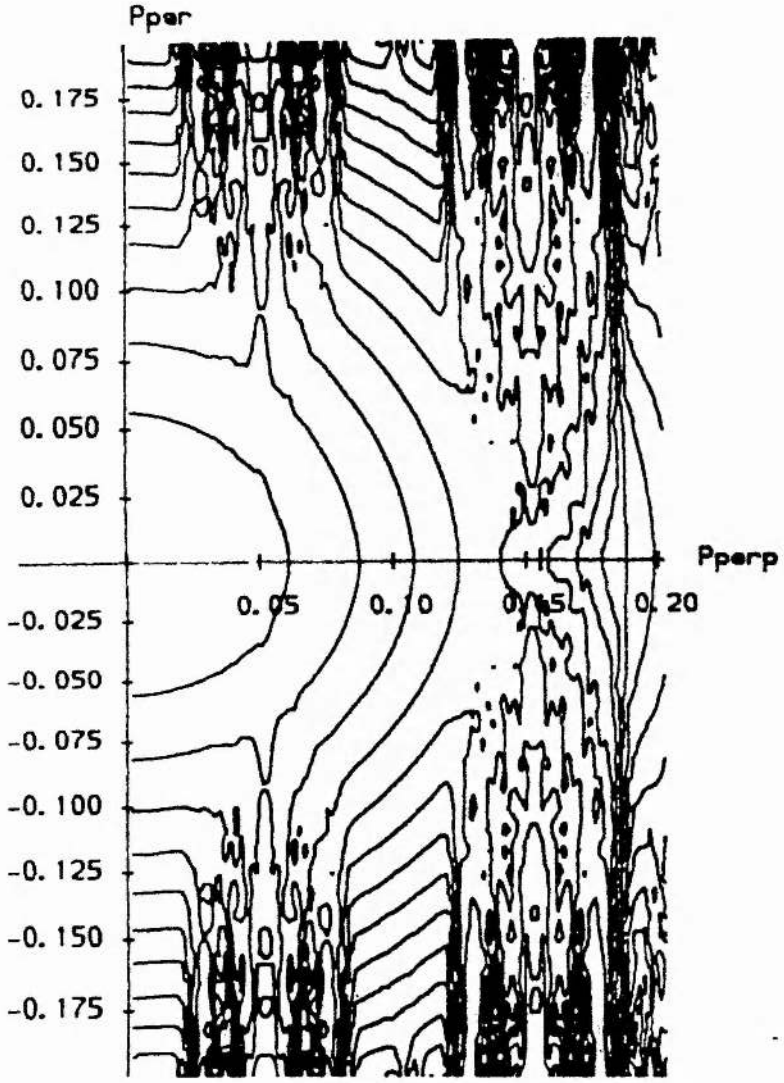

ω_{pe}/Ω	Ratio of plasma to cyclotron frequency	= 1/2
$T_\perp$	Perpendicular temperature	= 1 keV
$T_\parallel$	Parallel temperature	= 1 keV
B	Background field	= 2.5T
$n_{\parallel ec}$	Parallel refractive index	= 0
$ß_{EC}$	Ratio of cyclotron to EC wave frequency	= 1.01
$E_\parallel$	Parallel electric field	= $2.5*10^7$ Vm-1
L	Gaussian beam width	= 0.05m
$V_{\parallel c}$	Mixing parameter	= $10^8 ms^{-1}$

Horizontal axis $p_\perp$

Vertical axis $p_\parallel$

Note: the scale on this plot is not the same as that for Figure 4.4a

Figure 4.4c - Model Distribution Function.

Log(f) Against $p_\perp$

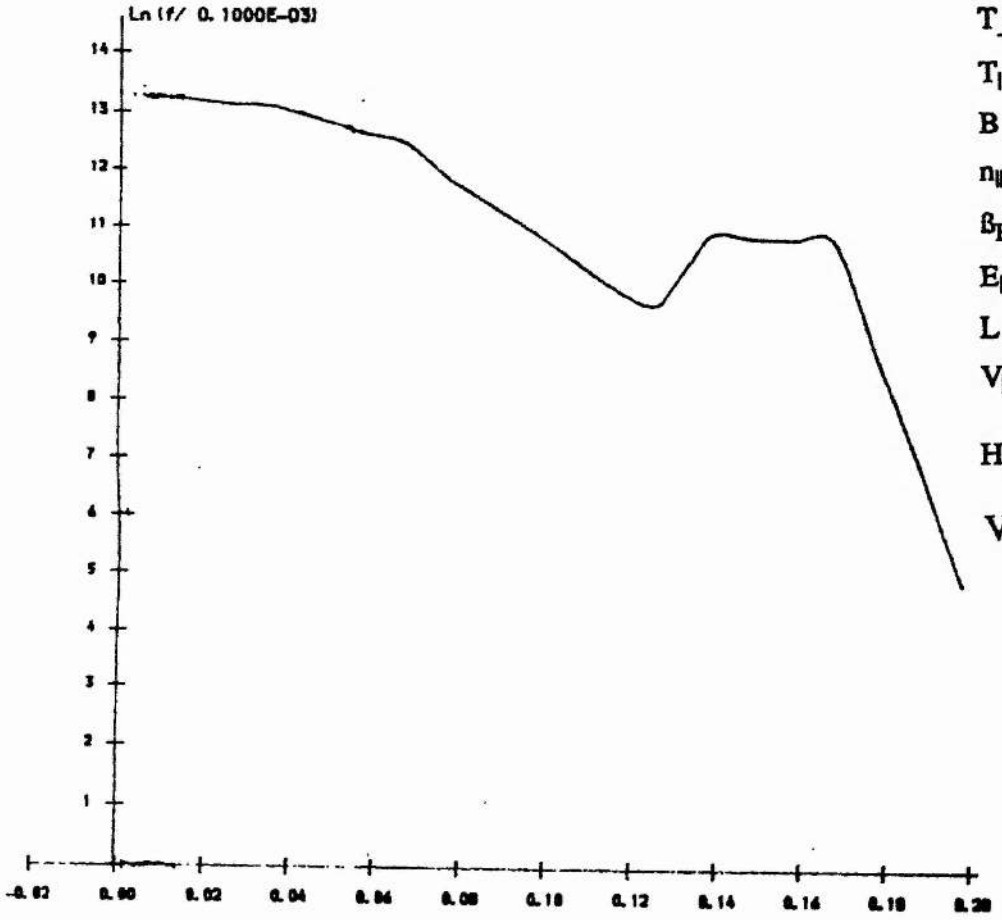

ω_{pe}/Ω	Ratio of plasma to cyclotron frequency	= 1/2
$T_\perp$	Perpendicular temperature	= 1 keV
$T_\parallel$	Parallel temperature	= 1 keV
B	Background field	= 2.5T
$n_{\parallel ec}$	Parallel refractive index	= 0
$ß_{EC}$	Ratio of cyclotron to EC wave frequency	= 1.01
$E_\parallel$	Parallel electric field	= $2.5*10^7$ V_I
L	Gaussian beam width	= 0.05m
$V_{\parallel c}$	Mixing parameter	= $10^8 ms^{-1}$

Horizontal axis $p_\perp$

Vertical axis $\log_e(1000_I, N)$

Figure 4.4d - Numerical Distribution Function.

Log(f) Against $p_\perp$

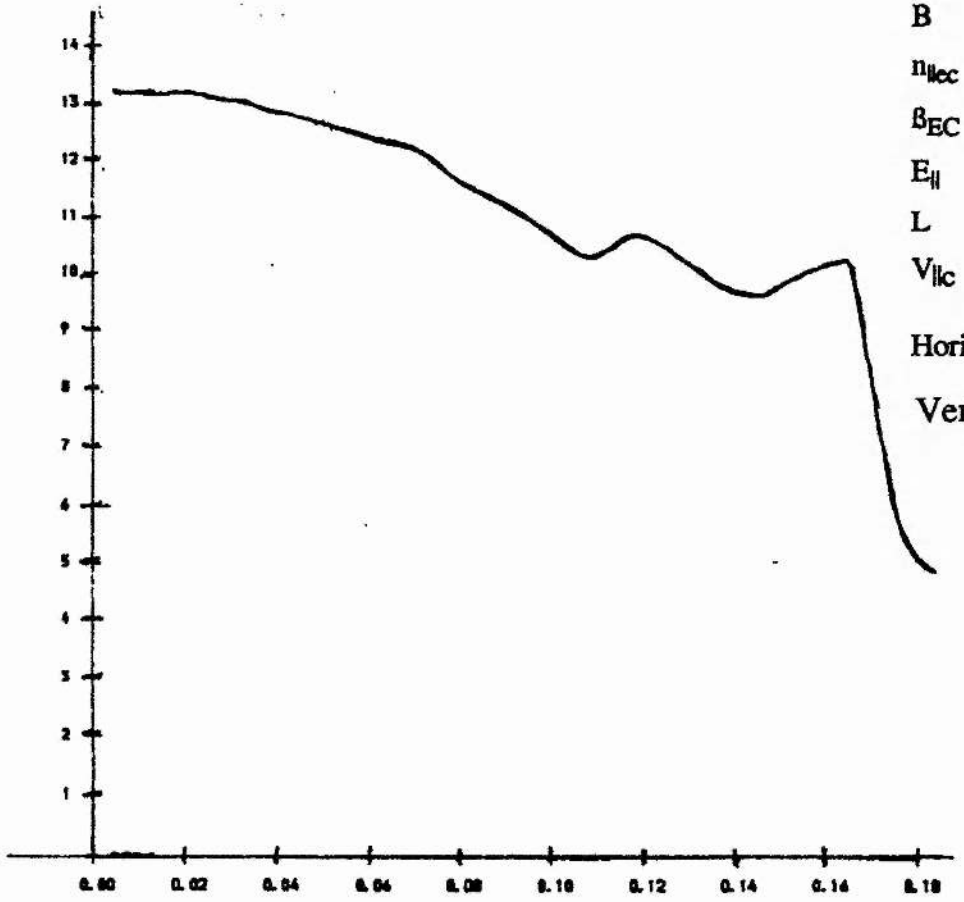

ω_{pe}/Ω	Ratio of plasma to cyclotron frequency	= 1/2
$T_\perp$	Perpendicular temperature	= 1 keV
$T_\parallel$	Parallel temperature	= 1 keV
B	Background field	= 2.5T
$n_{\parallel ec}$	Parallel refractive index	= 0
β_{EC}	Ratio of cyclotron to EC wave frequency	= 1.01
$E_\parallel$	Parallel electric field	= $2.5*10^7$ Vm-1
L	Gaussian beam width	= 0.05m
$V_{\parallel c}$	Mixing parameter	= $10^8 ms^{-1}$

Horizontal axis $p_\perp$

Vertical axis $\log_e(1000f/N)$

nature of the distributions demanded it.

Finally much could be said about the means used to obtain the numerical distribution. The amount of CPU required for each run was very substantial. The first distribution (ß=1.05) was found by use of two weeks' CPU time on a VAX at St Andrews. The remaining two were found using the Harwell Cray, and each run required a little under one hour of CPU time.

We now proceed to attempt to find an analytic condition for the approximation to be valid.

4.4 An Analytic Condition that the Adiabatic Approximation is Valid.

The adiabatic model presented in Chapter three relies on the constancy of the Hamiltonian. However if $E_{||}$ changes in time there will be a time dependent part causing a difference between the numerically determined distribution functions and those obtained analytically. Using the Hamiltonian of Nevins et al, equation (3.1),

$$H = \frac{1}{2}\left(\mu - P_r\right)^2 + \alpha\sqrt{\mu}\sin\psi$$

and letting $\tau=\Omega t$ we have

$$\frac{dH}{d\tau} = \frac{\partial H}{\partial \tau} = \frac{d\alpha}{d\tau}\sqrt{\mu}\sin\psi \qquad (4.3)$$

which will lead to a change ΔH when integrated over the electron's passage through the beam. Now for a Gaussian beam the equation relating the change in the Hamiltonian and the initial and final relativistic factors are given by

$$\gamma_i - \frac{\gamma_i^2}{2\beta} = \gamma_f - \frac{\gamma_f^2}{2\beta} + \Delta H$$

giving

$$\gamma_f = \beta \pm \sqrt{\left(\left(\beta - \gamma_i\right)^2 + 2\beta\Delta H\right)}$$

so if ΔH is approximately independent of β-γ_i the nonadiabatic heating will be most significant for β-$\gamma_i \approx 0$. More specifically the adiabatic approximation will be valid at a point in phase space if

$$\left|\frac{2\beta\Delta H}{\left(\beta-\gamma_i\right)^2}\right| << 1 \qquad (4.4a).$$

Likewise it will be valid for a given distribution if

$$2\beta\left|\frac{\int \Delta H d^3\underline{v}}{\int\left(\beta-\gamma\right)^2 d^3\underline{v}}\right| << 1 \qquad (4.4b).$$

We take $z = 0$ and $\tau = 0$ at the centre of the beam whose profile we shall take to be

$$\alpha(z) = \alpha_{pk} e^{-\frac{z^2}{L^2}}$$

L being the Gaussian width. Using Hamilton's equations the equations of motion in this approximation read

$$\frac{d\psi}{d\tau} = P_r - \mu + \frac{\alpha \sin\psi}{2\sqrt{\mu}}$$

and

$$\frac{d\mu}{d\tau} = -\alpha\sqrt{\mu}\cos\psi$$

The latter will be of use in obtaining an order of magnitude approximation to ΔH, which, from (4.3), is

$$\Delta H = \int_{-\infty}^{+\infty} d\tau \frac{d\alpha}{d\tau}\sqrt{\mu}\sin\psi \qquad (4.5)$$

Unfortunately this integral cannot be accurately evaluated, so we must resort to some intuitive methods for determining an order of magnitude approximation to it. We note that the Hamiltonian changes through the beam, so in particular the integrals $\Delta H_1 + \Delta H_2$ ($\equiv \Delta H$) where

$$\Delta H_1 = \int_{-\infty}^{0} d\tau \frac{d\alpha}{d\tau}\sqrt{\mu}\sin\psi \text{ and } \Delta H_2 = \int_{0}^{+\infty} d\tau \frac{d\alpha}{d\tau}\sqrt{\mu}\sin\psi$$

are both non-zero. In the adiabatic approximation however they cancel when added. Rather than perform the integration from $-\infty$ to $+\infty$ we take the change in value of the Hamiltonian over one *cycle* ie over the time for a complete orbit around the fixed point in phase space in the case of trapped particles and over the time to change ψ by 2π in the case of untrapped orbits. We use the result as an **order of magnitude approximation** to ΔH. Our estimate will be in error for two reasons: firstly we consider only the change in the Hamiltonian at one point along the path. For example if we consider a cycle about the fixed point when $\tau>0$ we will be evaluating part of ΔH_2. Our estimate will certainly underestimate the magnitude of ΔH_2. On the other hand as $d\alpha/d\tau$ is anti-symmetric about $\tau = 0$ there is likely to be significant cancellation in (4.5) and we will have $\Delta H_1 \approx -\Delta H_2$. Our approximation is more likely to be an over rather than an underestimate of ΔH. Our approach may appear to lack mathematical rigour but no other method of evaluating ΔH is readily apparent. The justification of our approach will therefore be partly a priori. Its real value lies in providing a *rough measurement*

of the accuracy of the approximation.

Using the approximate constancy of the Hamiltonian we can rewrite the equation for $d\mu/d\tau$ as

$$\frac{d\mu}{d\tau} = \pm\sqrt{\left(\alpha^2\mu - \left\{H + (1/2)(P_r - \mu)^2\right\}^2\right)} \qquad (4.6)$$

where we note the sign of the answer is + for $\cos(\psi) < 0$ and vice versa. Again using the constancy of the Hamiltonian our expression for ΔH is now

$$\Delta H = \frac{\dot{\alpha}}{\alpha}\oint d\tau\left(H + \frac{(P_r - \mu)^2}{2}\right)$$

where the line integral is over a complete cycle. We therefore have

$$\Delta H = \frac{\dot{\alpha}}{\alpha}\int_{\tau(\mu_{min})}^{\tau(\mu_{max})} d\tau\left\{H + (1/2)(P_r - \mu)^2\right\} + \frac{\dot{\alpha}}{\alpha}\int_{\tau(\mu_{max})}^{\tau(\mu_{min})} d\tau\left\{H + (1/2)(P_r - \mu)^2\right\}$$

$$= \frac{\dot{\alpha}}{\alpha}\int_{\mu_{min}}^{\mu_{max}} \frac{d\mu}{\dot{\mu}}\left\{H + (1/2)(P_r - \mu)^2\right\} + \frac{\dot{\alpha}}{\alpha}\int_{\mu_{max}}^{\mu_{min}} \frac{d\mu}{\dot{\mu}}\left\{H + (1/2)(P_r - \mu)^2\right\}$$

where the first integral in each expression is evaluated for $\cos\psi \le 0$ and the second for $\cos\psi \ge 0$. The two integrals add together rather than cancel as the sign of $d\mu/d\tau$ is different for each integral, so employing the very weakly relativistic approximation that $H + (1/2)(P_r - \mu)^2 \approx P_r(\mu - \mu_0)$, and using (4.6) we have,

$$|\Delta H| = \left| 2\frac{\dot{\alpha}}{\alpha}\int_{\mu_{min}}^{\mu_{max}} d\mu \frac{P_r(\mu - \mu_0)}{\sqrt{\alpha^2\mu - P_r^2(\mu - \mu_0)^2}} \right| \qquad (4.7a)$$

so that

$$|\Delta H| = |\pi\varepsilon(\alpha/P_r)^2| \qquad (4.7b)$$

where

$$\varepsilon = \frac{\dot{E}}{\Omega E} = \frac{\dot{\alpha}}{\Omega\alpha}$$

is a dimensionless measure of how quickly the field changes, which varies along the beam profile. We have not yet specified at what point we are calculating the integral (4.7a), and hence at what point we calculate ε in (4.7b).

The maximum contribution to (4.7a) for |ΔH| clearly comes when dα/dt has a maximum , ie at $z = \pm\frac{L}{\sqrt{2}}$. Choosing $z = +\frac{L}{\sqrt{2}}$ we have $\varepsilon = -\sqrt{2}\frac{V_{\|}}{L\Omega}$ and our condition that the heating is adiabatic (4.4a) becomes

$$\frac{2\sqrt{2}\,\pi V_{\|}\beta}{e\,L\Omega\,(\gamma-\beta)^2}\left\{\frac{\alpha_{pk}}{P_r}\right\}^2 << 1 \qquad (4.8a).$$

e being the exponential exp(1), <u>not</u> the electronic charge.

If we instead use (4.4b) the condition that the overall energy absorption of a distribution is accurately described by the adiabatic approximation is

$$\frac{2\pi\sqrt{2}\,\beta\int\left\{\frac{\alpha_{pk}}{P_r}\right\}^2 f\,d^3\underline{v}}{e\,L\,\Omega\int(\gamma-\beta)^2 f\,d^3\underline{v}} << 1 \qquad (4.8b).$$

The integral in the numerator of (4.8b) is not tractable (and can be problematic to evaluate numerically) but is the final measure of the accuracy of our approximation and the whole expression (4.8b) is henceforth referred to as the *critical ratio* . A graph of the logarithm of the critical ratio against ß for a single set of parameters is shown in figure (4.5). Again we note the approximation

improves as ß increases confirming the findings of the last section. It should be noted however that the graph cuts the axis at a fairly large value of ß ≈1.02. If our condition were accurate we would expect values of ß above this to fulfil the condition and those below it not to. In fact we have shown that with ß =1.01 we have reasonably good agreement and it would appear our condition is a little conservative, but basically in agreement with the conclusion from numerical work that the accuracy of the model increases with the frequency mismatch.

4.5 Discussion and Conclusion.

We have demonstrated that there are circumstances where the adiabatic approximation is highly accurate, and have found an approximate condition that this should be so. We have seen in Chapter three by examining individual particle orbits that the validity of the adiabatic assumption improves as ß increases away from γ_i, and in this chapter we have again seen that the approximation increases with ß by examining the effect of heating on an electron distribution. We have also examined contour plots and cross-sections of distribution functions arising after ECRH for the adiabatic and the numerical model when ß is relatively close to 1. In this case we observe good qualitative agreement, but relatively poor quantitative agreement.

Conclusion

Our theoretical model seems to work well for nonresonant particles. We have verified this using numerical and analytic techniques. They are in broad agreement although our analytic condition for validity of the theory may be somewhat conservative. We have seen that the essential feature of the distribution created by a FEL pulse, ie the inversion in $p_\perp$, is reproduced with our analytic distribution.

Figure 4.5

$\underline{\text{Log}_e\text{(Critical Ratio)}}$

Temperature	T	=1keV for Maxwellian distribution
Parallel refractive index	$n_{\|\|EC}$	=0
Parallel electric field	$E_{\|\|}$	$=5*10^7$ Vm^{-1} for the O mode
Magnetic field	B_0	=2.5T
Gaussian width	L	=0.05m

Vertical axis - Log_e(Critical Ratio)

Horizontal axis - $ß_{EC}$

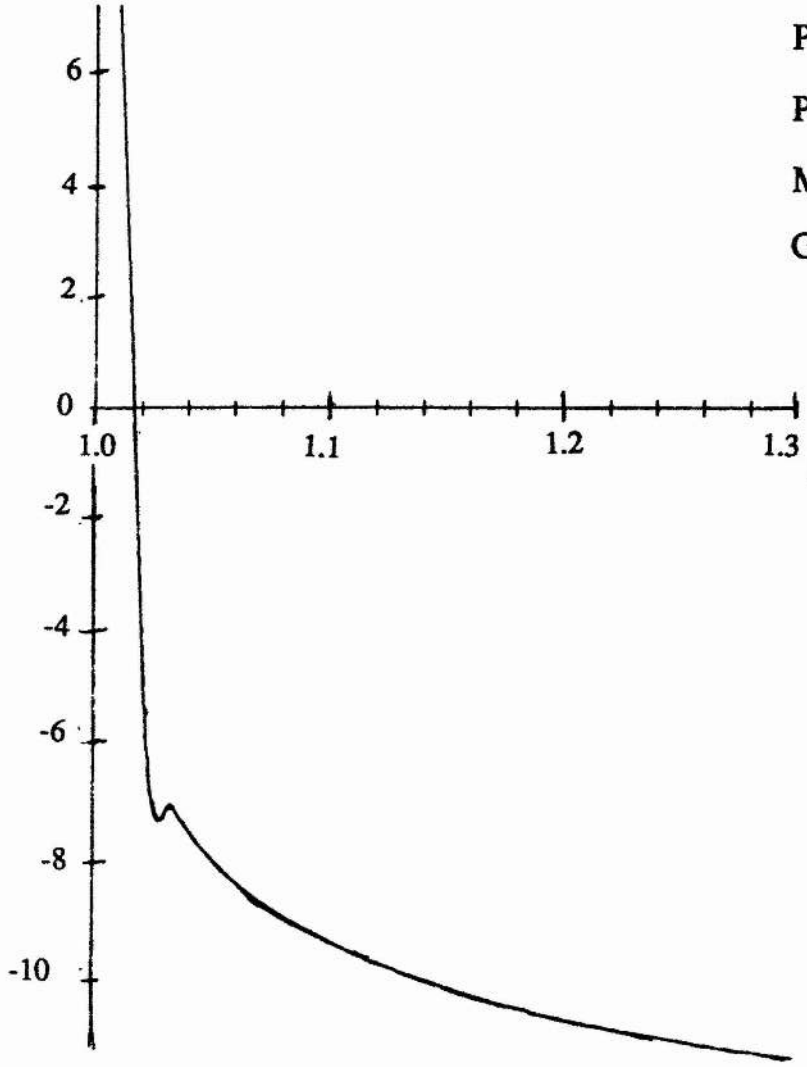

4.5 Discussion and Conclusion.

We have demonstrated that there are many circumstances where the adiabatic approximation is highly accurate, and have found an approximate condition that this should be so. We have seen in Chapter three by examining individual particle orbits that the validity of the adiabatic assumption improves as ß increases away from γ_i, and in this chapter we have again seen that the approximation increases with ß by examining the effect of heating on an electron distribution.

Here we note that the only test performed by Nevins et al to verify the accuracy of their model, which like ours rests on the assumption of adiabaticity, was comparison of the scaling law for power absorption with power laws found by numerically integrating the equations of motion through a beam. However all their result established was that the model was valid (to some extent at least) for obtaining a power absorption law in a certain parameter regime. What we have established here is that the model is valid for parameters which will be of considerable relevance for the work in the next chapter, ie ones for which the frequency mismatch is relatively large.

Conclusion

Our theoretical model seems to work well for nonresonant particles. We have verified this using numerical and analytic techniques. They are in broad agreement although our analytic condition for validity of the theory may be somewhat conservative. We have seen that the essential feature of the distribution created by a FEL pulse, ie the inversion in $p_\perp$, is reproduced with our analytic distribution.

CHAPTER FIVE

ELECTROMAGNETIC INSTABILITIES IN PLASMA HEATED BY ECRH

CHAPTER FIVE

Electromagnetic Instabilities in Plasma Heated by ECRH

In this chapter we present the main finding of this work, namely that distributions created by ECRH using FELs are unstable to e/m waves. The bulk of our results are numerical and use the theory of Chapter three and section 4.2 of Chapter four.

5.1 Introduction to Instabilities in Plasmas

The subject of instabilities in plasmas is so immense that no PhD thesis could contain an adequate introduction to the topic. Generally, instabilities may be classified as *parametric*, *macro* or *micro*.

Macroinstabilities involve the plasma as a whole and are detrimental to the confinement of plasma, as they involve a loss of containment of particles eg Wesson (1978). They are low frequency, tend to be magnetic in nature and are studied using MHD equations. Parametric instabilities are those involving nonlinear wave-wave interactions and are generally described using kinetic equations or 2-fluid equations. Microinstabilities, like parametric instabilities, tend to be high frequency and involve e/m or electrostatic instabilities. Both can cause anomalous transport of energy and can decrease the energy confinement time eg Tang (1978). However microinstabilities differ from parametric ones in that they involve only wave-particle interactions and can be studied using linear theory, while parametric instabilities typically involve the decay of one wave into two or three others (see Porkolab and Cohen (1988) for an analysis of parametric instabilities in FEL ECRH).

There are many types of microinstabilities possible in a plasma. Some involve both ion and electron distributions and many involve gradients in plasma quantities such as temperature or magnetic field. Some examples of well known instabilities are given below.

Harris instabilities.

Harris (1959 and 1961), Hall and Heckrotte (1964), Shima and Hall (1965), Guest and Dory (1965) and Soper and Harris (1965).

These can occur in a magnetised plasma if a single species - ions or electrons - has a sufficiently great temperature anisotropy. This type of instability is particularly relevant for this thesis as the instabilities we shall examine later in the chapter are of this nature. In particular Shima and Hall proved that a nonrelativistic Bimaxwellian in a magnetic field is stable provided $T_{\perp} < 2T_{\|}$. Intuitively therefore one would expect that only a significant change in perpendicular energy would cause instabilities of this nature in a plasma heated by ECRH.

Weibel instabilities.

Weibel (1959) and more recently Yoon (1989).

These are in some ways similar to Harris instabilities but can exist without the need for an external field. They involve zero frequency electromagnetic waves and increase with temperature anisotropy (Yoon).

Here we note that the choice of relativistic Bimaxwellian of Yoon is not unique. There is in fact no natural definition of a relativistic Bimaxwellian and later in this thesis we consider a Bimaxwellian of slightly different form.

Finally we come to the closest instabilities to those being examined in this thesis.

Whistler instabilities in ECRH in experiments on mirror machines.

Garner et al (1987) and Garner et al (1990).

Whistler instabilities have been observed and studied in mirror machines during ECRH, Garner et al (1987) and Garner et al (1990). They occur due to large anisotropies in the distribution function. In a tokamak different distribution functions may arise and so far no whistlers have been observed. It is one of the main conclusions of this thesis that instabilities may occur in laser ECRH and that whistler waves may be one of the unstable waves.

The above list is not complete but represents some types of instabilities that depend on the temperature anisotropy of a single plasma species.

5.2 Electromagnetic Instabilities.

(A note on symbols: the symbol $\beta=n_{harm}\Omega/\omega$ is used both where ω is the wave frequency of the incident ECRH and where it is the frequency of the unstable whistler wave. Where the distinction is not obvious the symbols are suffixed -EC and -w respectively. The same applies to the symbol $n_{||}$. Except where explicitly stated otherwise the harmonic number is 1 so that $\beta=\Omega/\omega$.)

Comparatively little work has been done on instability to e/m waves in tokamak relevant plasmas. Bornatici et al (1983B) and Yoon have investigated relativistic anisotropic distributions for instability, but it is not clear that these are directly related to tokamak distributions. In this thesis we are concerned with finding growth rates of e/m waves in ECRH heated plasmas, and the natural modes to examine are O, X and whistler modes. To this end we have developed a stability code to determine the stability to arbitrary distributions. The whistler mode is chosen for special attention because it propagates along magnetic field lines and hence is restricted to a single flux surface of a tokamak. Should the distribution on a flux surface be unstable to whistlers they will grow until nonlinear saturation occurs, and so it is possible that distribution functions may be substantially altered by this mechanism rather than through collisions, especially if the growth rate of the instability is much greater than the collision rate. The instability will not necessarily reduce the distribution to a Maxwellian one - for example any distribution function which is a function of v^2 only and has a negative gradient $df/d(v^2)$ must be stable (Bernstein et al, 1964). To obtain the growth rates we make the usual assumption that the linear dispersion relation applies and that the frequency may be written in a complex form $\omega_{com}=\omega_r+i\omega_i$, ω_i being the growth rate (sometimes denoted by γ in the literature; here that symbol is reserved for the relativistic factor though we later use the symbol γ_N as a quantity proportional to the growth rate). Further we assume $\omega_i/\omega_r << 1$ so we can write

$$\omega_i = \frac{-D_i}{\frac{\partial D_r}{\partial \omega_r}}$$

(5.1)

where the subscripts i and r refer to the imaginary and real parts respectively, and where $D(\omega_{com},k) = 0$ is the dispersion relation. Henceforth we drop the subscript r on the real part of the frequency. For the case of the O mode the dispersion relation must be relativistic and the polarisation is important. Calculation of the correct perpendicular refractive index and polarisation without making nonrelativistic approximations involves Shkarofsky functions (Shkarofsky, 1966) but in the case of parallel propagating whistlers it is permissible to obtain the parallel refractive index nonrelativistically because the polarisation is circular and the perpendicular refractive index is zero. The Shkarofsky functions are hard to calculate numerically (Owen, 1984, Airoldi and Orefice, 1982 and Krivenski and Orefice, 1983), but fortunately Owen's routines were available for inclusion into the code.

To simplify calculations we make a further approximation by neglecting ion effects. For a parallel propagating circularly polarised wave we have the following dispersion relation

$$D = \left(\varepsilon_{11} - n_{\|}^2\right)\left(\varepsilon_{22} - n_{\|}^2\right) - \varepsilon_{12}\varepsilon_{21} = 0$$

(5.2).

Using the small Larmor radius approximation we can write

$$\varepsilon_{11} = \varepsilon_{22} = 1+P+iQ$$

(5.3a)

$$i\varepsilon_{12} = -i\varepsilon_{21} = P+iQ$$

(5.3b)

where

$$P = -\frac{\omega_p^2}{2\omega(\omega+\Omega)} - \frac{\omega_p^2}{2\omega\Omega}\,\mathrm{PRINC}\left(\int d^3p\, p_\perp \frac{\mathcal{D}(f)}{\beta+n_{\|}p_{\|}-\gamma}\right)$$

(5.4a)

$$Q = - \frac{2\pi^2 \omega_p^2 \gamma_N}{\Omega \omega |n_{||}|}$$

(5.4b)

where

$$\gamma_N = \int_0^\infty dp_\perp \frac{p_\perp^3}{4} \mathcal{D}(f)$$

(5.5a),

PRINC (∫...) denotes the principal value of the integral,
and where $\mathcal{D}$ is the operator on the distribution function

$$\mathcal{D}(f) = \frac{\beta}{p_\perp} \frac{\partial f}{\partial p_\perp} + \frac{n_{||}}{\gamma} \frac{\partial f}{\partial p_{||}}$$

evaluated at $p_{||}=p_{||res}$ (5.5b).

Now from (5.2) we have

$$D = \left(1 + P + iQ - n_{||}^2\right)^2 - \left(P + iQ\right)^2$$

so that

$$Im(D) = 2\left(1 - n_{||}^2\right)Q \qquad \text{and}$$

$$Re(D) = \left(1 + P - n_{||}^2\right)^2 - P^2 .$$

Note that we have used a normalised distribution function f such that $\int d^3\underline{p}\ f=1$. Here and in equation (5.4a) the integration is over all momentum space.

The details of the calculation of P and Q are lengthy but are given in section

2.3.2 of Bornatici et al (1983A) where a similar but more general expression is derived. We have assumed the real parts of the dielectric tensor elements caused by the resonances at $n_{harm}=-1$ and $n_{harm}=0$ may be approximated by the cold plasma value. Note the parallel refractive index of the whistler $n_{||}$ must not be confused with the parallel refractive index of the incident ECRH which we denote $n_{||EC}$.

Equations (5.4a) and (5.4b) are formally correct for the nonrelativistic case provided (5.5a) is replaced by

$$\gamma_N = \frac{c}{2}\int_0^\infty dW_\perp \, W_\perp \, \mathcal{D}_{NR}(f) \qquad (5.5c),$$

where

$$\mathcal{D}_{NR}(f) = \frac{\beta \partial f}{\partial W_\perp} + \frac{n_{||}}{c}\frac{\partial f}{\partial V_{||}} \qquad (5.5d)$$

evaluated at $V_{||} = V_{||res} = \frac{\omega - \Omega}{k_{||}}$

is the nonrelativistic version of (5.5b), and where $W_\perp=\mu c^2=V_\perp{}^2/2$. Substituting (5.4) into (5.3a) and (5.3b); (5.3a) and (5.3b) into (5.2); and (5.2) into (5.1), we have

$$\omega_i = \frac{-\left(1-n_{||}^2\right)2Q}{\frac{\partial}{\partial \omega_r}\left(\left(1+P-n_{||}^2\right)^2 - P^2\right)}$$

$$= \frac{2\pi^2\omega_p^2}{\omega\Omega|n_{||}|} \frac{1-n_{||}^2}{\left(1+P-n_{||}^2\left(\frac{\partial P}{\partial\omega} - 2n_{||}\frac{\partial P}{\partial\omega}\right) - P\frac{\partial P}{\partial\omega}\right.} \gamma_N$$

(5.6)

where γ_N may be evaluated by (5.5a) or (5.5c) as appropriate. In the next section we describe the use of this integral to calculate growth rates of distributions obtained numerically from the BANDIT code (O'Brien et al (1986A) and O'Brien et al (1986B)) which were supplied by Mr M R O'Brien of the Culham Laboratory. In section 5.3 we use (5.6) to test distribution functions typical of gyrotrons for stability to whistlers, and in the remainder of the chapter we test the distribution function given by equation (4.2).

First however we wish to comment on the differences between (5.5a) and (5.5c). In the latter case the parallel resonant velocity is independent of the perpendicular velocity ie there is a complete decoupling of the perpendicular and parallel energy. A simple necessary and sufficient condition for instability is therefore that $\mathcal{D}_{NR}(f) > 0$ when evaluated at $V_{||}=V_{||res}$. This can with a little algebra be used to derive the condition for stability of a nonrelativistic Bimaxwellian originally found by Shima and Hall mentioned in section 5.1. Unfortunately in the fully relativistic case the parallel and perpendicular energies are coupled and we cannot obtain a necessary and sufficient condition for instability without performing the integral in (5.5a) as $\mathcal{D}(f)$ is dependent on momentum even when evaluated at the resonant parallel momentum. By using the weakly relativistic Bimaxwellian

$$f = N_{WRB}\, e^{-\lambda_{\|}\frac{p_{\|}^2}{2} - \lambda_{\perp}\frac{p_{\perp}^2}{2}} \quad \text{where} \quad 1/N_{WRB} = \int d^3\underline{p}\, e^{-\lambda_{\|}\frac{p_{\|}^2}{2} - \lambda_{\perp}\frac{p_{\perp}^2}{2}}$$

and the integral is over all momentum space, we arrive at the same condition as that obtained for the nonrelativistic distribution, though it is not obvious how well this will approximate the actual condition for instability using a fully relativistic distribution - especially at higher temperature.

There is in fact no unique definition of a fully relativistic Bimaxwellian. The form of the distribution in figures (5.3) and (5.5) is

$$f = N_{BM} e^{\frac{-(\lambda_{\perp}p_{\perp}^2 + \lambda_{\|}p_{\|}^2)}{1+\gamma}} \quad \text{where} \quad \frac{1}{N_{BM}} = \int d^3\underline{p}\, e^{\frac{-(\lambda_{\perp}p_{\perp}^2 + \lambda_{\|}p_{\|}^2)}{1+\gamma}} .$$

(see Chapter four). We identify $T_{\|,\perp}$ as $m_e c^2/\{k_B\lambda_{\|,\perp}\}$, k_B being Boltzmann's constant. However other authors - Garner et al (1990) - use other distributions to represent temperature anisotropy. The form most appropriate to tokamak heating is not immediately obvious, but what is important is the degree of anisotropy rather than the exact form of the distribution. Our rationale for choosing this form of the distribution is that despite the coupling of parallel and perpendicular energies which is an essential element of the relativistic distribution, it is still possible to identify effective perpendicular and parallel temperatures. This is of importance as we shall later discover that although the Bimaxwellian as a distribution is not always unstable to electromagnetic waves, it is possible to choose parameters $\lambda_{\|,\perp}$ such that the distribution is unstable.

5.3 Stability of Distributions Typical of ECRH Gyrotron Heating

In this section we consider plasmas heated by ECRH where the waves are not so intense that the linear resonance theory of O'Brien et al (1986A) and Taylor (1987) is invalid.

Firstly, as an illustration of the problem we consider a simplified case. We assume an initially Maxwellian distribution, and consider the effect of a single pulse of ECRH so short that no electron passes through the beam more than once. We consider only the part of the distribution function that has been heated and we ignore collisions. For simplicity we consider a nonrelativistic distribution. Later we consider the more realistic case that the heating is continuous and consider the steady state distribution calculated using the BANDIT code of O'Brien et al. Using (2.6a), the nonrelativistic expression for the heating of an electron we may derive (Taylor, 1987) a form for $P(W_\perp, \Delta W_\perp)$

$$P(W_\perp, \Delta W_\perp) = \frac{2}{K V_\perp \pi}\left(1 - \frac{4}{(KV_\perp)^2}\left\{ \Delta W_\perp - \frac{K^2}{8} \right\}^2 \right)^{-\frac{1}{2}} \qquad (5.7a)$$

$$\text{for } \left| \Delta W_\perp - \frac{K^2}{8} \right| < \frac{KV_\perp}{2}$$

and zero otherwise, from which we may easily derive

$$P(W_\perp - \Delta W_\perp, \Delta W_\perp) = \frac{2}{K V_\perp \pi}\left(1 - \frac{4}{(KV_\perp)^2}\left\{ \Delta W_\perp + \frac{K^2}{8} \right\}^2 \right)^{-\frac{1}{2}} \qquad (5.7b)$$

$$\text{for } \frac{K^2}{8} < \frac{KV_\perp^2}{2}$$

and zero otherwise.

The new distribution of electrons that have been heated by the beam, given that the distribution before application of ECRH is Maxwellian, can be calculated by the formula (2.2) using the above expression. It is convenient to introduce the dimensionless symbol

$$y = \frac{2}{KV_\perp}\left(\Delta W_\perp + \frac{K^2}{8}\right).$$

We shall take Q_{pass}=1 for convenience ie assuming all electrons on the flux surface are heated, and assume the following form for the Maxwellian

$$f_{max} = N_{NR} e^{-\frac{\left(\frac{V_\parallel^2}{2} + W_\perp\right)}{T}} \quad \text{where} \quad \frac{1}{N_{NR}} = \int d^3\underline{V}\, e^{-\frac{\left(\frac{V_\parallel^2}{2} + W_\perp\right)}{T}}$$

T being in units such that the Boltzmann constant and the electron mass are both unity. A minor modification of (2.2) gives us

$$f_{ECRH} = \int d(\Delta W_\perp)\, P(W_\perp - \Delta W_\perp, \Delta W_\perp)\, f_{max}(W_\perp - \Delta W_\perp, V_\parallel)$$

where the limits of integration are $-KV_\perp/2+K^2/8$ to $KV_\perp/2+K^2/8$, provided $W_\perp > K^2/8+KV_\perp/2$, so that the integral becomes

$$f_{ECRH} = \frac{N_{NR}}{\pi} e^{-\frac{\left(W_\perp + \frac{V_\parallel^2}{2}\right)}{T}} \int_{-1}^{+1} dy\, e^{xy}\left(1-y^2\right)^{-\frac{1}{2}} e^{-\frac{K^2}{8T}}$$

where $x = KV_\perp/(2T)$ again provided $W_\perp > K^2/8+KV_\perp/2$. Otherwise the limits of the integration are more complicated and the integral has no analytic solution (and in any case the linear theory is invalid). The result of the integration is (eg Gradshteyn and Ryzhik, 1965 p958):

$$f_{ECRH} = N_{NR}\exp\left(-\frac{2Tx^2}{K^2} - \frac{K^2}{8T} - \frac{V_{\parallel}^2}{2T}\right)I_0(x) \qquad (5.8),$$

again provided $W_\perp > K^2/8 + KV_\perp/2$, I_0 being the modified Bessel function of the first kind of order 0 (see figure (5.1) after Abramovitz and Stegun, 1972). The positive slope of the I_0 function gives grounds for investigating the stability of the distribution given in (5.8). We note from figure (5.1) that $d/dx(e^{-x}I_0(x)) < 0$ ie $I'_0 < I_0$. Differentiating (5.8) with respect to x we have

$$\frac{df_{ECRH}}{dx} = N_{NR}\exp\left(-\frac{2Tx^2}{K^2} - \frac{K^2}{8T} - \frac{V_{\parallel}^2}{2T}\right)\left(-\frac{4T}{K^2}x\,I_0 + I'_0\right)$$

and we see clearly we cannot have $df/dV_\perp > 0$ if $K < 2V_\perp$. We note also from (2.7b) that this is the same condition that the relativistic generalisation of (2.6) is valid. Although we have established for this distribution that $df/dV_\perp < 0$ under the stated condition we shall confirm analytically that no instability can exist when this condition is met.

The integral (5.5c) can be performed analytically if we choose $f = f_{ECRH}$ and ignore the contribution to f from unheated electrons on the rest of the flux surface. We assume equation (5.8) for f_{ECRH} is valid everywhere and we let

$$M(\sigma,\delta) = \int_0^\infty V_\perp I_0(\delta V_\perp)e^{-\sigma V_\perp^2}dV_\perp = \frac{e^{\frac{\delta^2}{4\sigma}}}{2\sigma}$$

(eg Gradshteyn and Ryzhik section 6.633 equation 4) so that

$$\frac{\partial M}{\partial \sigma} = -\frac{M}{\sigma}\left(1 + \frac{\delta^2}{4\sigma}\right) = \int_0^\infty V_\perp^3 I_0(\delta V_\perp)e^{-\sigma V_\perp^2}dV_\perp.$$

Figure (5.1) (After Abramovitz and Stegun)

$I^0(x)e^{-x}$ and $I_0(x)$

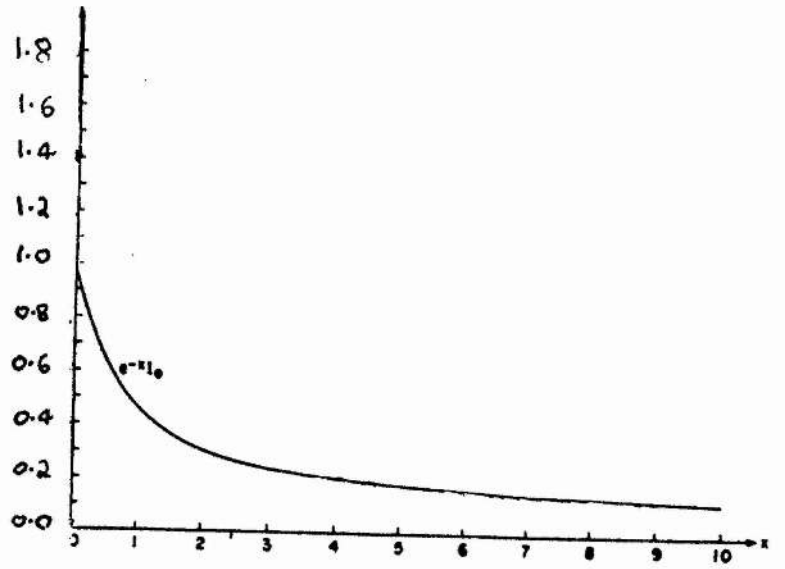

$e^{-x}I_0(x)$

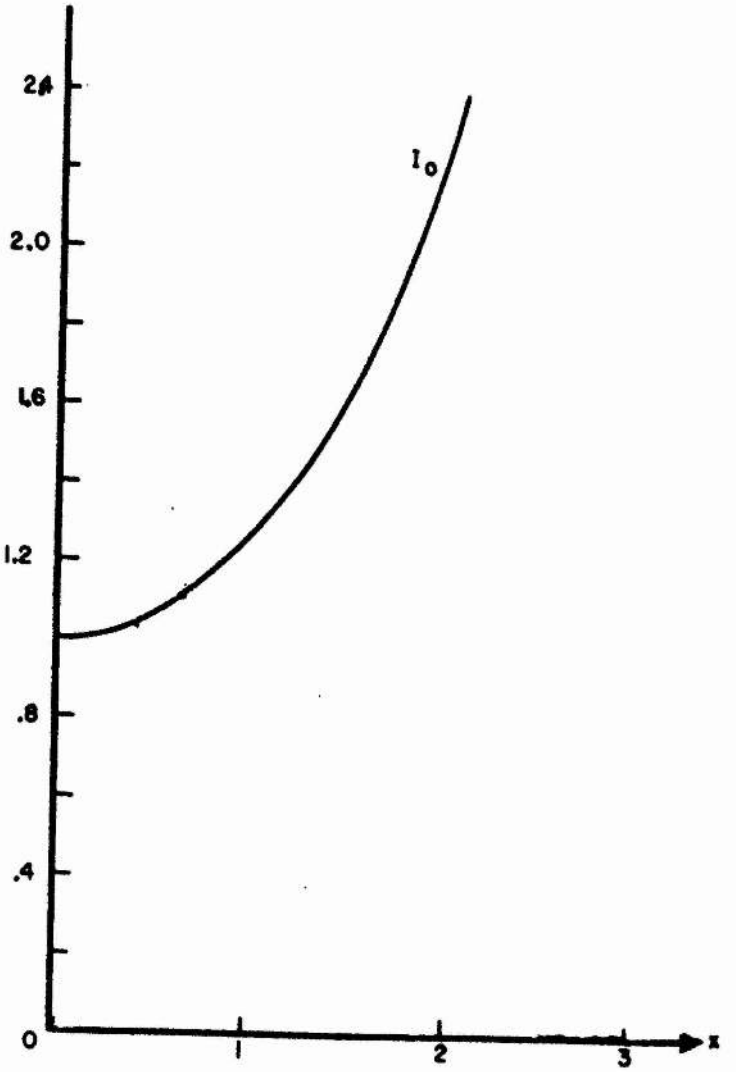

$I_0(x)$

Now we identify σ as 1/(2T) and δ as K/(2T). Further for simplicity we consider only the O mode propagating at the perpendicular. From now on it becomes important to distinguish between quantities belonging to the whistler wave and those belonging to the ECRH. Firstly we note that f_{ECRH}->0 as $W_\perp$->∞ and that $W_\perp \frac{\partial f_{ECRH}}{\partial W_\perp}$ -> 0 as $W_\perp$ ->0. This allows us to integrate the first terms in the integrand of (5.5a) by parts. Now from (5.5c) and (5.8) we have

$$\gamma_N = \frac{c}{2}\int_0^\infty dW_\perp W_\perp \left(\beta_W \frac{\partial}{\partial W_\perp} + \frac{n_\parallel}{c}\frac{\partial}{\partial V_\parallel}\right)\left(f_{max} e^{-\frac{K^2}{8T}} I_0(x)\right)$$

Identifying M with

$$\int_0^\infty dW_\perp \, I_0(x)\, e^{-\frac{W_\perp}{T}}$$

allows us to find the following expression for γ_N:

$$\gamma_N = \frac{c}{2} N_{NR}\left\{-M\beta_W e^{\frac{K^2}{8T}-\frac{V_\parallel^2}{2T}} - \frac{n_{\parallel W}}{2c}\frac{\partial}{\partial V_\parallel}\left(\frac{\partial M}{\partial \sigma} e^{\frac{K^2}{8T}-\frac{V_\parallel^2}{2T}}\right)\right\}$$

evaluated at the resonant parallel velocity

$$= cN_{NR}T\left\{-\beta_W + \frac{n_{\parallel W}}{c}\left(\frac{\partial}{\partial V_\parallel}\left(\frac{\delta^2}{4\sigma}\right) - \frac{V_{\parallel res}}{T}\left(1+\frac{\delta^2}{4\sigma}\right)\right)\right\} e^{-\frac{V_{\parallel res}^2}{2T}}$$

$$= -cN_{NR}T\left\{1+S_1\left(S_3-S_2\right)e^{-S_3}\right\} e^{-\frac{S_2^2}{S_4}}$$

where $S_4=\frac{v_{th}^2}{2c^2}$, $S_3=\frac{L^2\left(\omega_{EC}-\Omega\right)^2}{V_{\|res}^2}$, $S_2=\frac{\beta_W-1}{n_{\|W}}$ and $S_1=\frac{\delta^2}{4\sigma}$.

First consider the case where $S_2 \geq 1$. As $S_4 \ll 1$ any contribution to a damping or growth rate will be exponentially small. Now consider the case $S_2 \leq 1$. The above expression clearly has a maximum when the resonance of the ECRH and the unstable wave coincide ie $S_3 = 0$ when the contribution will certainly be negative as we have

$$\frac{\delta^2}{4\sigma} \equiv \frac{K^2}{8T} \ll 1.$$

If we suppose that this expression is correct provided the distribution function is a good approximation for $V_\perp{}^2 \leq 2T$ this condition again becomes identical to (2.7c).

So far we have neglected collisions and have essentially considered the effect of a pulse of ECRH of finite duration. In practice gyrotron heating will be continuous. Electrons continually pass through the beam but also suffer collisions. Rather than attempting to describe the combined effect of collisions and ECRH analytically we use the output from a sophisticated code developed at the Culham Laboratory over a number of years.

The BANDIT code models the effect of continuous ECRH at powers typical of gyrotrons, and collisions using a Fokker-Planck equation with an option to include the effect of a toroidal electric field. The basic equation solved is (2.1) where (O'Brien, 1990)

$$\left(\frac{\partial f}{\partial t}\right)_E = -\frac{eE}{m}\frac{\partial f}{\partial V_\|}$$

$\left(\frac{\partial f}{\partial t}\right)_c$ is given by a Fokker-Planck collision operator, and

$$\left(\frac{\partial f}{\partial t}\right)_W = \frac{1}{V_\perp}\frac{\partial}{\partial V_\perp}\left(V_\perp D_0 \frac{\partial f}{\partial V_\perp}\right).$$

In the latter expression the diffusion coefficient D_0 can be calculated using a model operator but is more usually calculated in the following manner. The mean change in velocity $<(\Delta V_\perp)^2>$ in time Δt is calculated using equation (2.6b) and D_0 is calculated as $<(\Delta V_\perp)^2>/2\Delta t$. The code can be used to calculate power absorption and current drive during ECRH.

Details of the code are beyond the scope of this thesis but are given in O'Brien et al (1986A) and O'Brien et al (1986B). The code was developed by Mr M R O'Brien at the Culham Laboratory and the numerical distributions used in this section were kindly supplied by him. Figures (5.2) show the damping rates of three steady state distributions produced by the code. Details of the parameters are given in the figure captions. The parameters were chosen to give maximum likely distortion to the distribution function; despite this the change in damping rate as compared with the Maxwellian distribution is small. In the first example we examine the distribution caused by the interaction of the O mode propagating perpendicular to the magnetic field with the fundamental resonance. The ECRH power is 1MW delivered in a Gaussian beam of form

$$e^{-\frac{(y^2+z^2)}{L^2}}$$

L being the Gaussian width, and equal to 0.05m. The background magnetic field is 3.42T and the ratio $ß_{EC}$ is 1.03. The unperturbed distribution is Maxwellian with temperature 1keV. The density of electrons is $10^{19}ms^{-1}$, and the size of the grid is 100 points in V space by 100 points in θ_p, θ_p being the pitch angle $V_\perp/V$. The vertical axis shows the damping rate normalised to the plasma frequency while the horizontal axis is the ratio $ß_W=\Omega/\omega$. The second example shows a similar example

but with the X mode interacting with the *second harmonic* (this is the only place in the whole thesis where we mention heating at any harmonic other than the first). This time the ECRH propagates at 19^0 to the perpendicular. The ratio $ß_{EC}=2\Omega/\omega$ is 1.06. Although the vertical axis is still ω_i/ω_{pe}, the horizontal axis is $ß_w=\Omega/\omega$ (***not*** $2\Omega/\omega_w$). For these two cases the damping rates are virtually indistinguishable from those of the unperturbed Maxwellian. The largest change is produced by the third example which includes simulation of the toroidal electric field - figure (5.2c), suggesting that the ohmic electric field creates a greater distortion to the distribution than the ECRH. In this example we have used a nonrelativistic model operator rather than simulation of a particular mode. Instead of calculating the value D_o by $<(\Delta V_\perp)^2>/2\Delta t$ we let

$$D_0 = D_{max}\, e^{-\left(\frac{V_{||} - 2\nu_e}{\frac{\upsilon_e}{2}}\right)^2}$$

where $D_{max}=5\nu_e V_{th}^2$, V_{th} is the thermal electron speed and ν_e is the electron collision frequency. The ohmic electric field is $0.1E_D$, E_D being the Dreicer field=$mV_{th}\nu_e/e$. As we use this model none of the other parameters such as power input nor the ratio $ß_{EC}$ for the flux surface we gave for figures (5.2a) and (5.2b) are applicable. The Dreicer field is of significance in the study of runaway electrons, i.e. electrons whose parallel velocity increases so much that they essentially become collisionless, causing possible confinement problems.

Given our analytic work and the more realistic distributions taken from the BANDIT code, we conclude that no instabilities to whistler waves are possible when a Maxwellian distribution is perturbed by the application of ECRH, the underlying reason being that the perturbation to the Maxwellian is not sufficiently large.

Figure 5.2a.

Damping rates of whistlers /ω_{pe} in flux surface distributions produced numerically by the BANDIT code

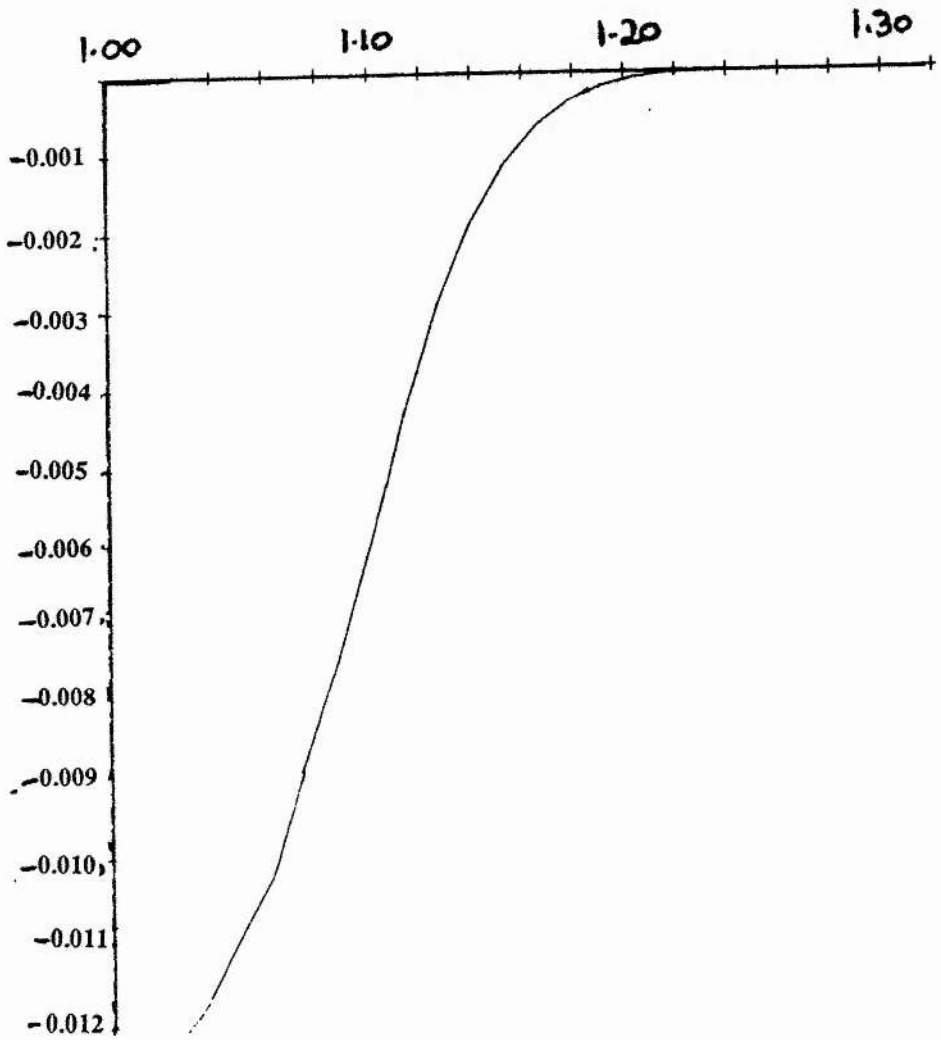

Mode	O mode fundamental perpendicular propagation
ECRH power	1 M W
Density	$10^{19} m^{-3}$
Profile	$\exp(-(y^2 + z^2)/L^2)$ where L = 0.05m
Grid size	100 * 100 points, (V,θ) space, max energy 150 keV
Distribution	Maxwellian temperature 1keV
Magnetic field	3.42T
Flux surface	Ω/ω =1.03 for the electron cyclotron wave at the flux surface where ECRH impinges

Vertical axis - damping rate/ω_{pe}

Horizontal axis - Ω/ω for the whistler wave

Figure 5.2b.

Damping rates of whistlers /ω_{pe} in flux surface distributions produced numerically by the BANDIT code

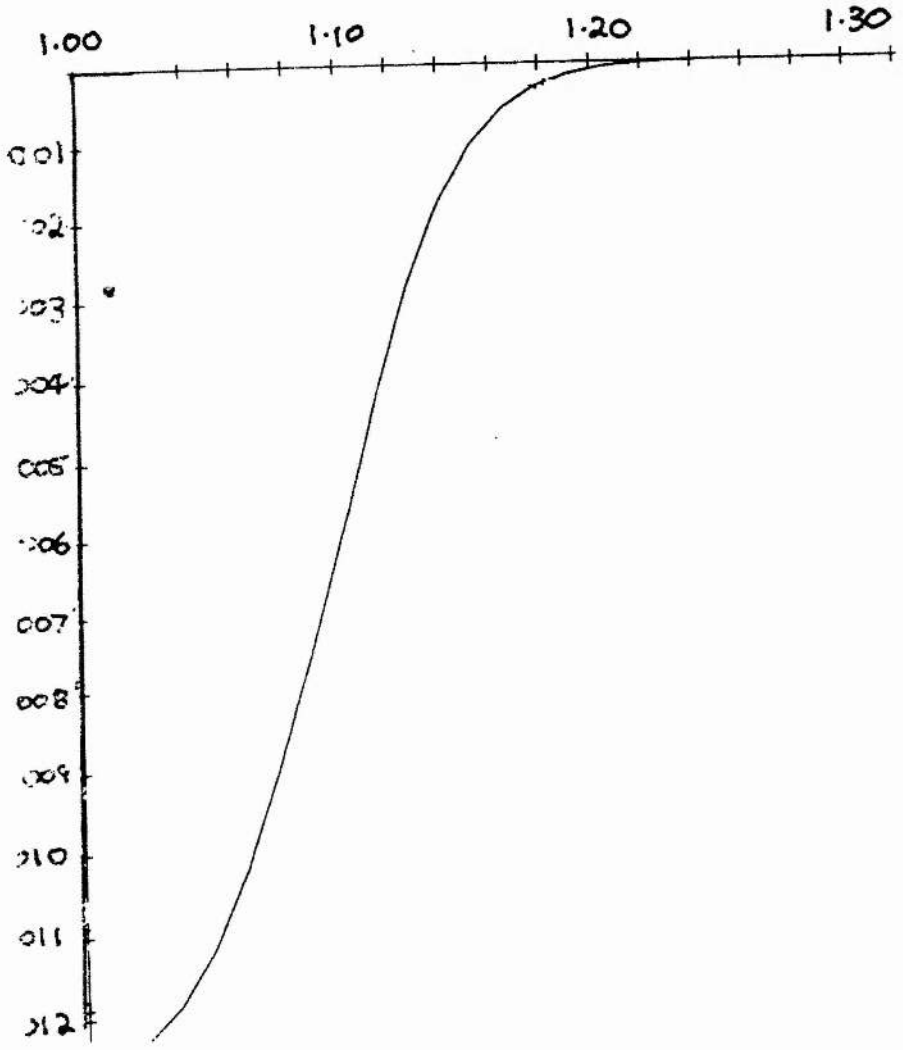

Mode	X mode second harmonic 19° to perpendicular
ECRH power	1 M W
Density	$10^{19} m^{-3}$
Profile	$\exp(-(y^2 + z^2)/L^2)$ where L = 0.05m
Grid size	100 * 100 points, (V,θ) space, max energy 150 keV
Distribution	Maxwellian temperature 1keV
Magnetic field	3.42T
Flux surface	$2\Omega/\omega = 1.06$ for the electron cyclotron wave at the flux surface where ECRH impinges

Vertical axis - damping rate/ω_{pe}

Horizontal axis - Ω/ω for the whistler wave

Figure 5.2c.

Damping rates of whistlers /ω_{pe} in flux surface distributions produced numerically by the BANDIT code

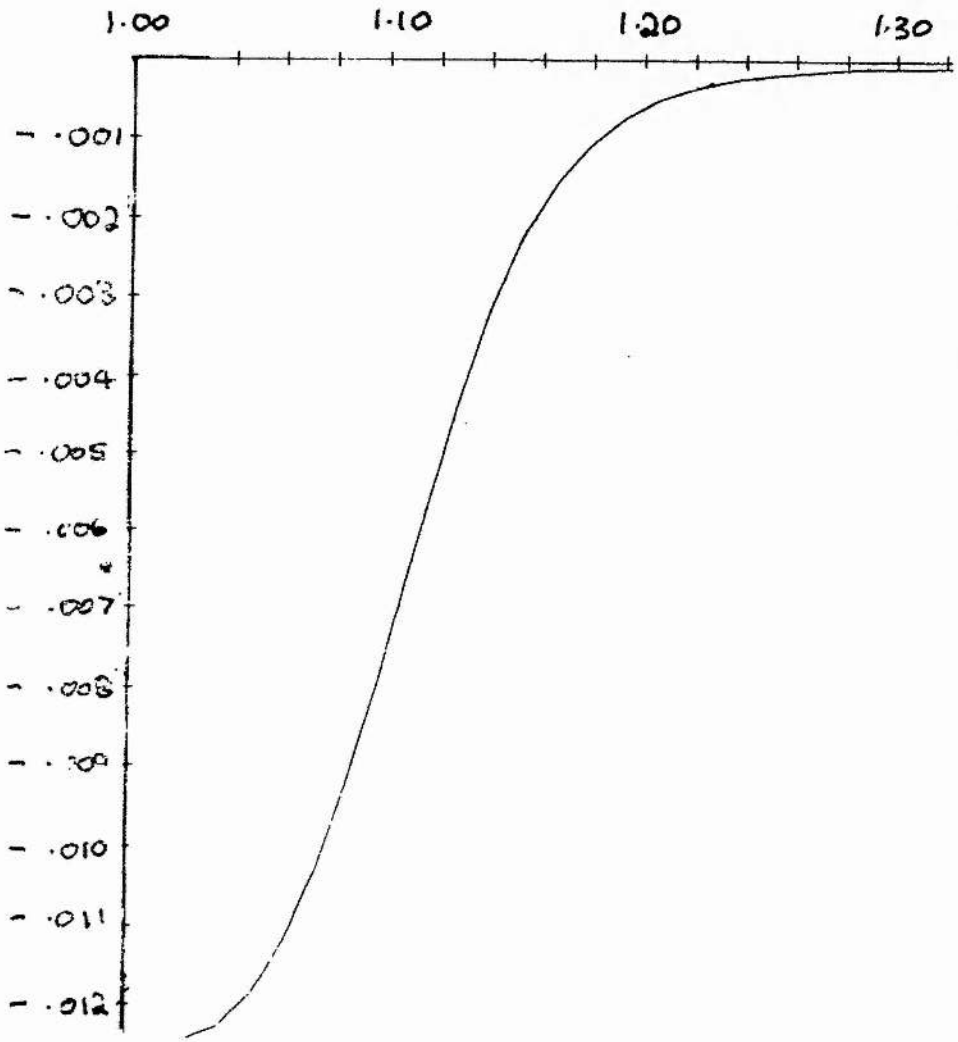

Nonrelativistic ECRH model operator

$$\frac{\partial f}{\partial t} = \frac{1}{V_\perp}\frac{\partial}{\partial V_\perp}\left(V_\perp D \frac{\partial f}{\partial V_\perp}\right)$$

$D = D_{max} \exp(-(V_\parallel - 2v_e/0.5v_e)^2)$

$D_{max} = 5 v_e V_{eth}^2$

v_e =electron collision frequency

V_{eth} thermal electron energy.

Ohmic electric field is 0.1 E_D, E_D = Dreicer Field = $mV_e v_e/e$.

Grid size	100 * 100 points, (V,θ) space, max energy 150 keV
Distribution	Maxwellian temperature 1keV
Magnetic field	3.42T

Vertical axis - damping rate/ω_{pe}

Horizontal axis - Ω/ω for the whistler wave

5.4 Instabilities in Distributions given by Nonlinear Heating.

In this section we consider instabilities to electromagnetic waves of the distributions found in Chapter four ie FEL ECRH produced distributions. In particular we will examine the stability to whistler waves. Because we are interested in small disturbances linear theory is sufficient to describe the growth rates. The expression for the growth rate can be found from (5.5a) by splitting up the interval of integration as follows:

$$\gamma_N = \int_{p_\perp \notin \mathbf{D}} dp_\perp \frac{p_\perp^3}{4} \mathcal{D}(f_{max}) + \int_{p_\perp \in \mathbf{D}} dp_\perp \frac{p_\perp^3}{4} \mathcal{D}(f_{ECRH})$$

(5.9),

where $\mathbf{D}$ is the set of all values of $p_\perp$ for which the three conditions of Chapter three are satisfied and which are in resonance with the unstable wave. We note that the universal set is $\mathbf{D} \cup \mathbf{D}' = (0,\infty)$ if the unstable wave is the whistler wave, but that this interval is finite if we consider a wave for which $n_{||w}^2 < 1$ (eg Bornatici and Ruffina, 1985), $\mathbf{D}'$ being the complement of $\mathbf{D}$. Our definition of f_{ECRH} is given in Chapter four and involves the quantity β_{EC}.

The integral over $p_\perp$ can be conveniently performed by using a transformation of coordinates given by Bornatici and Ruffina which gives the resonant velocity coordinates in terms of one parameter, η say:

$$\gamma = \frac{\beta_w}{1 - n_{||w}^2} + \frac{|n_{||w}|}{|1 - n_{||w}^2|}\left(n_{||w}^2 + \beta_w^2 - 1\right)\eta$$

(5.10a)

$$p_{\perp} = \frac{\sqrt{\left(n_{\|w}^2+\beta_w^2-1\right)}\sqrt{\eta^2-1}}{\sqrt{\left|1-n_{\|w}^2\right|}} \qquad (5.10b)$$

$$p_{\|} = \frac{\beta_w n_{\|w}}{1-n_{\|w}^2} + \frac{n_{\|w}}{|n_{\|w}|}\frac{\sqrt{\left(n_{\|w}^2+\beta_w^2-1\right)}\eta}{\left|1-n_{\|w}^2\right|} \qquad (5.10c).$$

This transformation is of use, and gives the resonant points in velocity space, not only for waves propagating with $\beta_w>1$, in which case $n_{\|w}{}^2>1$ and $\eta\geq 1$, but also when $\beta_w<1$, in which case $n_{\|w}{}^2<1$ and $\eta\in(-1,1)$, provided of course that $n^2{}_{\|w}+\beta^2{}_w>1$. In this chapter we will mainly be concerned with whistler waves, and we consequently restrict our analysis to $\eta\in(1,\infty)$. However in Appendix three we extend the analysis to $\eta\in(-1,1)$ to consider possible instabilities to the O mode.

Using the transformation (5.10) to determine $f_{max}(\eta)$, the Maxwellian distribution function at resonant points of velocity space is given by

$$f_{max} = N\, e^{\left(\lambda_T\frac{\beta_w}{n_{\|w}^2-1} - \lambda_T\frac{|n_{\|w}|}{\left|n_{\|w}^2-1\right|}\left(n_{\|w}^2+\beta_w^2-1\right)\eta\right)}$$

and the distribution $f_{ECRH}(\eta)$ (we shall take $Q_{pass}=1$ for the purpose of this discussion but not when presenting numerical work later in this chapter) is given by

$$f_{ECRH} = \frac{N}{2} e^{-\left(\lambda_T \frac{\beta_w}{n_{\|w}^2 - 1} - \lambda_T \frac{|n_{\|w}|}{|n_{\|w}^2 - 1|} \left(n_{\|w}^2 + \beta_w^2 - 1 \right) \eta \right) - 2 \lambda_T \beta_{EC}} + \frac{1}{2} f_{max}$$

and from (5.9) we have the following expression for γ_N (t being a dummy variable of integration),

$$\gamma_N = \left(\frac{n_{\|w}^2 + \beta_w^2 - 1}{n_{\|w}^2 - 1} \right)^2 \frac{N \lambda_T}{4} \times$$

$$\left(e^{\lambda_T \frac{\beta_w}{n_{\|w}^2 - 1}} \int_{t \in \clubsuit'} dt\, t\left(t^2 - 1\right) e^{-\lambda_T \frac{|n_{\|w}|}{|n_{\|w}^2 - 1|} \left(n_{\|w}^2 + \beta_w^2 - 1 \right) t} \frac{\beta_w + n_{\|w} p_\|}{\gamma} \right.$$

$$\frac{1}{2} e^{\lambda_T \frac{\beta_w}{n_{\|w}^2 - 1}} \int_{t \in \clubsuit} dt\, t\left(t^2 - 1\right) e^{-\lambda_T \frac{|n_{\|w}|}{|n_{\|w}^2 - 1|} \left(n_{\|w}^2 + \beta_w^2 - 1 \right) t} \frac{\beta_w + n_{\|w} p_\|}{\gamma} +$$

$$\left. \frac{1}{2} e^{-\lambda_T \frac{\beta_w}{n_{\|w}^2 - 1}} \int_{t \in \clubsuit} dt\, t\left(t^2 - 1\right) e^{\lambda_T \frac{|n_{\|w}|}{|n_{\|w}^2 - 1|} \left(n_{\|w}^2 + \beta_w^2 - 1 \right) t + 2 \lambda_T \beta_{EC}} \frac{\beta_w + n_{\|w} p_\|}{\gamma} \right)$$

(5.11)

where ♣ is the image set of **D** under transformation (5.10b), ie the set of values of the integration variable giving resonant points in velocity space which satisfy the three conditions of Chapter three. Also ♣' =(1,∞)/♣ ie the complement of ♣ in (1,∞). Noting that $\gamma = \beta_w + n_{\|w} p_\|$, we can evaluate (5.11) readily if we know the set ♣. We now proceed to determine it using some straightforward but tedious algebra. We shall in fact find that ♣ is approximately equal to an interval (η_{min}, η_{max}), so that the evaluation of (5.11) will be straightforward.

Analysis of implications of the three conditions of Chapter three.

Condition 1.

Firstly we consider condition 1 of Chapter three. We consider final velocities which are functions of η given by equations (5.10) with $\eta \geq 1$. We note that (3.5b) must automatically be satisfied if we have $\gamma_f = \gamma_f(\eta)$ and $p_{||} = p_{||}(\eta)$ with $\eta \geq 1$, as this guarantees $\gamma_f > \gamma_0$. We have from (3.5a)

$$\gamma_f \leq 2\beta_{EC} - \gamma_0$$

$$\Rightarrow 1 + p_{||}^2 \leq \left(\beta_- - n_{||w} p_{||}\right)^2$$

where $\beta_- = 2\beta_{EC} - \beta_w$,

$$\Rightarrow \left(1 - n_{||w}^2\right) p_{||}^2 + 2\beta_- n_{||w} p_{||} + \left(1 - \beta_-^2\right) \leq 0$$

$$\Rightarrow p_{||} \leq p_{||-} \text{ or } p_{||} \geq p_{||+} \text{ subject of course to } p_{||} = p_{||}(\eta) \text{ for } \eta \in (1, \infty)$$

where $p_{||-} < p_{||+}$ and $p_{||-}$ and $p_{||+}$ are solutions of

$$\left(1 - n_{||w}^2\right) p_{||}^2 + 2\beta_- n_{||w} p_{||} + \left(1 - \beta_-^2\right) = 0.$$

We now restrict attention to perpendicular propagation. We note that we may without loss of generality consider only $n_{||w} < 0$ since we have no preferred direction along the z axis (our distribution function is symmetric in $p_{||}$). We note at this stage that in the nonrelativistic case choice of $n_{||w} < 0$ determines the sign of the resonant parallel velocity, (positive for $\beta_w > 1$). In the relativistic case however there are generally two resonant values of $p_{||}$ corresponding to $p_\perp$ and it is possible

that these may be of opposite sign. We note from (5.10c) that with our choice of $n_{\|w}$, $p_{\|0}=p_{\|}(\eta=0)$ is positive but that $p_{\|} \to -\infty$ as $\eta \to \infty$. We therefore have the additional restriction that $p_{\|} \leq p_{\|0}$. It turns out in fact that it is the negative values of $p_{\|}$ which are of most interest to us.

With our choice of $n_{\|w}$ we can determine $p_{\|-}$ and $p_{\|+}$ subject to $p_{\|-}<p_{\|+}$. Explicitly we have

$$p_{\|\pm} = \frac{\beta_- n_{\|w} \pm \sqrt{n_{\|w}^2 \beta_-^2 + \left(n_{\|w}^2 - 1\right)\left(1-\beta_-^2\right)}}{n_{\|w}^2 - 1} \tag{5.12a}$$

We note that $|p_{\|-}|$ has a very large magnitude for typical parameters. This is most easily seen by noting $\beta_- \approx 1$ and by making a Taylor expansion of the square root of (5.12a) so that

$$p_{\|+} \approx \frac{\beta_-^2 - 1}{2 n_{\|w} \beta_-} \tag{5.12b}$$

and

$$p_{\|-} \approx \frac{2\beta_- n_{\|w}}{n_{\|w}^2 - 1} \tag{5.12c}$$

These last two expressions are valid provided

$$\left| \frac{\left(n_{\|w}^2 - 1\right)\left(1-\beta_-^2\right)}{n_{\|w}^2 \beta_-^2} \right| \ll 1 \tag{5.12d}$$

which will always be the case for parameters of interest.

Condition 2

Now let us consider the trapping condition. To make analytic progress we make further simplifications. We assume the incident ECRH is in the O mode and that we can make the weakly relativistic approximation. Together with our earlier assumption that propagation is perpendicular we can use condition (3.7b) and neglecting the factor γ (consistent with our weakly relativistic approximation) we have the approximate condition $|p_{||}|>p_{||T}$ where

$$p_{||T}=\left(\frac{B_0 c}{E_{||}}\right)\frac{1}{\beta_{EC} n_{\perp EC}}\left(\frac{2(\beta_{EC}-\gamma_0)}{3\beta_{EC}}\right)^{\frac{3}{2}} \qquad (5.13),$$

where $\gamma_0^2=1+p_{||T}^2$.

We note at once that this is not an explicit expression for $p_{||T}$. There is really no suitable approximation to $p_{||T}$ that we can make here that would be of assistance to later analysis. We therefore content ourselves with this expression.

Suppose now that $\beta_-<1$. We will then have an interval $(p_{||+},-p_{||T})$ on which the first two of our conditions are satisfied provided $p_{||+}<-p_{||T}$. Obviously we have also an interval $(p_{||T},p_{||0})$ on which our conditions are also valid, but we are less interested in this interval because it corresponds to very much smaller values of γ_f, and hence very much larger values of γ_i , so $\exp\{\lambda_T(\gamma_f-1)\}$ is exponentially small and any contribution to the growth rate will be negligible. It can therefore be seen that we have one significant interval of $p_{||}$ and hence η in which the first two of our conditions are fulfilled. We will refer to the maximum and minimum values of $p_{||}$ and η with a 'min' and 'max' subscript ie

$p_{||min} = p_{||+}$ and

(5.14a)

$p_{\|max} = -p_{\|T}$

(5.14b).

Using (5.10c) our expressions for η_{min} and η_{max} are

$$\eta_{min/max} = \frac{n_{\|w}^2 - 1}{\sqrt{n_{\|w}^2 + \beta_w^2 - 1}} \left\{ \frac{\beta_w n_{\|w}}{n_{\|w}^2 - 1} - p_{\|max/min} \right\}$$

(5.15)

subject to the restriction $\eta_{min} \geq 1$ (η_{min} can be 1 if $p_{\|max}$ is large enough). (Note that η_{min} corresponds to $p_{\|max}$ and vice versa).

Condition 3

We still have one more condition to satisfy, namely the third condition. We see from Chapter three that in order to check this condition we need to calculate $p_{\perp FP}$ from an implicit equation, so we will be able to make very little analytic progress on this condition. Instead it must be determined implicitly and this is done for numerical work. It is clear that as $|p_{\|}|$ increases so $T_{rot}/T_{transit}$ will decrease, so condition 3 imposes an upper limit on $|p_{\|}|$. For most typical parameters the maximum imposed on $|p_{\|}|$ by condition 1 is more restrictive than that imposed by condition 3, although this is by no means *always* the case. To simplify analytic calculations we ignore the possibility that it is condition (3.7) which imposes a maximum on $|p_{\|}|$ for the duration of this section, but stress that this is *not* ignored in the code used to calculate the growth rates which we will discuss later.

Summary of Conditions (1) to (3).

Firstly suppose that $p_{||T}<p_{||0}$. We will have an interval $(p_{||T},p_{||0})$ on which the conditions are satisfied. However this interval corresponds to

$\gamma_f \in \left(\gamma_{min},\beta_w+n_{||w}p_{||T}\right)$ and therefore to $\gamma_i \in \left(\beta_- - n_{||w}p_{||T},2\beta_{EC}-\gamma_{min}\right)$, where

$\gamma_{min} = \gamma(\eta=0)$.

As

$$e^{-\lambda_T\left(\beta_- - n_{||w}p_{||T} - 1\right)}$$

is exponentially small, relatively few electrons are heated/cooled to resonant parallel velocities in $(p_{||T},p_{||0})$. We therefore ignore this interval completely and seek other intervals in which the conditions are satisfied.

Now if $p_{||+}<p_{||-}$ then we have an interval $(p_{||+},p_{||-})$in which our conditions are fulfilled. This interval corresponds to

$\gamma_f \in \left(\beta_w+n_{||w}p_{||+},\beta_w-n_{||w}p_{||T}\right)$ and therefore to $\gamma_i \in \left(\beta_w+n_{||w}p_{||T},\beta_w-n_{||w}p_{||+}\right)$.

Now

$$e^{-\lambda_T\left(\beta_- + n_{||w}p_{||T} - 1\right)}$$

is **not** exponentially small and many electrons may be heated into velocities which are resonant in this interval.

This having been stated, we now have well defined values of η_{min} and η_{max} and hence a completely defined integral in (5.11).

The evaluation of the growth rate.

As we have now defined the limits of the integral in (5.11) at least implicitly we have the following expression for γ_N:

$$\gamma_N = - g(z,1) - g_H(z,\eta_{min}) - g_H(z,\eta_{max}) \tag{5.16a}$$

where

$$g(z,\eta) = -Ce^{-z\eta}\left(\frac{6}{z^4} + \frac{6\eta}{z^3} + \frac{\left(3\eta^2-1\right)}{z^2} + \frac{\eta\left(\eta^2-1\right)}{z}\right) \tag{5.16b}$$

and where

$$z = \frac{\left| n_{\|w} \right|}{\left| 1 - n_{\|w}^2 \right|} \left(n_{\|w}^2 + \beta_w^2 - 1 \right) \lambda_T \tag{5.16c}$$

and

$$C = \frac{N\lambda_T}{4} \frac{\left(n_{\|w}^2 + \beta_w^2 - 1 \right)^2}{\left| 1 - n_{\|w}^2 \right|^2} e^{-\frac{\lambda_T \beta_w}{1 - n_{\|w}^2}} \tag{5.16d}$$

and

$$g_H(z,\eta) = \frac{g(z,\eta) - g(-z,\eta) e^{-2\lambda_T \beta_{EC} - \frac{2\lambda_T \beta_w}{n_{\|w}^2 - 1}}}{2} \tag{5.16e}.$$

Clearly there is endless scope for discussion as we have not even considered a realistic distribution (we have taken $Q_{pass}=1$ instead of $Q_{pass} \propto p_{||}$). Although it is possible to evaluate the integral in (5.5a) with a more realistic distribution such as (4.1c) by adapting equations (5.16) slightly, no analytic expression for γ_N may be found if we introduce a temperature anisotropy (ie we have a Bimaxwellian with $T_{||} \neq T_{\perp}$ instead of a Maxwellian). Clearly by using a more realistic distribution given by (4.1c), $df/dp_{\perp}$ will not be as large, especially near $p_{||} \approx 0$, as far fewer electrons are heated. The waves are therefore less likely to be unstable. In contrast the existence of temperature anisotropy may well increase instability as it tends to increase $df/dp_{\perp}$ as discussed in section 5.2. Finally we could speculate on the differences we would expect if we were to use a more accurate theory for the heating of electrons which took into account the nonadiabatic heating of electrons.

So far we have not given explicit conditions that instabilities should occur, and although it is obvious that the implicit condition $\gamma_N>0$ is both a necessary and sufficient condition, the resulting algebra is too cumbersome to yield illuminating results. The reader may therefore be wondering whether we will have any instabilities at all. In the next section we must give a brief description of the stability code and in the next but one we redress the balance by giving plenty of numerical examples of instances of instability. First though we examine analytically the limiting case that negative terms in (5.16a) for the growth rate can be neglected compared with those positive terms which contribute to instability. We suppose now that the condition $\eta_{min} < \eta_{max}$ is fulfilled and that furthermore we have $\eta_{min}=1$. This will enable us to estimate the order of magnitude of growth rates that are possible. We note first that (5.16a) has five terms (the $g_H(z,\eta)$ functions contain two terms each). However with $\eta_{min}=1$ the first two cancel. Let us examine the exponential factors in the remaining terms with the help of (5.16b-e). The arguments of the exponential function are $\lambda_T(1-\gamma_{min})$, $\lambda_T(1-2\beta_{EC}+\gamma_{min})$ and

$\lambda_T(1--\gamma_{max})$ respectively (the last two are in fact equal). We see therefore the growth rate will grow as γ_{min}->1, ie as the unstable wave is in resonance with low velocity electrons. As z is typically >>1 g(η=1) will be dominated by the third term in equation (5.16b) and γ_N will be dominated by

$$\frac{N' e^{-\lambda_T\left(\gamma_{min}-1\right)}}{2n_{\|w}^2\lambda_T}$$

where

$$N' = \frac{\lambda_T}{4\pi K_{2red}(\lambda_T)}$$

and

$$K_{2red}(\lambda_T) = e^{\lambda_T}K_2(\lambda_T)$$

As λ_T->∞ we have (eg Gradshteyn and Ryzhik, 1965 p963)

$$K_{2red} \approx \sqrt{\frac{\pi}{2\lambda_T}}$$

We now make an order of magnitude estimate of γ_N. Taking $\lambda_T \approx 500$, γ_{min}=1 and $n_{\|w} \approx 2$ we see that $\gamma_N \approx 1/5$. The order of magnitude of the other factors in equation (5.6) is hard to calculate; however if ω_{pe}, Ω and ω all have the same order of magnitude and we use the cold plasma approximation in which $P = -\frac{\omega_p^2}{\omega(\omega+\Omega)}$ then the order of magnitude of (5.6) is simply ω/5. Unless heating

is in the low density region of the tokamak so that ω_{pe} is not of the same order of magnitude as ω this very large value will be large enough to question the assumption that $\omega_i/\omega<<1$.

We have of course considered very extreme cases to arrive at our order of magnitude estimate of the maximum possible growth rate of instabilities, and have not justified many of our assumptions. Nonetheless our numerical examples from the rest of the chapter will show that for certain choices of parameter growth rates may be surprisingly large and in some instances may be of the order of magnitude indicated here.

The reader may be wondering why we have not produced necessary or sufficient conditions for our instability to occur. The reason lies mainly in the complexity of the expression for γ_N in (5.11) together with the difficulty in obtaining the appropriate limits of integration. In particular because we do not have an explicit expression for $p_{\|T}$ we are not able even to determine a condition that an interval of resonant velocity space lies in the velocity space of heated electrons, from which we could deduce a necessary condition for the instability.

Although this may seem unsatisfactory it must be remembered that our aim is not simply to prove that the distribution function is unstable, but to show also that the typical growth rates involved are an order of magnitude larger than the collision time. This we do using numerical techniques. The results of the stability code are therefore critical to our conclusion.

5.5 Details of the Stability Code.

The stability codes can determine growth or damping rates for a variety of distributions and electromagnetic waves. The distribution may either be specified numerically on a Cartesian or polar grid in velocity, in which case the distribution is interpolated using a cubic spline in order to provide the distribution function and its derivatives for use in the integral (5.4). Alternatively it may be of a specified analytic form chosen through an input flag. In this section we mainly describe its use to determine the growth or damping rates of whistler waves. Its use to determine growth rates of numerical distributions is limited because it is numerically problematic to take derivatives of distributions specified on grids, especially if the distributions are not smooth or if we are interested in regions where the distribution function is small. We have already mentioned figures (5.2a) to (5.2c) which were calculated using numerical data. In these examples however the distributions were smooth and there was little difficulty in taking derivatives. Unfortunately the same could not be said for the distributions displayed in the last chapter which we would have liked to have tested for stability in order to make a more direct comparison of semi-analytically derived growth rates and those derived from fully numerical means.

In the last section we have given a detailed account of the way in which γ_N, the integral in (5.5a), is calculated. We have said very little about the actual calculation of the growth rate given by (5.6). Now equations (5.2) to (5.4) provide an implicit equation for $n_{||w}$, which is solved using NAG routine C05AJF. However we make a number of approximations in the process.

First we consider the evaluation of (5.4a). We note first that in cylindrical coordinates $(p_\perp, p_{||}, \phi)$ the ϕ integration is trivial since the integrand is independent of ϕ. Secondly it is important to appreciate that the most significant effect a distortion to a Maxwellian distribution has is to alter the absorption properties rather than to alter the basic polarisation and dispersion of the waves. Hence it is typical in numerical work to assume the distribution is Maxwellian for the purposes of calculating (5.4a), so the double integral can be evaluated in

terms of Shkarofsky functions using the code of Owen (1984) if the calculation is performed relativistically, or using the plasma dispersion function otherwise. We adopt this approach. We calculate the integral in (5.4a) nonrelativistically for the purpose of obtaining $n_{||w}$ by solving (5.2), and for the purpose of calculating the denominator in (5.6). The reason for the nonrelativistic approximation in the former case is that many evaluations of the LHS of (5.2) are needed to calculate $n_{||w}$ implicitly, and the plasma dispersion function is far easier to calculate than the Shkarofsky functions. In the latter case it is because the plasma dispersion function is relatively easy to differentiate with respect to ω, whereas the Shkarofsky functions are not. However we use the relativistic approach to evaluate the numerator of (5.6).

The routine proceeds by calculating the growth rates for the instabilities for a number of given values of the *whistler frequency* . Optionally the maximum growth rate and the whistler frequency at which it occurs may be found. Then these maximum growth rates can be found as a function of the ECRH frequency and a maximisation over the *ECRH frequency* can be performed using a crude search procedure.

The calculation of the growth rates of the O mode is similar to those of whistlers, but is more complicated and involves either four or eight integrals depending on the approximations being used. Details are given in Appendix three.

The actual results are calculated by using numerical integration to calculate the integral in (5.5a). In the case of numerically specified distributions it is essential to use numerical integration, but when we use the distribution predicted by the adiabatic model and the initial distribution is Maxwellian this is not necessary as we have an analytic formula (5.13) which is exact. Although the numerical integration is still performed, the formula is still of use in order to check the coding.

The amount of CPU time required for the numerical integrations is negligible in the case that the distribution is specified analytically. If the distribution is specified numerically it can take a minute or so of CPU time to set up the spline coefficients, but the overall timing is still relatively short.

Despite the apparent simplicity of the code, it is really not possible to make many comparisons of the results with completely analytic results because of the difficulty of evaluating analytically the factors in (5.6) other than γ_N.

We have already fully explained in the previous section how the distribution function is obtained in the simplified case that the propagation is perpendicular to the field. We have described how the limits of the numerical integration are determined by checking that the conditions (1) and (2) are satisfied on (η_{min},η_{max}). The only difference between the analysis in section 5.4 and the code is that in the latter case we also determine numerically $T_{rot}/T_{transit}$ to check that condition (3) is satisfied on (η_{min},η_{max}) (which is generally the case). In the case of oblique propagation the approach is similar but requires greater use of the numerical solution of complicated equations to calculate quantities given implicitly which had explicit values in the perpendicular case.

5.6 Results from the Stability Code.

This section gives the results from the stability code for a range of parameters showing substantial growth rates in some cases. Firstly we note from figures (5.3a) to (5.3d) that the instability increases with $n_{||EC}$ near $n_{||EC}=0$. These figures are calculated using a Bimaxwellian distribution where $T_{\perp}/T_{||}=2$, and for a flux surface which is heated by the beam where $ß_{EC}=1.01$. We note that for the chosen parameters the distribution is stable for perpendicular propagation (figure 5.3a). To reinforce this point we show the maximum growth rate with respect to the whistler wave frequency in figure (5.4) as a function of $n_{||EC}$. The reason for the increase in growth rate is that an increase in $n_{||EC}$ increases the maximum possible energy to which an electron may be accelerated.

To illustrate the dependence of the growth rates on the temperature anisotropy we calculate growth rates for a Bimaxwellian which has not been heated using a FEL in figure (5.5). At this point we should point out that a Bimaxwellian is not necessarily an unstable distribution. In the nonrelativistic case it was proved by Shima and Hall that in a magnetic field a distribution is stable provided $T_{\perp}<2T_{||}$. Intuitively introducing a relativistic distribution brings greater stability, though no simple condition can be given for stability in the relativistic case. The example is given purely to demonstrate the role played by temperature anisotropies in instabilities. We conclude that the underlying physical reason for the instability is an increase of perpendicular energy over parallel energy, increasing $df/dp_{\perp}$. The dependence of the growth rate on the quantity $ß_{EC}$ at the point on the flux surface where the ECRH occurs is illustrated in figure (5.6). The essential point to note is that the growth rate has a maximum well away from $ß_{EC}=1.0$ or even $ß_{EC}=\gamma(V_{th})\approx 1.002$. This is fortuitous as it is well away from $ß_{EC}=1.0$ that our adiabatic model most closely approximates the actual heating.

The dependence of the growth rate on the electric field of the ECRH is

Figure 5.3a.

Growth rate/ω_{pe} as a function of Whistler Frequency.

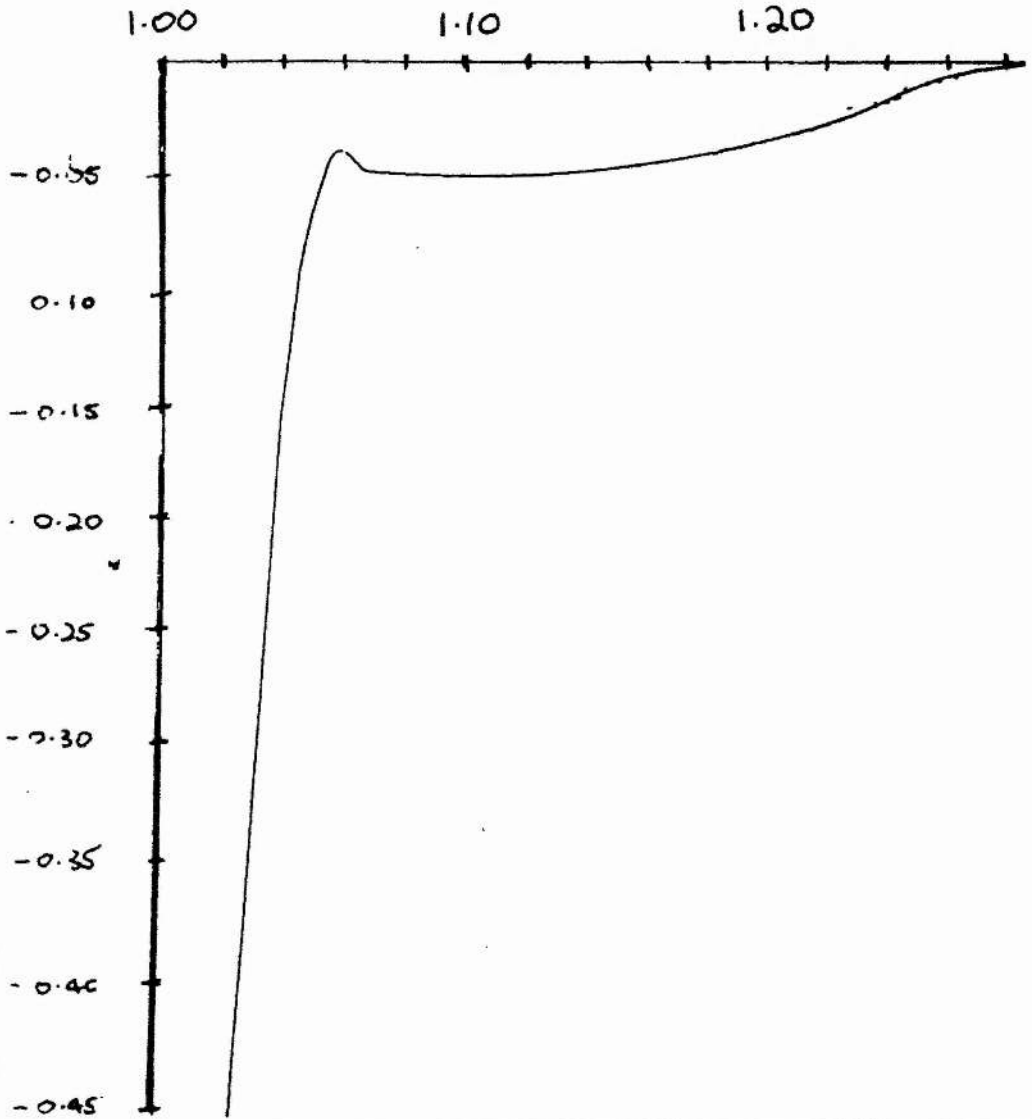

ω_{pe}/Ω	=1/2	Ratio of plasma to cyclotron frequency
$T_{\|\|}$	= 1keV	Parallel temperature
$T_{\perp}$	= 2keV	Perpendicular temperature (Bimaxwellian
L	= 0.05	Gaussian width
B	= 2.5T	Background field
$E_{\|\|}$	= $5 * 10^7$ Vm^{-1}	Parallel electric field
$ß_{EC}$	= 1.01	Ratio of cyclotron to O mode wave frequer
$V_{\|\|c}$	= $10^9 ms^{-1}$	Mixing parameter
$n_{\|\|ec}$	= 0	Parallel refractive index

Vertical axis - damping rate/ ω_{pe}

Horizontal axis - $ß_w=\Omega/\omega$ for whistler

Figure 5.3b.

Growth rate/ω_{pe} as a function of Whistler Frequency.

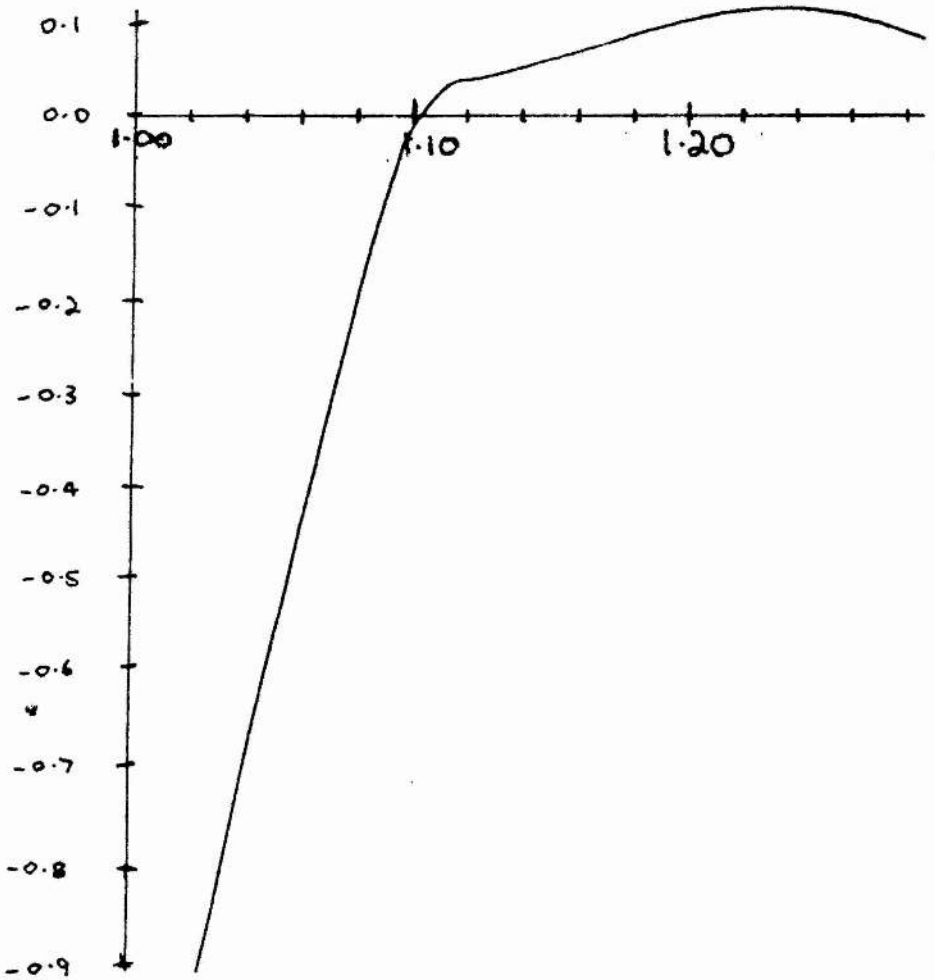

ω_{pe}/Ω	=1/2	Ratio of plasma to cyclotron frequency
$T_{\|\|}$	= 1keV	Parallel temperature
$T_{\perp}$	= 2keV	Perpendicular temperature (Bimaxwellian)
L	= 0.05	Gaussian width
B	= 2.5T	Background field
$E_{\|\|}$	= $5 * 10^7$ Vm^{-1}	Parallel electric field
β_{EC}	= 1.01	Ratio of cyclotron to O mode wave frequenc
$V_{\|\|c}$	= $10^9 ms^{-1}$	Mixing parameter
$n_{\|\|ec}$	= 0.05	Parallel refractive index

Vertical axis -growth- damping rate/ ω_{pe}

Horizontal axis - $\beta_w=\Omega/\omega$ for whistler

Figure 5.3c.

Whistler Growth rate/ω_{pe} as a function of Whistler Frequency.

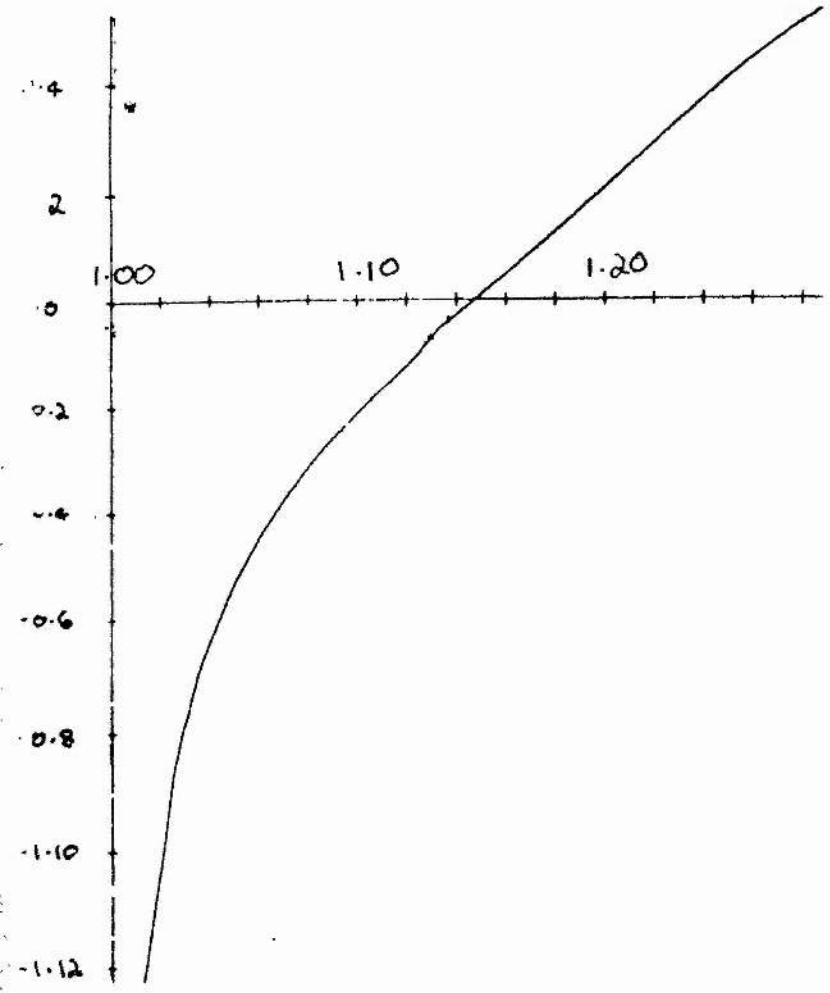

ω_{pe}/Ω	=1/2	Ratio of plasma to cyclotron frequency
$T_{\|\|}$	= 1keV	Parallel temperature
$T_{\perp}$	= 2keV	Perpendicular temperature (Bimaxwellian)
L	= 0.05	Gaussian width
B	= 2.5T	Background field
$E_{\|\|}$	= $5 * 10^7$ Vm^{-1}	Parallel electric field
$ß_{EC}$	= 1.01	Ratio of cyclotron to O mode wave frequency
$V_{\|\|c}$	= $10^9 ms^{-1}$	Mixing parameter
$n_{\|\|ec}$	= 0.1	Parallel refractive index

Vertical axis - growth rate/ω_{pe}

Horizontal axis - ß for whistler wave

Whistler growth rate /ω_{pe} against whistler frequency.

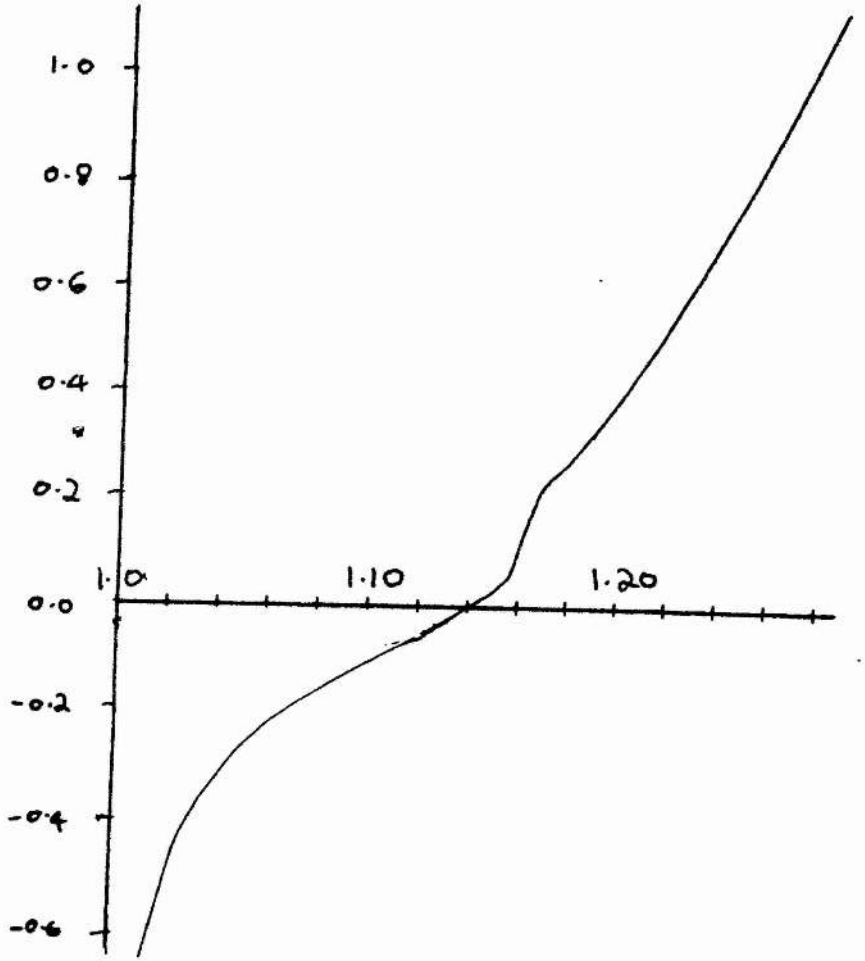

ω_{pe}/Ω	=1/2	Ratio of plasma to cyclotron frequency
$T_{\|\|}$	= 1keV	Parallel temperature
$T_{\perp}$	= 2keV	Perpendicular temperature (Bimaxwellian)
L	= 0.05	Gaussian width
B	= 2.5T	Background field
$E_{\|\|}$	= $5 * 10^7$ Vm^{-1}	Parallel electric field
$ß_{EC}$	= 1.01	Ratio of cyclotron to O mode wave frequency
$V_{\|\|c}$	= $10^9 ms^{-1}$	Mixing parameter
$n_{\|\|ec}$	= 0.15	Parallel refractive index

Vertical axis - growth rate/ω_{pe}

Horizontal axis - ß for whistler wave

Figure 5.4.

Whistler Growth rate/ω_{pe} as a function of Parallel Refractive Index of incoming ECRH

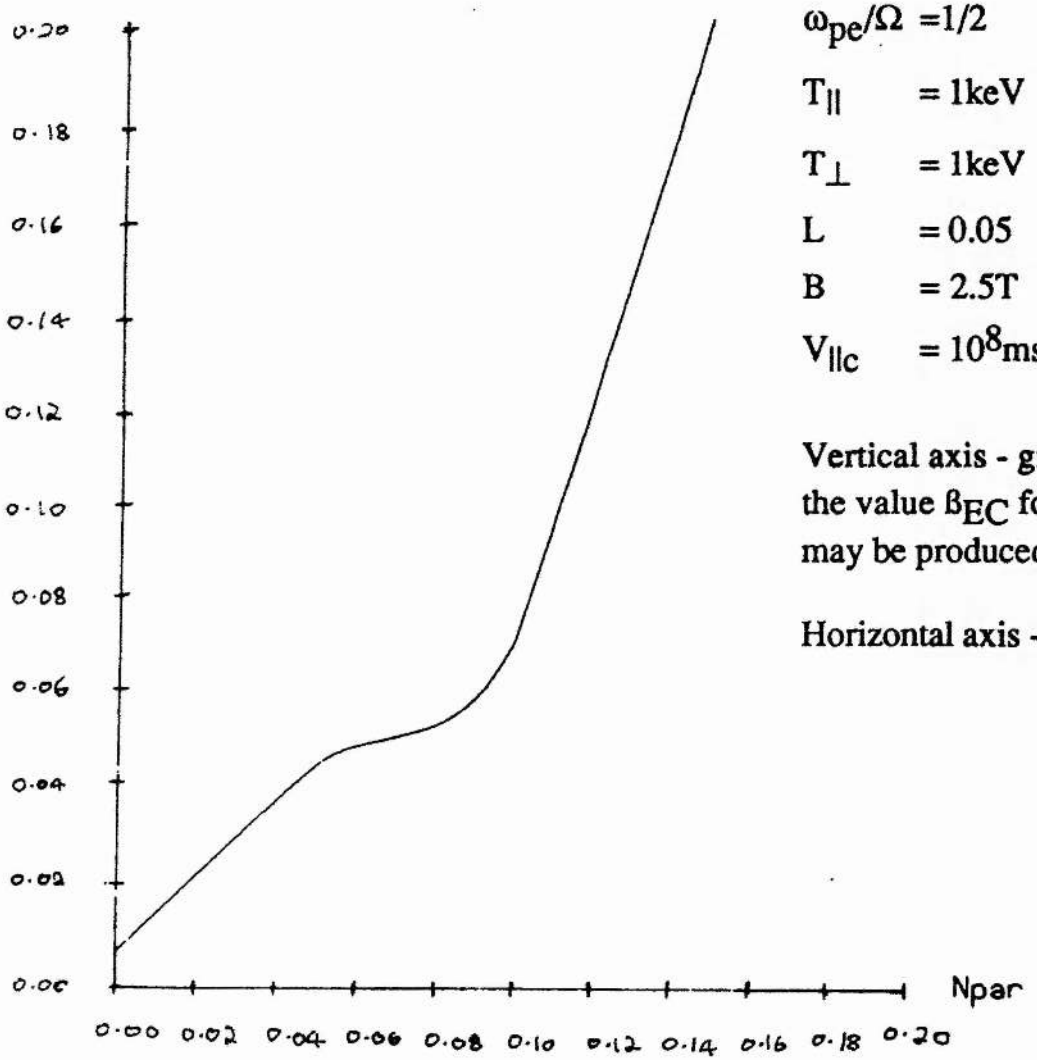

ω_{pe}/Ω	=1/2	Ratio of plasma to cyclotron frequency
$T_{\|\|}$	= 1keV	Parallel temperature
$T_{\perp}$	= 1keV	Perpendicular temperature
L	= 0.05	Gaussian width
B	= 2.5T	Background field
$V_{\|\|c}$	= $10^8 ms^{-1}$	Mixing parameter

Vertical axis - growth rate/ω_{pe} maximised over both the whistler frequency and the value β_{EC} for a flux surface. Physically it represents the largest growth that may be produced in the plasma.

Horizontal axis - $n_{\|ec}$ for the incoming ECRH

Figure 5.5.

Whistler Growth rate/ω_{pe} as a function of whistler frequency for a Bimaxwellian without application of ECRH

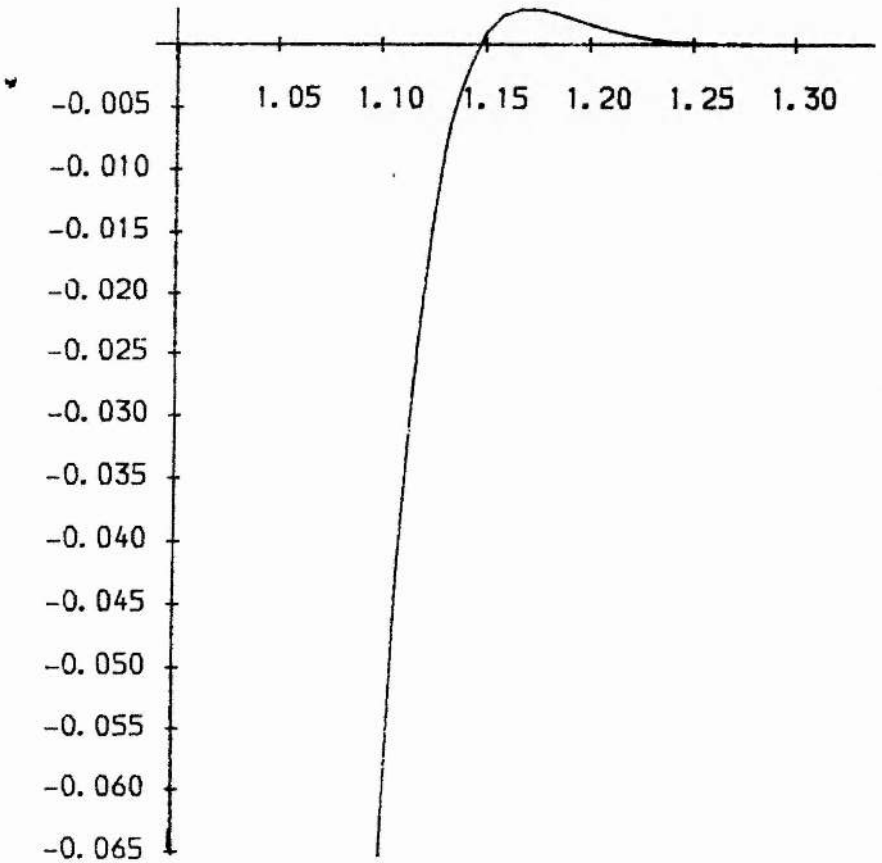

ω_{pe}/Ω	Ratio of plasma to cyclotron frequency	= 1/2
$T_\perp$	Perpendicular temperature	= 5 keV (Bimaxwellia
$T_\parallel$	Parallel temperature	= 0.5 keV
B	Background field	= 2.5T
$n_{\parallel ec}$	Parallel refractive index	= 0
$ß_{EC}$	Ratio of cyclotron to EC wave frequency	= 1.15
$E_\parallel$	Parallel electric field	= $5*10^7$ Vm-1
L	Gaussian beam width	= 0.05m

Vertical axis - growth/damping rate/ω_{pe}

Horizontal axis - ß for whistler wave

Figure 5.6.

Whistler Growth rate/ω_{pe} as a function of the ratio $ß_{EC}$

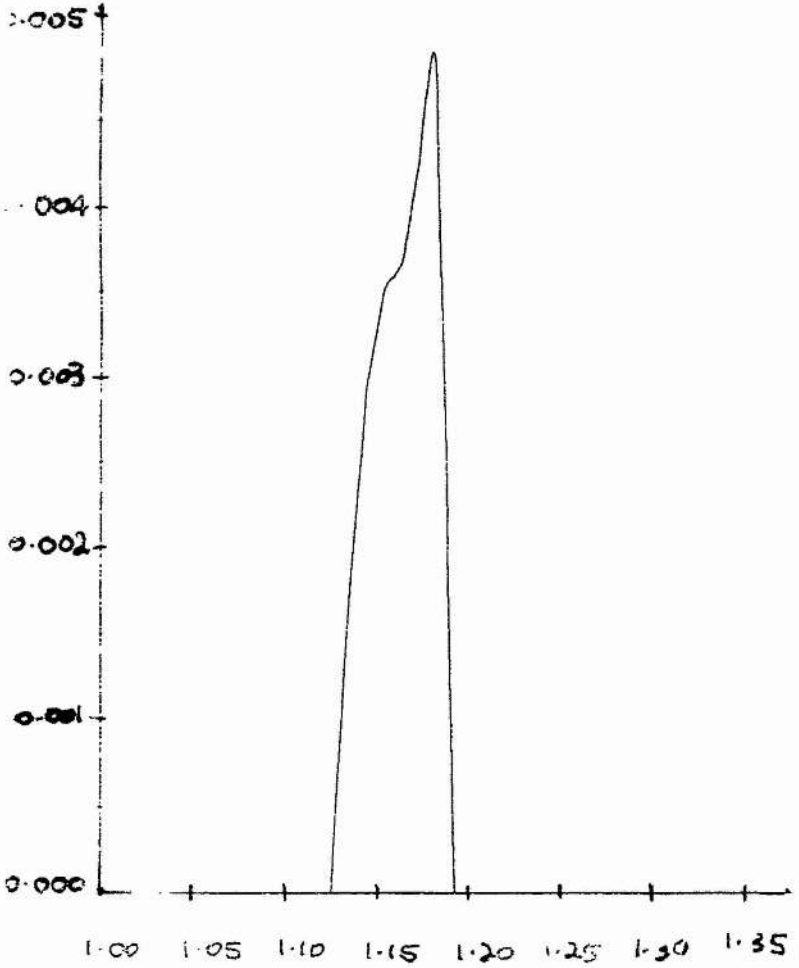

ω_{pe}/Ω	Ratio of plasma to cyclotron frequency	= 1/2
$T_\perp$	Perpendicular temperature	= 1 keV
$T_\parallel$	Parallel temperature	= 1 keV
B	Background field	= 2.5T
$n_{\parallel ec}$	Parallel refractive index	= 0
$E_\parallel$	Parallel electric field	= $5*10^7$ Vm-1
L	Gaussian beam width	= 0.05m
$V_{\parallel c}$	Mixing parameter	= $10^8 ms^{-1}$

Horizontal axis - $ß_{EC}$ for flux surface

Vertical axis - whistler growth rate maximised over whistler frequency

Figure 5.7a.

Whistler Growth rate/ω_{pe} as a function of Electric field of incoming ECRH

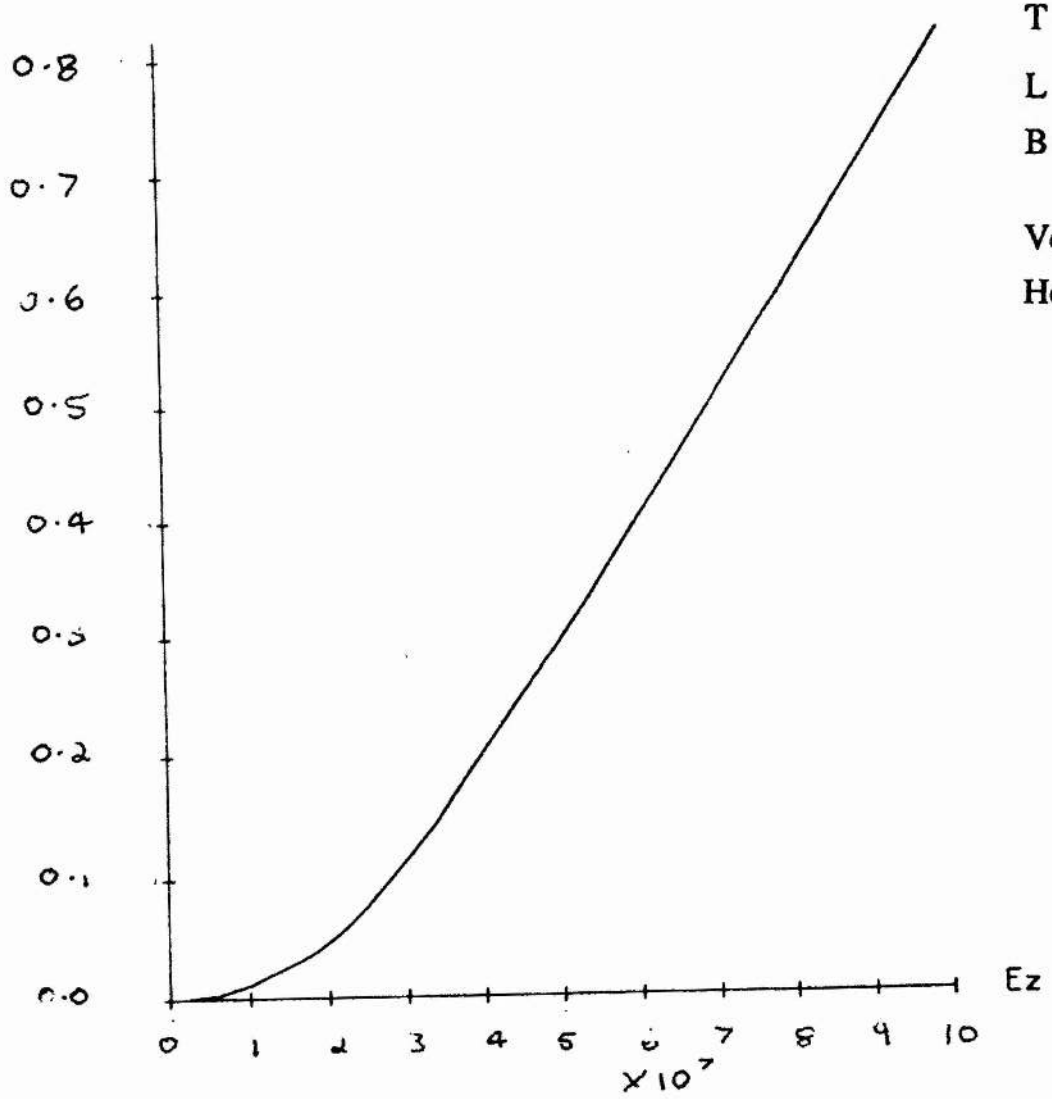

ω_{pe}/Ω	=1/2	Ratio of plasma to cyclotron frequency
T	= 1keV	Temperature (Maxwellian)
L	= 0.05	Gaussian width
B	= 2.5T	Background field

Vertical axis - β_{EC} for flux surface where maximum growth occur

Horizontal axis - $E_{||}$ for the incoming ECRH

Figure 5.7b.

Value of β_{EC} where maximum whistler growth rate occurs as a function of $E_{||}$

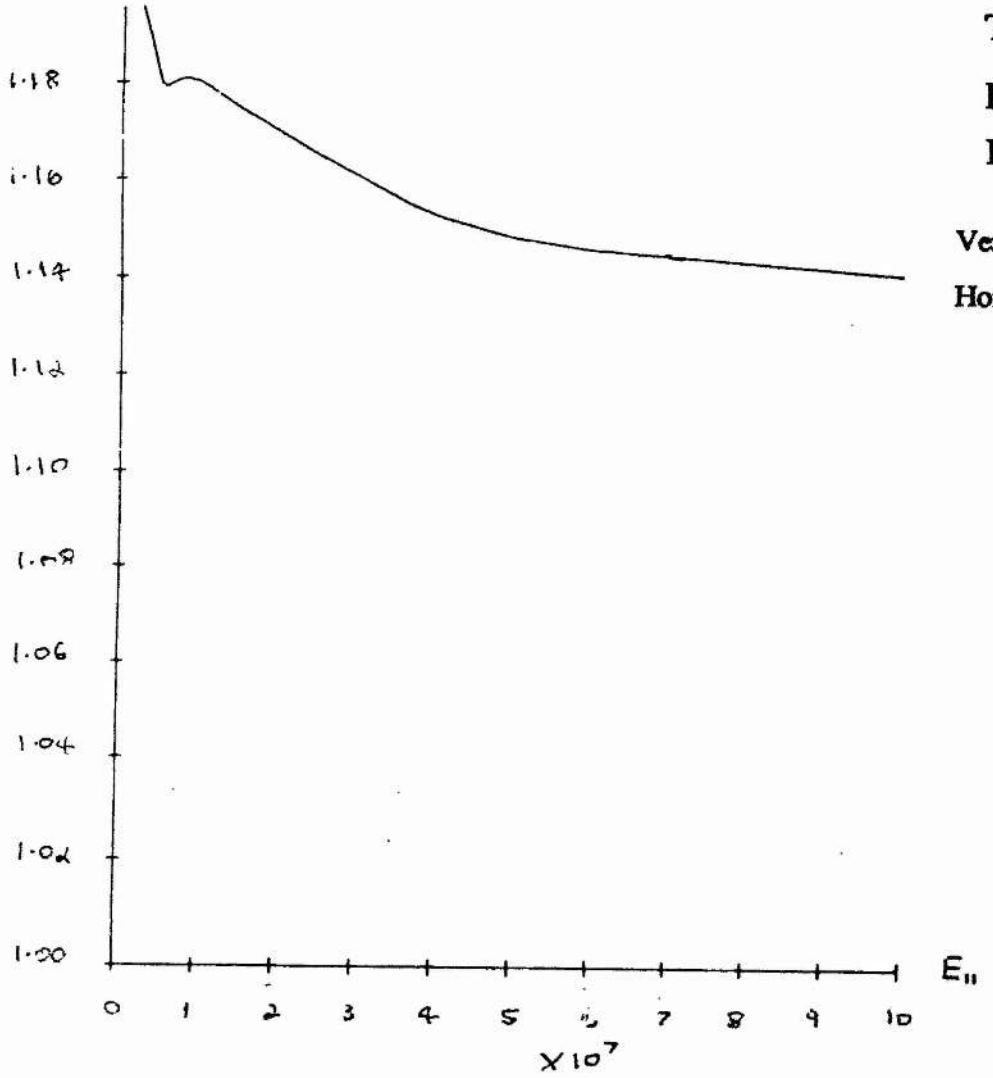

ω_{pe}/Ω	=1/2	Ratio of plasma to cyclotron frequency
T	= 1keV	Temperature (Maxwellian)
L	= 0.05	Gaussian width
B	= 2.5T	Background field

Vertical axis β_{EC} on flux surface where maximum growth rate occurs

Horizontal axis $E_{||}$

examined numerically in figure (5.7a) and a linear relationship is observed in the regime of interest. The vertical axis is the growth rate maximised over both the ratio $ß_{EC}$ *and* the whistler frequency. The horizontal axis is the electric field of the incoming ECRH in Vm^{-1}. Figure (5.7b) shows the value of $ß_{EC}$ at which the maximum growth rate occurs on the vertical axis with $E_{||}$ again on the horizontal axis. We note again that the values of $ß_{EC}$ at which the maxima occur are all much greater than $\gamma(V_{th})\approx 1.002$.

The growth rates for the whistler are compared with those for the O mode in figures (5.8a) and (5.8b) where we see that O mode instability can occur even when instability to whistlers does not. However the interpretation of the results is more problematic in the case of the O mode as is discussed in Section (5.8). We do not present results for the X mode as it cannot propagate just above the cyclotron frequency (see Chapter one).

Figure 5.8a

O mode growth rate/ω_{pe} against O mode frequency.

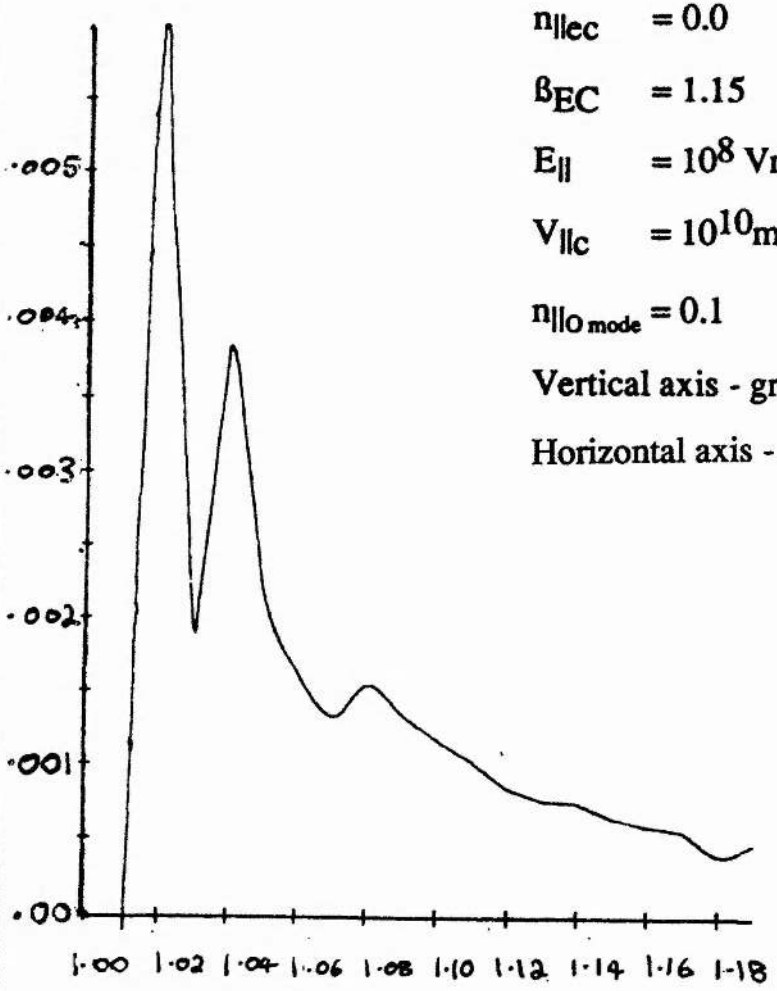

T	= 1keV	Temperature (Maxwellian)
$n_{\|ec}$	= 0.0	Perpendicular EC wave
$ß_{EC}$	= 1.15	Ratio of cyclotron to EC wave
$E_{\|}$	= 10^8 Vm^{-1}	Parallel electric field
$V_{\|c}$	= $10^{10}ms^{-1}$	Mixing parameter
$n_{\|O\ mode}$	= 0.1	Parallel refractive index of O mode unstable wave

Vertical axis - growth rate/ω_{pe} of O mode

Horizontal axis - $ß=\Omega/\omega$ for O mode

Figure 5.8b

Whistler Damping rate/ω_{pe} against whistler frequency

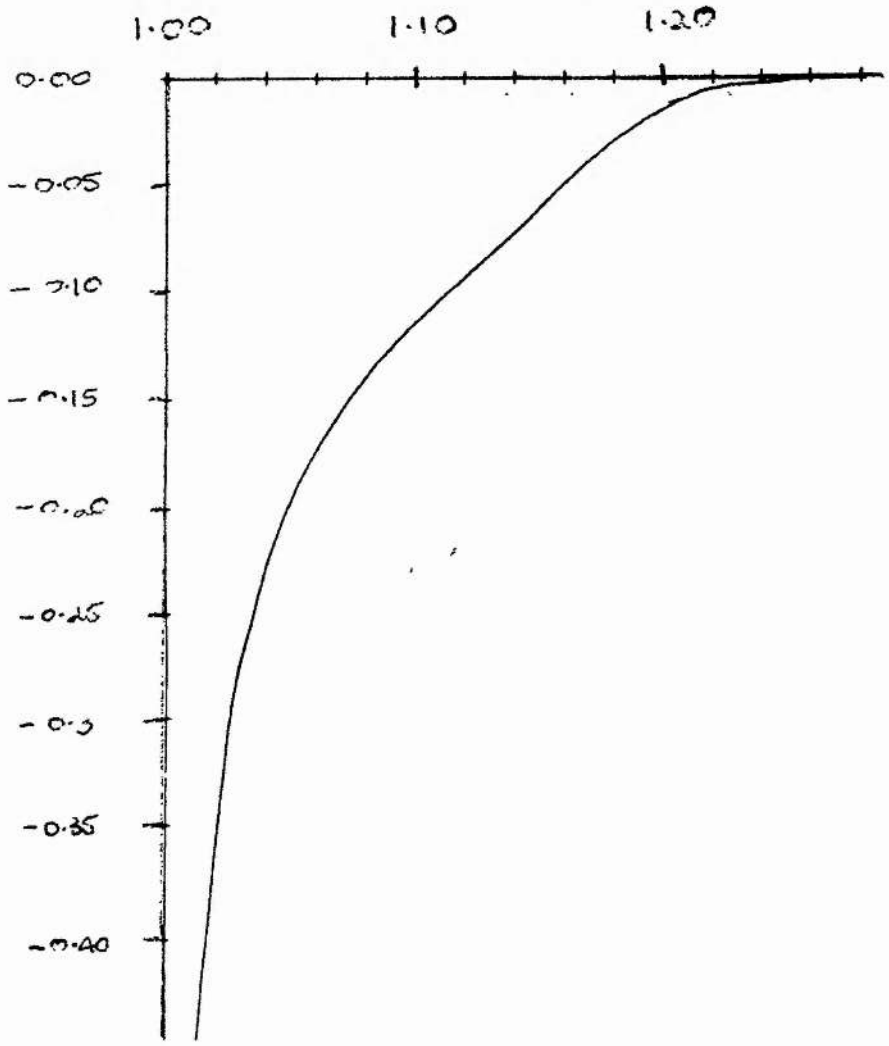

T	= 1keV	Temperature (Maxwellian)
$n_{\|\|ec}$	= 0.0	Perpendicular EC wave
$ß_{EC}$	= 1.15	Ratio of cyclotron to EC wave
$E_{\|\|}$	= 10^8 Vm^{-1}	Parallel electric field
$V_{\|\|c}$	= $10^{10}ms^{-1}$	Mixing parameter

Vertical axis - damping rate/ω_{pe} of whistler

Horizontal axis - ß for whistler frequency

5.7 Collision Rates.

We now proceed to find a typical collision time for the plasmas under consideration so we can compare collision rates with instability growth rates. The rate at which electrons collide is given by the inverse of the electron-electron collision time τ_{ee} (eg Cairns, 1985)

$$\tau_{ee} \approx \frac{3^{\frac{1}{2}} 6\pi\varepsilon_0^2 T^{\frac{3}{2}} m^{\frac{1}{2}}}{n_e e^4 \log_e \Lambda}$$

where $\log_e\Lambda$ is the coulomb logarithm whose properties will not be discussed here (again see Cairns for a discussion) but whose value can be taken to be about 10, and ε_0 is the permittivity in a vacuum. Using the values T=1keV and $n_e=1.0*10^{19}$ m^{-3} we find $\tau_{ee}\approx 10^{-6}$s. Thus we shall be particularly interested in any instabilities whose growth rates are greater than 10^6Hz, as in this case the physics is dominated by instabilities rather than collisions.

5.8 Discussion.

Firstly we consider the order of magnitude of the growth rates we have found numerically. We note from (5.3b)-(5.3d) and (5.7) that it is possible for growth rates to be of a similar order of magnitude to the real part of the wave frequency, invalidating the assumption on which the growth rate was calculated in the first place. This confirms our somewhat crude order of magnitude estimate in section 5.4. Taking figure (5.3b) as an example we see that the maximum growth rate is given as $\omega_i/\omega_{pe}\approx 0.1$. Using the value $\omega_{pe}/\Omega=1/2$ and $B_0=2.5T$ we see $\Omega\approx 4.4*10^{11}$ and hence $\omega_i\approx 2*10^{10}$Hz. The essential point however is that this is higher than the collision frequency by several orders of magnitude. This is reassuring because despite the large number of assumptions that have been made in obtaining these results our conclusion that the physics will be dominated by instabilities rather than collisions cannot be in serious doubt.

In this chapter we have concentrated mainly on whistler instabilities rather than the O mode. We present a calculation of O mode growth rates for comparison even though the physical relevance of them is difficult to interpret. Firstly it is not clear whether there will be any wave-wave interaction during the pulse which could itself have a significant effect on the physics. More importantly it is not clear how O mode waves will behave as they propagate away from the heating region. Unlike whistlers they cross flux surfaces and hence will experience a rapidly changing electron distribution function. It may be that instabilities are damped strongly near the source of the wave. Furthermore it is not clear that the expression for the growth rate of the wave is still valid in a highly non-homogeneous plasma. This is of no importance to the whistler calculations as the whistler will experience a homogeneous plasma along its path as it propagates.

Despite this it is still possible that instability to the O mode may occur and that it may be this wave which depletes the distribution of heated electrons of energy, rather than the whistler wave. If this is the case there is likely to be much increased diffusion of energy perpendicular to the magnetic field. However the

basic conclusion that the underlying distribution will be dominated by instabilities rather than collisions remains valid. The existence of such instabilities casts doubt on the accuracy of current drive calculations based on FEL heating (Nevins, 1987). The reason is that faster collisionless particles are more likely to give up energy to the wave and so become more collisional, instead of carrying current around the torus. If there are instabilities in the plasma the unstable wave will grow until nonlinear saturation occurs. The resultant distribution function will not necessarily be Maxwellian and may still give rise to a current in the plasma, but the exact form of the distribution function cannot be determined using linear analysis. An exact description of the saturation mechanism is beyond the scope of this thesis. Nonetheless it is an important consideration, especially if the instability is caused by a large increase in energy of a relatively small number of electrons, as it is possible the instability may saturate quickly without affecting the bulk of the distribution. It may still be possible to produce current drive if desired, although not with the same high efficiency that would otherwise be expected in the absence of instabilities.

A further consequence of instability is enhanced transport of energy in a direction perpendicular to the magnetic field, which could lead to poor energy confinement especially if the O mode were the unstable wave, or if the whistler were to propagate at a small angle to the magnetic field. Clearly in any situation only one instability will dominate, and it is not the purpose of this thesis to determine which one it will be; we have concentrated on the whistler mode simply because it is relatively easy to analyse and because some of the complications involved in studying waves propagating in a spatially varying magnetic field do not arise.

5.9 Conclusion.

We have examined the stability to whistler waves of distributions obtained when tokamak plasmas are heated by ECRH. Firstly we examined the effects of a pulse of ECRH at powers typical of gyrotrons using linear theory developed by O'Brien et al and Taylor et al, and found that by making some simplifying assumptions and neglecting collisions, no significant instability could occur for parameters for which the model is valid. Next we tested numerical data from the BANDIT code which models continuous operation ECRH, accounting for collisions with a Fokker-Planck collision operator. We again found that there was very little effect on the damping rate of whistlers due to the ECRH. Finally we used the adiabatic theory of heating developed in Chapter three to examine non steady-state distributions that we believe may be typical of those that will arise if lasers are used to produce ECRH. We find that the whistler and possibly other e/m waves are so unstable that the subsequent evolution in time will be dominated by instabilities rather than collisions.

CHAPTER SIX

SUMMARY AND CONCLUSION

CHAPTER SIX

Summary and Conclusion.

In this thesis we have examined high power electron cyclotron heating as recently proposed experiments have included the use of a free electron laser to generate large pulsed powers. In the past the effect of waves on the plasma has been described by quasilinear theory which becomes completely invalid for high wave fields, so a more sophisticated way of determining the final distribution function must be obtained. Under the assumption that the change in wave amplitude seen by electrons crossing the pulse is sufficiently slow we derived an analytic form for the final distribution function after a single pulse of ECRH given that the original distribution is Maxwellian.

In Chapter one we reviewed the background and history of fusion together with an outline of cold plasma theory, warm plasma theory, other means of additional heating, ECRH and current drive.

In Chapter two we reviewed the theory of ECRH in the context of gyrotrons and in particular gave a critique of the work of Taylor et al (1988) for the heating of resonant particles. We extended the gyroaveraged equations in several ways, by including non zero $k_{||}$, a Gaussian beam, terms for the rate of change of the wave amplitude with time, second order effects and finally included the Bessel functions correctly instead of making the small Larmor radius approximation. We compared the improved equations with those obtained by Taylor (1987) and the exact equations and found that the improved equations were much more accurate. We also showed how the equations of motion used by Taylor can be simplified without loss of accuracy, so that the CPU requirement for the code can be substantially reduced, when there is no magnetic field inhomogeneity.

In Chapter three we examined the theory of electron motion in a pulsed intense Gaussian beam in detail using the adiabatic assumption. Next we considered mainly nonresonant electrons which dominate the absorption at high wave intensities. We reviewed the work of Nevins et al (1987) and produced a more accurate and concise account of the nonlinear interaction. We then tested

the adiabatic model numerically by integrating the equations of motion through the beam for individual particles at single points in phase space. We showed numerically that the exact nature of the beam can be important by comparison of a Gaussian triangular and tophat profile for the beam. We found that the theory is good for particles which are not exactly in resonance but is highly inaccurate for those particles which are exactly in resonance where the adiabatic model predicts that no heating should take place.

In Chapter four we tested the accuracy of the adiabatic model by again integrating the equations of motion, but this time for an entire distribution of electrons, assuming that the original distribution is Maxwellian, and displaying the new distribution as a contour plot and by taking a cross section through the perpendicular velocity. We concluded by finding a condition that the adiabatic approximation is valid, and showed that it is most accurate in the regime where instabilities are likely to occur.

In Chapter five we examined the theory of linear instability in plasmas. Firstly we considered the problem analytically neglecting collisions and considering the non steady state distribution function obtained after a short time period. Next we used numerical output from the BANDIT code which models both collisions and ECRH in a plasma to demonstrate that no instability exists in distributions typical of gyrotron heating. Then we showed that using the nonlinear model derived in Chapter three instabilities may exist in distributions typical of those that may be produced in experiments using FELs to heat the plasma. Further work had to be done numerically, and we demonstrated that off perpendicular heating can give rise to far greater instabilities, and that the growth rate is proportional to the electric field amplitude of the ECRH in the region of interest. Comparison was made with growth rates for the O mode and it was seen that the O mode may have even larger growth rates than the whistler.

Our basic conclusion was that using FELs to heat plasmas will produce microinstabilities, possibly the whistler instability, and that these will dominate the subsequent evolution in time of the distribution function. This in turn may cast doubt on the accuracy of current drive calculations based on the assumption that the distribution function is stable.

Suggestions for further work.

It would be highly desirable to be able to obtain a first order correction to the adiabatic model by allowing for the effects of nonadiabatic motion. As the condition, obtained in Chapter four, that the adiabatic approximation is valid involves an order of magnitude estimate of the change in the Hamiltonian, and not a first approximation to it, there is clearly scope for refinement. As mentioned in Chapter three there are situations in which neither the linear resonance heating theory of O'Brien et al nor the adiabatic theory of Nevins et al is valid, so finding a theory to fit these situations would be a useful step towards solving this problem.

Secondly it would be interesting to determine what mechanisms are responsible for nonlinear saturation and to find the equilibrium distribution function in a pulsed system of intense ECRH by calculating the self-consistent effect of the unstable wave on the distribution function, perhaps using the approach of Davidson and Yoon (1989). In this way we may be able to make revised estimates of the ability of FELs to induce currents in tokamaks.

Thirdly it might be interesting to consider the effect of magnetically trapped particles on the new distribution function after a pulse of FEL ECRH, to determine whether the presence of such particles enhances or diminishes the instability.

APPENDICES AND REFERENCES

Appendices

Appendix I

Derivation of the Gyroaveraged Equations of Motion for an Electron in a Beam of ECRH

The Lagrangian for a particle of mass m and charge -e in an electromagnetic field is

$$L = (m\underline{U}-e\underline{A}).\dot{\underline{x}} - \gamma mc^2$$

where $\underline{A}$ is the magnetic potential, and $d\underline{x}/dt$ the nonrelativistic velocity and where we have chosen a gauge such that the electric field potential vanishes. We write the magnetic potential as

$$\underline{A} = B_0 x\left(1+\frac{z}{G}\right)\hat{\underline{y}} + \underline{A}_1$$

$\underline{A}_1$ being the magnetic part of the wave and G being the magnetic field gradient of Taylor et al (where the quantity was denoted by R) and the wave is assumed to have time and space dependence exp $i(k_\perp x+k_{||}z-\omega t)$. We now transform to guiding centre coordinates:

$$\underline{x} = \underline{X}+\frac{U_\perp}{\Omega}\sin(\phi)\hat{\underline{x}} - \frac{U_\perp}{\Omega}\cos(\phi)\hat{\underline{y}}$$

$$\underline{U} = U_\perp\cos(\phi)\hat{\underline{x}} + U_\perp\sin(\phi)\hat{\underline{y}} + U_{||}\hat{\underline{z}}$$

$$\dot{\underline{x}} = \dot{\underline{X}}+\frac{\dot{U}_\perp}{\Omega}\sin(\phi)\hat{\underline{x}} + \frac{U_\perp\dot{\phi}}{\Omega}\cos(\phi)\hat{\underline{x}} - \frac{\dot{U}_\perp}{\Omega}\cos(\phi)\hat{\underline{y}} + \frac{U_\perp\dot{\phi}}{\Omega}\sin(\phi)\hat{\underline{y}}$$

where $\underline{X} = (X,Y,Z)$ is the position of the guiding centre. We assume that the wave frequency is close to the cyclotron frequency so that we can average over the cyclotron oscillations and define an averaged Lagrangian

$$L_{av} = \frac{1}{2\pi}\int_0^{2\pi} L\, d\phi .$$

After use of the Jacobi identity

$$e^{iasinx} = \sum_{n=-\infty}^{+\infty} J_n(a)\, e^{inx}$$

the space dependence becomes

$$e^{ik_\perp\left(X + \frac{U_\perp}{\Omega}sin\phi\right)} = e^{ik_\perp X} \sum_{n=-\infty}^{n=+\infty} J_n(a)\, e^{in\phi}$$

Using the identity

$$\frac{1}{2\pi}\int_0^{2\pi} e^{in\phi} d\phi = \begin{cases} 1 \text{ for } n=0 \\ 0 \text{ otherwise} \end{cases}$$

and similar expressions for

$$\frac{1}{2\pi}\int_0^{2\pi} e^{in\phi} sin\phi d\phi \text{ and } \frac{1}{2\pi}\int_0^{2\pi} e^{in\phi} cos\phi d\phi$$

we obtain with straightforward but lengthy algebra the following expression for the averaged Lagrangian:

$$L_{av} = \frac{mU_\perp^2 \dot{\phi}}{2\Omega} + mU_\parallel \dot{z} - eB_0 X\dot{Y}\left(1 + \frac{z}{G}\right)$$

$$-e\left[A_{1x}e^{i\psi} + c.c.\right]J_1\dot{X} - \frac{e}{2i}\left[A_{1x}\frac{d}{dt}\left(\frac{u_\perp}{\Omega}\right)e^{i\psi} - c.c.\right]J_0 - e\left[A_{1x}\frac{\dot{\phi}}{k_\perp}e^{i\psi} + c.c.\right]J_1$$

$$-\frac{e}{i}\left[A_{1y}e^{i\psi} + c.c.\right]\dot{Y}J_1 + \frac{e}{2}\left[A_{1y}\frac{d}{dt}\left(\frac{u_\perp}{\Omega}\right)e^{i\psi} - c.c.\right]J_0 - \frac{e}{i}\left[A_{1y}\frac{\dot{\phi}}{k_\perp}e^{i\psi} + c.c.\right]J_1$$

$$-e\left[A_{1z}J_1 e^{i\psi} + c.c.\right]\dot{z} - \gamma mc^2$$

which reduces to A2.8 of Taylor (1987) on making the small Larmor radius approximation.

The suffices $\parallel$ and $\perp$ refer to parallel and perpendicular components respectively for

V electron velocity

U $=\gamma V$

k wave number.

The argument of the Bessel function is $a=\frac{k_\perp U_\perp}{\Omega}$ where Ω is the cyclotron frequency.

A_1 is regarded as a function of position,

$\omega' = \omega - k_\parallel V_\parallel$

and G is the magnetic field gradient of Taylor et al.

The phase of the particle here is denoted by ψ and is related to the phase of the electron, ϕ, by $\psi = \phi - \omega t$.

Now we let $\underline{A}_1 = \underline{E}/(2i\omega)$, $E_- = E_x - iE_y$ and $E_\parallel = E_z$ and note that we can take $X=Y$, $=dX/dt=dY/dt$, $=0$. The Lagrangian becomes

$$L_{av} = \frac{mU_\perp^2\dot{\phi}}{2\Omega} + mU_\parallel\dot{z} + \frac{e}{2\omega}E_-\frac{d}{dt}\left(\frac{U_\perp}{\Omega}\right)J_0\cos\psi - \frac{e}{\omega}E_-\frac{\dot{\phi}}{k_\perp}J_1\sin\psi - \frac{e}{\omega}E_\parallel V_\parallel J_1\sin\psi - \gamma mc^2.$$

We now obtain the following equations of motion from Lagrange's equations (see also equation (2.5) of Chapter two):

$$\frac{d}{dt}\left(\frac{\partial L_{av}}{\partial \dot{\phi}}\right) - \frac{\partial L_{av}}{\partial \dot{\phi}}$$

yields

$$\frac{d}{dt}\left(\frac{mu_\perp^2}{2\Omega} - \frac{e}{\omega}\frac{E_-}{k_\perp}J_1\sin\psi\right) - \left(-\frac{e}{2\omega}E_-\frac{d}{dt}\left(\frac{u_\perp}{\Omega}\right)J_0\sin\psi - \frac{e}{\omega}E_-\frac{\dot{\phi}}{k_\perp}J_1\cos\psi - \frac{e}{\omega}E_\parallel V_\parallel J_1\cos\psi\right)$$

$$\Rightarrow \frac{mu_\perp}{\Omega}\frac{du_\perp}{dt} - \frac{mu_\perp^2}{2\Omega^2}\dot{\Omega} - \frac{e}{\omega}\frac{\dot{E}_-}{k_\perp}J_1\sin\psi - \frac{e}{2\omega}\frac{E_-}{k_\perp}\frac{k_\perp\dot{u}_\perp}{\Omega}J_0\sin\psi - \frac{e}{\omega}\dot{\psi}\frac{E_-}{k_\perp}J_1\cos\psi$$

$$= -\frac{e}{2\omega}E_-\frac{\dot{u}_\perp}{\Omega}J_0\sin\psi + \frac{e}{2\omega}E_-\frac{u_\perp}{\Omega^2}\dot{\Omega}\,J_0\sin\psi - \frac{e}{\omega}E_-\frac{\dot{\phi}}{k_\perp}J_1\cos\psi - \frac{e}{\omega}E_\parallel V_\parallel J_1\cos\psi.$$

Cancelling two of the terms, noting that $\dot{\Omega} = \frac{\Omega_o V_\parallel}{G}$ and $\omega' = \dot{\psi} - \dot{\phi}$ and multiplying through by $\frac{\Omega}{mu_\perp}$ we have

$$\frac{du_\perp}{dt} = \frac{\Omega_0 u_\perp V_\parallel}{2G\Omega} + \frac{e}{m\omega}\dot{E}_-\frac{J_1}{a}\sin\psi + \frac{e}{m\omega}E_-\frac{J_1}{a}\omega'\cos\psi + \frac{e}{2m}E_-\frac{\Omega_0 V_\parallel}{\Omega^2 G}J_0\sin\psi - \frac{e}{2m\omega}\frac{E_\parallel V_\parallel k_\perp J_1}{a}\cos\psi.$$

Similarly,

$$\frac{d}{dt}\left(\frac{\partial L_{av}}{\partial \dot{z}}\right) - \frac{\partial L_{av}}{\partial z} = 0$$

yields

$$\frac{du_\parallel}{dt} = -\frac{u_\perp^2(\omega' + \dot{\psi})\Omega_0}{2\Omega^2 G} - \frac{e}{2m\omega}E_\parallel\frac{aV_\parallel}{\Omega}\frac{\Omega_0}{G}J_0\sin\psi + \frac{e}{2m\omega}\frac{\dot{E}_-}{V_\parallel}\frac{d}{dt}\left(\frac{u_\perp}{\Omega}\right)J_0\cos\psi - \frac{e}{m\omega}\frac{\dot{E}_-}{V_\parallel}\frac{(\omega' + \dot{\psi})}{k_\perp}J_1\sin\psi$$

$$-\frac{k_\parallel e}{2m\omega}E_-\frac{d}{dt}\left(\frac{u_\perp}{\Omega}\right)J_0\sin\psi + \frac{e}{2m\omega}E_-\frac{\dot{u}_\perp}{\Omega^2}\frac{\Omega_0}{G}J_0\cos\psi - \frac{e}{m\omega}E_-\frac{d}{dt}\left(\frac{u_\perp}{\Omega}\right)\frac{a}{\Omega}\frac{\Omega_0}{G}J_1\cos\psi - \frac{k_\parallel e}{m\omega}E_-\frac{(\omega' + \dot{\psi})}{k_\perp}J_1\cos\psi$$

$$- \frac{e}{2m\omega} E_- (\omega' + \dot{\psi}) \frac{aV_\perp \Omega_0}{\Omega^2 G} \sin\psi - \frac{k_{||} e E_{||} V_{||} J_1 \cos\psi}{m\omega}$$

where have used $\frac{\partial \psi}{\partial z} = k_{||}$, and

$$\frac{d}{dt}\left(\frac{\partial L_{av}}{\partial \dot{U}_\perp} \right) - \frac{\partial L_{av}}{\partial U_\perp} = 0$$

yields

$$\frac{d\psi}{dt} = \omega' + \frac{\frac{e\Omega E_- J_0 \cos\psi}{2m\omega u_\perp} + \frac{eE_- \Omega_0 V_{||} J_0 \cos\psi}{2m\omega\Omega u_\perp G} + \frac{eE_-}{2m\omega} \frac{d}{dt}\left(\frac{u_\perp}{\Omega}\right) \frac{k_\perp}{u_\perp} J_1 \cos\psi + \frac{eE_{||} V_{||} J_0 k_\perp \sin\psi}{2m\omega u_\perp}}{\left(1 - \frac{eE_- J_0 \sin\psi}{2m\omega U_\perp}\right)}$$

In his derivation Taylor neglected terms of the form (rate of change of ψ, $U_{||}$ or $U_\perp$) * ($E_{||}$ or E_-). He had no need to include terms involving dE/dt in his equations and furthermore made the small Larmor radius expansion. Taylor's own equations are given in (2.4a) to (2.4c) for comparison.

Appendix 2

The Gyroaveraged Hamiltonian Governing Motion of an Electron in a Beam of ECRH.

The Hamiltonian governing interaction of an electron charge e mass m with an electromagnetic wave in dimensionless units is

$$H=\sqrt{1+\left(\underline{p}+\frac{e}{m}\underline{A}\right)^2}$$

where $\underline{p}$ is the canonical relativistic momentum normalised to mc, H is the Hamiltonian normalised to mc^2, $\underline{A}$ is the magnetic vector potential (including any background magnetic field) normalised to c, and the potential is zero by choice of gauge. We consider the case of the O mode propagating perpendicular to a background magnetic field with potential $\underline{A}_0$. We assume the magnetic potential due to the wave $\underline{A}$ is small so that $(A_1/A_0)^2$ can be ignored. Making this approximation we find

$$H=\sqrt{1+p_\perp^2+p_\parallel^2+\frac{2e\underline{p}.\underline{A}_1}{m}}$$

where the canonical coordinates are now $(p_\parallel, z)$ and (μ,ϕ) with $\mu=p_\perp{}^2/2$.

Now we make a transformation to $\varnothing=\psi+\omega\tau/\Omega$ where we let $\tau=\Omega t$. Using a generating function $F=-\mu(\psi+\tau/ß)$ we have from Hamiltonian theory that $H\rightarrow H+dF/d\tau$ so $H\rightarrow H-\mu/ß$. We can make another two useful transformations without altering the Hamiltonian, viz the transformation to guiding centre coordinates $(x,y)\rightarrow(X,Y)$ as in Appendix one. Now for the O mode

$$A_{1z} = -\frac{E_{\|}}{2\omega}\cos\left(k_{\perp}x - \frac{\tau}{\beta}\right),$$

$$= -\frac{E_{\|}}{2\omega}\cos\left(k_{\perp}\rho\sin(\phi) - \frac{\tau}{\beta}\right)$$

under a suitable shift of the origin of ø, or by taking X=0. We now use the Jacobi identity and average over the gyrophase ψ as in Appendix one. We find

$$\underline{p}.\underline{A}_1 = \frac{p_{\|}E_{\|}J_1\left(\frac{n_{\perp}p_{\perp}\omega}{\Omega}\right)\sin\psi}{\omega}$$

$$\approx \frac{p_{\|}E_{\|}\left(\frac{n_{\perp}p_{\perp}\omega}{\Omega}\right)\sin\psi}{2\omega}$$

so that

$$H_{av} = \sqrt{1+2\mu+p_{\|}^2+\frac{E_{\|}p_{\|}n_{\perp}\sqrt{2\mu}\sin\psi}{B_0c}} - \frac{\mu}{\beta} \quad .$$

As we have already neglected terms second order in the field strength we linearise our basic Hamiltonian and apply Hamilton's equations, finding

$$\dot{p}_{\perp} = -\frac{e}{2m}\frac{E_{\|}V_{\|}}{\omega}k_{\perp}\cos\psi$$

$$\dot{\psi} = \frac{\Omega}{\gamma} - \omega + \frac{E_{\|}V_{\|}}{\omega}\sqrt{\frac{2}{\mu}}\sin\psi$$

$$\dot{z} = \frac{p_{\|}\text{real}}{\gamma}$$

$$\dot{p}_{\|\text{real}} = 0$$

where $p_{\|\,real}$ is the actual normalised parallel momentum, and not the canonical momentum. The linearisation is not strictly necessary but is done here as we wish to recover the Hamiltonian of Nevins et al. Our equations agree with the equations derived by Taylor et al, in the case of magnetic field homogeneity.

We shall not give the full details of extension to oblique incidence, but instead we note that the transformation $\phi = \psi + \omega\tau/\Omega$ becomes $\phi = \psi + \omega'\tau/\Omega$ so that the exact Hamiltonian is now

$$H = \sqrt{1 + \left(\underline{p} + \frac{e}{m}\underline{A}\right)^2} \; - \; \frac{\mu(1 - n_{\|} p_{\|}/\gamma)}{\beta}$$

where the canonical variables are (ψ,μ) and $(z,p_{\|can})$. We note here that this Hamiltonian involves no approximation whatsoever. By gyroaveraging we can eliminate the time dependence of the Hamiltonian and so use the constancy of the averaged Hamiltonian to derive our adiabatic theory on the assumption that the electric field changes sufficiently slowly, demonstrating that the adiabatic theory does not depend on a linearisation of the Hamiltonian.

The Hamiltonian of Nevins et al may easily be derived from ours by linearising, adding the constant $-P_r^2/2$ and making a weakly relativistic expansion to obtain

$$H = \frac{\left(P_r - \mu\right)^2}{2} + \alpha\sqrt{\mu}\,\sin\psi \text{ with } \alpha = \frac{E_{\|} p_{\|} n_{\perp}}{B_0 c \gamma \sqrt{2}}$$

where we have defined the phase angle so as to be consistent with the definition given by Taylor et al, rather than that of Nevins et al.

Appendix 3.
Growth Rate of O/X Mode Instabilities.

In this Appendix we describe the calculation of the growth/damping rate of the O mode as it is performed in the stability code.

The growth rate of the O/X mode is derived in the same manner as for a whistler wave. Now however the dispersion relation is much more complicated. Let $D_{i,j} = \varepsilon_{i,j} - n_i n_j$ where n_i are components of the refractive index (which of course depends on the direction of propagation) then $D=\det(D_{i,j})$. We again use the formula

$$\omega_i = \frac{-D_i}{\frac{\partial D_r}{\partial \omega_r}}$$

but to simplify the calculations we make a number of further simplifications. Firstly we calculate the denominator by using the nonrelativistic formulae for $\varepsilon_{i,j}$ and hence for $D_{i,j}$. By making the small Larmor radius approximation we can reduce the expressions for the dielectric tensor coefficients to the following form (Owen, 1984, but see also section 2.3.2. of Bornatici et al, 1983A):

$$\begin{aligned}
\varepsilon_{1,1} &= \varepsilon_{2,2} &&= 1+P \\
i\varepsilon_{1,2} &= -i\varepsilon_{2,1} &&= P \\
\varepsilon_{1,3} &= \varepsilon_{3,1} &&= n_\perp T \\
i\varepsilon_{2,3} &= -i\varepsilon_{3,2} &&= n_\perp T \\
\varepsilon_{3,3} & & &= R+n_\perp{}^2 S,
\end{aligned}$$

where P, T (not to be confused with the temperature), R and S may be complex.

We now consider the values of P, T, R and S when the distribution is Maxwellian. The nonrelativistic expressions for P, T, R and S are

$$P = \frac{\omega_p^2}{\omega^2}\sqrt{\frac{\lambda_T}{2}}\,\frac{Z(z_1)}{2n_{||}}$$

$$R = \frac{\omega_p^2}{\omega^2}\sqrt{\frac{\lambda_T}{2}}\,\frac{2(1+z_0 Z(z_0))z_0}{n_{||}}$$

$$S = \frac{\frac{\omega_p^2}{\Omega^2} z_1\left(1+z_1 Z(z_1)\right)}{n_{||}\sqrt{2\lambda_T}}$$

$$T = \frac{\omega_p^2}{\omega\Omega}\,\frac{\left(1+z_1 Z(z_1)\right)}{2n_{||}}$$

where Z is the plasma dispersion function (calculated by a standard routine FRDCNT written by Terry Martin of the Culham Laboratory)

$$Z(z) = \pi^{-1/2}\int_{-\infty}^{+\infty}\frac{dt\, e^{-t^2}}{t-z}$$

and

$$z_0 = \frac{\sqrt{\frac{\lambda_T}{2}}}{n_{||}} \text{ and } z_1 = (1-\beta)z_0.$$

Here we have assumed that only the antihermitian dielectric tensor elements in the numerator of our expression for the growth rate need to be calculated using our arbitrary distribution f. Otherwise we assume that the dielectric tensor elements can be calculated using a Maxwellian of form $N\exp(-\lambda_T\gamma)$. These expressions are straightforward to differentiate as $dZ/dz = -2(1+zZ)$ and so this completes our description of the calculation of the denominator.

The numerator is more difficult to evaluate. Here we use the relativistic version of the above equations to determine the hermitian parts of $\varepsilon_{i,j}$ but integrate the arbitrary distribution function to obtain the anti-hermitian parts.

We now have (Owen and Bornatici et al)

$$P = \frac{\omega_p^2 \lambda_T}{\omega^2 2} f_{\frac{5}{2}}\left(\frac{\lambda_T \Omega}{\omega}, n_{\|}\right)$$

$$R = \frac{\omega_p^2}{\omega^2} \lambda_T \frac{\partial}{\partial n_{\|}} \left(n_{\|} f_{\frac{5}{2}}\left(0, n_{\|}\right)\right)$$

$$S = -\frac{\omega_p^2}{\omega^2} \frac{1}{2\beta^2} \frac{\partial}{\partial n_{\|}} \left(n_{\|} f_{\frac{7}{2}} \left(\frac{\lambda_T \Omega}{\omega}, n_{\|}\right)\right)$$

$$T = \frac{\omega_p^2}{\omega^2} \frac{\lambda_T}{2} \frac{n_{\|}}{\beta} \frac{\partial}{\partial(\lambda_T \beta)} f_{\frac{7}{2}}\left(\lambda_T \beta, n_{\|}\right)$$

where f is the Shkarofsky function

$$f_q\left(\lambda_T \beta, n_{\|}\right) = -i \int_0^{\infty} \frac{\exp\left\{\lambda_T - \lambda_T\left[(1-it)^2 + n_{\|}^2 t^2\right]^{\frac{1}{2}} - i\lambda_T \beta t\right\}}{\left[(1-it)^2 + n_{\|}^2 t^2\right]^{\frac{q}{2}}} \, dt$$

which is calculated using a routine of Owen which also calculates $n_{\perp}$ for the chosen mode. Only the real parts of the above quantities are required. The anti-hermitian parts of $\varepsilon_{i,j}$ (which essentially determine whether or not an instability occurs) are calculated as follows (see again Bornatici et al):

$$\mathrm{Im}(\varepsilon_{1,1}) = \mathrm{Im}(\varepsilon_{2,2}) = \mathrm{Re}(\varepsilon_{1,2}) = -\mathrm{Re}(\varepsilon_{2,1}) = I_1$$

$$\mathrm{Im}(\varepsilon_{1,3}) = -\mathrm{Re}(\varepsilon_{2,3}) = I_2$$

$$\mathrm{Im}(\varepsilon_{3,1}) = \mathrm{Re}(\varepsilon_{3,2}) = I_3$$

$$\mathrm{Im}(\varepsilon_{3,3}) = I_4$$

where

$$I_1 = -\frac{\omega_p^2}{\omega^2}\frac{2\pi^2}{|n_\parallel|}\int_0^\infty dp_\perp \frac{p_\perp^2}{4} U$$

$$I_2 = -\frac{\omega_p^2}{\omega^2}\frac{2\pi^2}{|n_\parallel|}\int_0^\infty dp_\perp \frac{p_\perp^2}{4} W\, p_\parallel\left(\frac{n_\perp p_\perp}{\beta}\right)$$

$$I_3 = -\frac{\omega_p^2}{\omega^2}\frac{2\pi^2}{|n_\parallel|}\int_0^\infty dp_\perp \frac{p_\perp^2}{4} U p_\parallel\left(\frac{n_\perp p_\perp}{\beta}\right)$$

$$I_4 = -\frac{\omega_p^2}{\omega^2}\frac{2\pi^2}{|n_\parallel|}\int_0^\infty dp_\perp \frac{p_\perp^2}{4} W\, p_\parallel\left(\frac{n_\perp p_\perp}{\beta}\right)^2$$

and where

$$U = \frac{\partial f}{\partial p_\perp} + \frac{n_\parallel}{\gamma} F \text{ and } W = \frac{\partial f}{\partial p_\parallel} - \frac{\beta}{\gamma p_\perp} F \text{ and } F = p_\perp \frac{\partial f}{\partial p_\parallel} - p_\parallel \frac{\partial f}{\partial p_\perp} .$$

Inclusion of the Bessel functions J_0 and J_1 would have forced us to evaluate eight integrals instead of the four mentioned above, as otherwise the only identity we would have between the anti-hermitian parts would be $\varepsilon_{1,2} = -\varepsilon_{2,1}$.

REFERENCES

ABRAMOVITZ M and STEGUN I A (1972), *'Handbook of Mathematical Functions '*, Dover Publ Inc, New York.

AIROLDI A C and OREFICE A (1983), *J Plasma Physics* **27**, 515.

BEHN R et al (1984), *Plasma Physics and Contr Fusion* **26,** 173.

BERNABEI S et al (1982), *Phys Rev Lett* , **49**, 1255.

BICKERTON R J et al (1986), *Plasma Physics and Contr Fusion* **28**, 1943.

BERNSTEIN I B, TREHAN S K and WEENIK M P H (1964), *Nucl Fusion* **4**, 61.

BORNATICI M, CANO R, DE BARBIERI O AND ENGELMANN F (1983A), *Nucl Fusion* **23,** 1153.

BORNATICI M, CRESTANI M and FERRI P (1983B), *Proc14th Int Conf on Contr Fusion and Plasma Physics* **1,** 383.

BORNATICI M and RUFFINA U (1985), *Il Nouvo Cimento* **6D,** 231.

CAIRNS R A (1985), *'Plasma Physics '*, Blackie, Glasgow and London.

CAIRNS R A, OWEN J A and LASHMORE-DAVIES C N (1983), *Phys Fluids* **26,** 3475.

CAIRNS R A and LASHMORE-DAVIES C N (1986), *Plasma Physics and Contr Fusion* **28,** 1539.

CLEMMOW, P C and DOUGHERTY, J P (1969), *'Electrodynamics of Particles and Plasmas'*, Addison-Wesley, London.

CONSOLI T (1986), *Proc 13th Int Conf on Contr Fusion and Plasma Physics, Schliersee* **2**, 223.

DAVIDSON R C, YANG T S and AAMODT R E (1989), *J Plasma Physics* **41**, 405.

DAVIDSON R C and YOON P H (1989), *Phys Fluids* **B1**, 195.

DAVYDOVSKII V Ya (1963), *Sov Phys* JETP **16**, 629.

DENDY R O and O'Brien (1989), *Nucl Fusion* **29**, 480.

FIDONE I, GIRUZZI G, GRANATA G and MEYER R L (1984) *Phys Fluids* **27**, 661.

FIELDING P J (1980), *Proceedings of the Joint Workshop on Electron Cyclotron Emission and Electron Cyclotron Resonance Heating*, Oxford CLM-ECR , 69.

FISCH N J (1987), *Reviews of Modern Physics* **59**, 175.

FISCH N J and BOOZER A H (1980), *Phys Rev Lett* **45**, 720.

GARNER R C , MAUEL M E, HOKIN S A, POST R C and SMATLAK D L (1987), *Phys Rev Lett* **59**, 1821.

GARNER R C , MAUEL M E, HOKIN S A, POST R C and SMATLAK D L (1990), *Phys Fluids* **B2**, 242.

GILL R D et al (1986), *Proc 13th Int Conf on Contr Fusion and Plasma Physics, Schliersee* **1**, 21.

GOLDSTEIN H (1950), '*Classical Mechanics* ' Addison - Wesley.

GOLOVANIVSKY K S (1985), *Soviet J Plasma Physics* **11**, 171.

GRADSHTEYN I S and RYZHIK. I M (1965), '*Tables of Integrals, Series and Products* ' Academic Press, New York and London.

GUEST G E and DORY R A (1965), *Phys Fluids* **8**, 1853.

HALL L S and HECKROTTE W (1964), *Phys Rev* **134 A,** 1474.

HARRIS E G (1961), *J Nucl Energy* **C2**, 138.

JAEGER F, LICHTENBERG, A J and LIEBERMAN M A (1972), *Plasma Physics* **14,** 1073.

KOTEL'NIKOV I A and STUPAKOV G V (1990), *Phys Fluids* **B2**, 881.

KRIVENSKI V and OREFICE A (1983), *J Plasma Physics* **30**, 125.

LANGDON A B and LASINSKI B F (1976), *Methods Comput Phys* **16,** 327.

LICHTENBERG and A J LIEBERMAN M A (1983), ' *Regular and Stochastic Motion* ' Springer - Verlag, New York.

LIEBERMAN M A and LICHTENBERG, A J (1973), *Plasma Physics* **15,** 125.

LITTLEJOHN R G (1983), *J Plasma Physics* **29,** 111.

MENYUK C R, DROBOT A T, PAPADOPOULUS K and KARAMABADI H (1987), *Phys Rev Lett* **58**, 2071.

MENYUK C R, DROBOT A T and PAPADOPOULUS K (1988), *Phys Fluids* **31,** 3768.

NEVINS W M, ROGNLIEN T D and COHEN B I (1987), *Phys Rev Lett* **59,** 60.

OKHAWA T (1970), *Nucl Fusion* **10,** 185.

O'BRIEN (1990), *Private Communication* .

O'BRIEN M R, COX M, and START D F H (1986A), *Nucl Fusion* **26,** 1625.

O'BRIEN M R, COX M, and START D F H (1986B), *Comp Physics Communications* **40,** 123.

OWEN J A (1984), *PhD Thesis.*

PORKOLAB M and COHEN B I (1988), *Nucl Fusion* **28,** 239.

PRATER R et al (1987), *Proceedings of the American Institute of Physics Conference, Kissimmee* **159,** 9.

ROGNLIEN T D (1983), *Phys Fluids* **26,** 1545.

SHIMA Y and HALL L S (1965), *Phys Rev* **139A,** 1115.

SHKAROFSKY I P (1966), *Phys Fluids* **9,** 561.

SOPER G K and HARRIS E G (1965), *Phys Fluids* **8,** 985.

START D F H et al (1982), *Phys Rev Lett* **48,** 624.

STIX T H (1962), *'The Theory of Plasma Waves'* McGraw-Hill, New York.

SUVOROV E V and TOKMAN M D (1983), *Plasma Physics* **25,** 723.

TAYLOR A W (1987), *PhD Thesis.*

TAYLOR A W, CAIRNS R A and O'BRIEN M R (1988), *Plasma Physics and Contr Fusion* **30**, 1039.

THOMASSEN K I (1988), *Plasma Physics and Contr Fusion* **30**, 57.

TIMOFEEV A V (1978), *Sov Phys JETP* **48,** 656.

WESSON J (1987), *'Tokamaks'* OUP.

YOON P H (1989), *Phys Fluids* **B1**, 1336.